Universidade de Aveiro Departamento de Engenharia Civil
2013

Rui André
Simões Dias Maio

Seismic Vulnerability Assessment of Old Building Aggregates

Avaliação da Vulnerabilidade Sísmica de Agregados de Edifícios Antigos

Universidade de Aveiro Departamento de Engenharia Civil
2013

Rui André
Simões Dias Maio

Seismic Vulnerability Assessment of Old Building Aggregates

Avaliação da Vulnerabilidade Sísmica de Agregados de Edifícios Antigos

Valutazioni della Vulnerabilità Sismica di un Aggregato di Edifici Antichi

Dissertação apresentada à Universidade de Aveiro para cumprimento dos requisitos necessários à obtenção do grau de Mestre em Engenharia Civil, realizada sob orientação científica do Professor Doutor Romeu da Silva Vicente, Professor Auxiliar da Universidade de Aveiro, do Professor Doutor Humberto Varum, Professor Auxiliar da Universidade de Aveiro e do Professor Doutor Antonio Formisano, Professor Auxiliar da Universidade de Nápoles Federico II.

Dedico este trabalho aos meus pais, irmão e namorada.

o júri / the jury

presidente / president

Prof. Doutora Ana Luísa Pinheiro Lomelino Velosa
Professora Associada da Universidade de Aveiro

Prof. Doutor Alexandre Aníbal Meira Guimarães Costa
Professor Adjunto Convidado do Instituto Superior de Engenharia do Porto

Prof. Doutor Romeu da Silva Vicente
Professor Auxiliar da Universidade de Aveiro

agradecimentos / acknowledgements

Aproveito esta ocasião para manifestar a minha gratidão a todos aqueles que, directa ou indirectamente contribuiram para a minha formação académica e cívica ao longo dos últimos cinco anos, cujos ensinamentos não vou seguramente esquecer. Começo por agradecer à Universidade de Aveiro e ao Departamento de Engenharia Civil pelas infraestruturas e ambiente de trabalho favorável e motivador, e também pela oportunidade de estudos no estrangeiro, experiências das quais ficarei eternamente grato.

A presente dissertação marca o final de uma etapa importante da minha vida, pelo que devo agradecer primeiramente às pessoas que mais me auxiliaram na sua elaboração. Assim, ao professor Romeu Vicente, que na qualidade de orientador despertou em mim um sentido mais crítico na abordagem de problemas e dificuldades, o meu obrigado pela simpatia, paciência e apoio demonstrados ao longo deste último ano.

My warmest appreciation goes to my co-supervisor, professor Antonio Formisano, for his constant wise guidance, in particular throughout the period of studies in Naples, and also for ceding me the tools and data to initiate this dissertation.

Uma palavra de agradecimento ao professor Humberto Varum, pelos sábios comentários, atenção e acompanhamento prestado no âmbito desta dissertação. Deixo aqui também um obrigado ao professor Carlos Coelho pela simpatia e competência com que, desempenha as funções de docente e ao mesmo tempo coordena o gabinete de mobilidade internacional do departamento.

To Eng. Davide Seni and to STA DATA, for ceding me the software license of 3muri®. To Dr. Serena Cattari and Eng. Marina Russo for helping me on the use and interpretation of the mentioned software.

Obrigado a todos os meus colegas de curso sem excepcção e em especial ao João Oliveira, companheiro inseparável, pelo apoio incondicional prestado durante todo este percurso.

Por último, agradeço profundamente aos meus pais Rui e Eva e irmão Diogo, pela eterna amizade e valores transmitidos e ainda pelo investimento realizado durante toda a minha formação académica que aqui termina. Agradeço igualmente à Marta, pelo amor, paciência e dedicação. Agradeço aos meus familiares e amigos, pelo apoio constante quer nos bons, quer nos maus momentos.

keywords

Seismic Vulnerability; Building Aggregates; 3muri®; Non-linear Static Analysis; Macro-elements; Fragility Curves; Damage Distribution; Vulnerability Index.

abstract

The present dissertation approaches the assessment of the seismic vulnerability of old stone masonry building aggregates. With this topic it is presented a review on the most recent methods and tools used for the seismic vulnerability assessment of masonry buildings, focusing the research developed both in Italy and Portugal. Moreover, a case study of an old stone masonry building aggregate was assessed, which is located in *San Pio delle Camere* (*Abruzzo*, Italy), slightly affected by the 6th April 2009 *L'Aquila* earthquake. This building aggregate was modelled using the STA DATA software 3muri®. On one hand, static non-linear numerical analysis was performed to obtain capacity curves and a prediction of the damage distribution in the structure, caused by the input seismic action (hybrid method), on the other hand indirect methods were used, based on different vulnerability index formulations.

palavras-chave

Vulnerabilidade Sísmica; Agregados de Edifícios; 3muri®; Análise Estática não-linear; Macro-elementos; Curvas de Fragilidade; Distribuição de Danos; Índice de Vulnerabilidade.

resumo

A presente dissertação insere-se no estudo da avaliação da vulnerabilidade sísmica de agregados de edifícios antigos de alvenaria de pedra. É feita uma revisão geral da literatura sobre os mais recentes estudos e ferramentas para a avaliação da vulnerabilidade sísmica de agregados de edifícios de alvenaria de pedra, enfatizando o trabalho de investigação desenvolvido em Itália e em Portugal nesta temática. É avaliada a vulnerabilidade sísmica de um caso de estudo de um agregado de edifícios, localizado em *San Pio delle Camere* (na região de *Abruzzo*, em Itália), afectado pelo sismo de L'Aquila e modelado com o recurso ao programa da STA DATA 3muri®. Numa primeira fase, a avaliação da vulnerabilidade sísmica do agregado foi conseguida através de uma metodologia híbrida, que estima as curvas de fragilidade com base nos deslocamentos espectrais resultantes de análises estáticas não-lineares. Posteriormente foram aplicados métodos indirectos, baseados na estimativa de um índice de vulnerabilidade, para diferentes formulações correntes.

parole chiave

Vulnerabilità Sismica; Aggregati di Edifici; 3muri®; Analisi Statica non Lineare; Macro-elementi; Curve di Fragilità; Distribuizione di Danni; Indice di Vulnerabilità.

riassunto

La presente tesi di laurea magistrale si propone di contribuire allo sviluppo dello studio sulla valutazione della vulnerabilità sismica degli aggregati di edifici in muratura di pietra. È stata fatta una ricerca e una revisione sui più recenti metodi e strumenti utilizzati per la valutazione della vulnerabilità sismica di edifici in muratura, con particolare attenzione per la ricerca sviluppata in Italia e in Portogallo. È stato presentato il modello equivalente di un caso di studio che ha coinvolto un edificio aggregato situato a San Pio delle Camere (Abruzzo, Italia) paese colpito dal terremoto de l'Aquila nell'aprile del 2009. Per la redazione del modello è stato utilizzato il software di STA DATA 3muri®, dove sono stati discussi l'influenza di alcuni parametri sulla costruzione del comportamento globale e delle corrispondenti pushover curve. Sono stati anche discussi i risultati ottenuti per le curve di fragilità e le distribuzioni di danni dovuti all' azione sismica considerata. In una seconda fase sono stati applicati e discusse metodologie semplificate basate nella valutazione dell'indice di vulnerabilità. Infine è stato fatto il confronto tra metodologie per ulteriori sviluppi della ricerca.

Contents

List of Tables

List of Figures

Nomenclature

1 General

a_g	–	Peak ground acceleration
b	–	Generic width
CM_i	–	Center of mass
CT_i	–	Center of torsion
d_{uv}	–	Ultimate diagonal shear displacement
E	–	Young (elasticity) modulus of a generica material
f_k	–	Characteristic compressive strength
f_m	–	Average compressive strength of masonry
f_{ym}	–	Average yield strength for steel
g	–	Acceleration of gravity
G	–	Shear modulus of a generica material
h	–	Generic height
h_1	–	Windows height
I_{MCS}	–	Earthquake intensity in Mercalli-Cancani-Sieberg scale
I_{EMS-98}	–	European Macroseismic Scale
M_w	–	Moment magnitude
$N70$	–	Control node 70, on storey level 3
S	–	Soil factor
s_l	–	Horizontal structure supporting length
S_S	–	Stratigraphic amplification coefficient
S_T	–	Topographical amplification coefficient
U_x	–	Longitudinal modelling direction
U_y	–	Transversal modelling direction
$v_{s,30}$	–	Average value of propagation velocity of S waves in the upper 30 m of the soil profile at shear strain of 10^{-5} or less
t_{min}	–	Minimum thickness value of the walls supporting the horizontal structure
t_{max}	–	Maximum thickness value of the walls supporting the horizontal structure
γ	–	Specific Weight of materials
γ_m	–	Partial factor for material property
τ	–	Average shear strength value

2 Capacity Spectrum Method

2.1 Performance Point Determination

$a_{g_{DLS}}$ – Peak ground acceleration assumed for the DLS limit state
A_u – Ultimate capacity of the SDoF system
D_d – Maximum displacement of the structure for DLS limit state
$d^*_{e,max}$ – Performance point of the equivalent SDoF system with unlimited elastic behaviour
d_{max} – Performance point corresponding to the control node of the MDoF system
d^*_{max} – Performance point of the equivalent SDoF system
D_{max} – Maximum spectral displacement for ULS, demanded by the Italian code, according to the elastic response spectrum formulation
$D_{max_{DLS}}$ – Demand displacement for the DLS limit state
d_n – Control node displacement of the equivalent MDoF system
d^*_n – Control node displacement of the equivalent SDoF system
D_u – Maximum displacement offered by the structure, corresponding to a 20% decay on the pushover curve peak base shear value
d^*_u – Ultimate displacement of the equivalent SDoF system
d^*_y – Yield displacement of the equivalent SDoF system
E^*_m – Actual deformation energy up to the function of the plastic mechanism
F_b – Base shear force of the MDoF system
F^*_b – Base shear force of the equivalent SDoF system
$\overline{F_i}$ – Normalised lateral force
F^*_y – Yield force of the equivalent SDoF system
k^* – Secant stiffness of the equivalent SDoF system
m^* – Mass of the equivalent SDoF system
m_i – Mass in the i–th storey
q^* – Ration between the acceleration in the structure with unlimited elastic behaviour $S_e(T^*)$ and with limited strength $\frac{F^*_y}{m^*}$
S_a – Spectral acceleration
S_d – Spectral displacement
T^* – Period of the equivalent SDoF system
α_u – Minimum safety factor
Γ – Mass participation factor
Φ_i – Normalised displacements

2.2 Elastic Response Spectrum

C_C – Coefficient related to the soil category

F_0	–	Maximum amplification factor of the horizontal acceleration spectrum on ground type A
S	–	Soil factor
S_{De}	–	Elastic displacement response spectrum
S_e	–	Spectral acceleration response
$S_e(T)$	–	Elastic acceleration response spectrum
$S_e(T^*)$	–	Elastic acceleration response spectrum at the period T^*
T	–	Vibration period of a linear SDoF system
T_B	–	Lower limit of the period of the constant spectral acceleration branch
T_c^*	–	Perid that defines the beginning of constant velocity range in the horizontal elastic acceleration spectrum
T_C	–	Upper limit of the constant spectral acceleration branch
T_D	–	Value defining the beginning of the constant displacement response range of the spectrum
η	–	Damping corrector factor
ξ	–	Viscous damping ratio (in percent)

2.3 Inelastic Response Spectrum

R_μ	–	Reduction factor in terms of ductility μ
S_{ae}	–	Elastic spectral acceleration
S_{ay}	–	Inelastic spectral acceleration
S_{de}	–	Elastic spectral displacement

3 Fragility Curves and Damage Distribution

a	–	Distribution limit of the Probability densuty function
b	–	Distribution limit of the Probability densuty function
d_s	–	General damage state
D_k	–	Structural damage limit state k
D_{k_i}	–	Damage grade i
D_u	–	Ultimate capacity of the equivalent SDoF system
D_y	–	Yielding capacity of the equivalent SDoF system
p_β	–	Simplified probability density function, assuming $a = 0$ and $b = 5$
$P\left[d_S \vert S_d\right]$	–	Conditional probability of reaching or exceeding a given damage state d_s
p_k	–	Probability of the occurrence of a damage grade D_k
$P\left[d_{s_k} \vert S_d^*\right]$	–	Damage probability histograms for different damage states d_s
Q	–	Ductility coefficient of a determined building typology, represents the ratio between the growth of damage and the seismic intensity

r	–	Probability density function dispersion control paramter
$\overline{S_{dds}}$	–	Median value of the spectral displacement at which the structure reaches the threshold of damage state d_s
S_{d_i}	–	Damage limit state i
S_d^*	–	Spectral displacement of the performance point of the structure
$S_d^{NV}{}_i$	–	Damage limit state i obtained through nominal mean values, as a function of D_y and D_u
t	–	Probability density function dispersion control parameter
V	–	Vulnerability Index for the estimation of the mean damage grade μ_D using the macroseismic methodology
β_{ds}	–	Standard deviation of the natural logarithm of spectral displacement for damage state d_s
Γ	–	*Gamma* function
Φ	–	Standard normal cumulative distribution function
μ_D	–	Mean damage grade
σ_D^2	–	Variance of the damage with a discrete probability distribution

4 Vulnerability Index Methodologies

C_{vi}	–	Class values of each parameter
I_V^*	–	General vulnerability index after applying the weight sum of the respective parameters
I_V	–	General normalised vulnerability index
I_{V_m}	–	Mean normalised vulnerability index, representing the mean of all the evaluated structural units
I_{V_a}	–	Normalised vulnerability index of the building aggregate
$I_{V_a}^*$	–	Vulnerability index of the building aggregate
$I_{V_{for}}$	–	Normalised vulnerability index of a single structural unit evaluated through Formisano *et al.* methodology
$I_{V_{vic}}$	–	Normalised vulnerability index of a single structural unit evaluated through Vicente methodology
$I_{V_{for,m}}$	–	Normalised vulnerability index representing the mean of all the evaluated structural units evaluated through Formisano *et al.* methodology
$I_{V_{vic,m}}$	–	Normalised vulnerability index representing the mean of all the evaluated structural units evaluated through Vicente methodology
p_i	–	Weight of each parameter

Acronyms

ADRS	–	Acceleration Displacement Response Spectrum
CF	–	Confidence Factor
CSM	–	Capacity Spectrum Method
DLS	–	Damage Limit State
EC8	–	Eurocode 8
FEM	–	Frame by Macro-Elements
FEMA	–	Federal Emergency Management Agency
FRP	–	Fibre-Reinforced Plastic
GNDT	–	*Grupo Nazionale per la Difesa dai Terremoti* (National Earthquake Defense Group)
INE	–	*Instituto Nacional de Estatística* (Statistics National Institute)
LNEC	–	*Laboratório Nacional de Engenharia Civil* (National Laboratory of Civil Engineering)
MDoF	–	Multi Degree of Freedom
NTC08	–	*Norme Tecniche per le Costruzioni* (Italian building code)
PDF	–	Probability Density Function
PGA	–	Peak Ground Acceleration
PIB	–	*Produto Interno Bruto* (Gross Domestic Product)
PMF	–	Probability Mass Function
RC	–	Reinforced Concrete
ReLUIS	–	*Rete dei Laboratori Universitari di Ingegneria Sismica* (Laboratories University Network of seismic engineering)
SDoF	–	Single Degree of Freedom
SLS	–	Serviceability Limit State
T_R	–	Return Period
ULS	–	Ultimate Limit State
UMI	–	*Unità Minime di Intervento* (Minimum reliable unit)
US	–	*Unità Strutturali* (Structural unit)

Part I

Introduction and Literature Review

Chapter 1

Introduction

1.1 Foreword

Earthquakes are one of the most frightening, destructive and deadliest natural disaster ever known by human kind. History has punished the Mediterranean bordering countries making them the most vulnerable seismic areas in Europe. Following the XVIII Century the most two relevant seismic events, in terms of fatalities were the 1st November 1755 Lisbon and the 28th December 1908 Messina earthquake, occurred precisely in Portugal and in Italy, respectively.

Portugal's mainland and Azores island are an important seismic area in Europe due to both tectonic and volcanic activity, respectively. The historical seismic activity of Portugal is highly significant, with the contribution of the well known 1755 Lisbon earthquake, still one of the most severe earthquakes ever recorded in Europe. Until the XX Century the seismic activity in Portugal mainland decreased, although the 1926, 1973, 1980 and 1998 major earthquakes occurred in Azores island.

The Italian territory predisposition to earthquakes is even more worrying being such events generally stronger and more frequent, a statement explained by recent events occurred in *Molise*, *Abruzzo* and *Emilia-Romagna* regions, in 2002, 2009 and 2012, respectively. It's a consensus that Italy's building and architectural heritage is unmeasurable, thence emerges the intrinsic necessity of protect efficiently the built environment to be able to face these devastating but inevitable events.

The damage caused by earthquakes depends not only on its intensity but also on the vulnerability of structures to this kind of phenomenon. In Portugal, a great part of our building stock was not submitted to specific seismic design and ancient buildings are in need of rehabilitation. Moreover, in historical centres these buildings were weakened due to economical interests, for example, with the opening of gaps on the façade walls at the ground floor level, reducing the resistant section of those walls.

The necessity of reducing the hazard due to earthquakes emerged in the 90's, with professor Frank Press, to which is associated the first notion of anti-seismic strengthening solutions for buildings [Ravara *et al.* 2001]. Since back then, scientists are challenging the after-effects of earthquakes by predicting and identifying the most vulnerable areas and establishing mandatory anti-seismic design giving a better response to earthquakes, minimizing both human and material losses.

In 2001, Portuguese National Association of Engineers came with a complete framework regarding the reduction of the seismic vulnerability of the Portuguese building

stock [Ravara *et al.* 2001] through its seismic rehabilitation, increasing their strength and rendering them capability of:

- "Ensuring the protection of people, goods, as well as the serviceability of the elements in risk for a moderate and relatively frequent earthquake (short recurrence interval)";
- "Preventing the collapse of constructions for an intensive and relatively rare earthquake (long recurrence interval)".

In 2005, LNEC advanced with the damage scenario estimation simulated for an earthquake with a similar return period as the 1755 Lisbon earthquake [Oliveira 2008]. This study brought the following expressive numbers with respect to the metropolitan area of Lisbon:

- Human losses in between 10,000–20,000;
- 267,973 damaged buildings;
- 8,394 collapsed buildings;
- unmeasurable economical losses.

To further exacerbate the situation, the Portuguese demographic distribution is massively concentrated along the sea side border which, may worsen this prediction. As it is easy to imagine, the consequences would be even more catastrophic if this earthquake occurred during the summer season.

Recently, the European Facility for Earthquake Hazard and Risk published the European Seismic Hazard Map in which the region of Lisbon and Tagus Valley were assigned with a probability equal or larger than 10% of in the next 50 years being attained by a peak ground acceleration superior than 0.3 g, considered equivalent to earthquakes with moderate intensity and potential damage.

Nevertheless, Portuguese scientists, civil protection and other responsible authorities for the national security must give their best to reduce the repercussions of an already advertised devastating earthquake.

1.2 Motivation

Regardless its size, when compared to other European countries, Portugal has a vast architectural heritage to preserve. Over the last decade, the construction sector contribution to PIB (Gross Domestic Product) decreased when compared to the mean of 15 European countries [Almeida 2009] and many factors has been appointed to this decrease. The ageing population and the low birth index, associated to the financial-economic crisis installed in Portugal, explains the balance of 1 million inhabited dwellings in our country. As urban development strategies are a relative recent matter in the priorities of Portugal's construction sector, we've been erecting buildings for decade, squeezing every square meter of our cities without concerning about the immediate needs. Therefore, historical centres have been progressively suffering several transformations. In Lisbon, particularly buildings from the down-town area *Baixa Pombalina* (known for Pombaline "cage" type buildings), are known to have been profoundly modified at ground floor levels,

compromising the structural resistant sections and the global safety. Another illustrative example is the abusive increasing of number of floors and attics, without anti-seismic concerns.

Nowadays, in historical centres, it is very difficult to analyse a building as an independent structure when, for example, it shares the same boundary walls. It is in this context that the necessity of studying this new "class" of building aggregates appeared. Moreover, our historical centres, once overpopulated, are nowadays in need of structural rehabilitation to bring them back to life again. The majority of these old buildings are known to have been designed without seismic concerns [Ravara *et al.* 2001]. Thus, in recent years we've been focusing our attention in historical city centres, where the most vulnerable buildings are concentrated.

Despite this negative trend, the effort made to improve the preservation state of our building stock during the last decade led to some novelties, according to INE (Census 2011), with 71.1% of this building stock with no need of structural rehabilitation and a reduction to 1.7% in the percentage of buildings in severe preservation state [INE and LNEC 2013]. Although this general improvement on structural preservation conditions of buildings, these numbers don't account for the seismic safety of the building stock. This way, structural interventions should consider the seismic vulnerability of these buildings in order to improve their response when subjected to earthquakes.

1.3 Objectives

The present dissertation aspires to contribute for the development of the seismic vulnerability assessment of a distinct class of buildings that prevails in our historical centres, the building aggregates. An important feature linked to the study of the seismic vulnerability of historical centres is the evolution of the urban layout and the chronological construction process, in which buildings share the mid-walls with adjacent buildings and façade walls are aligned. In this way, buildings don't have an independent structural behaviour, but they interact amongst themselves mainly due to horizontal actions and so the structural performance should be studied at the level of the building aggregate, where such interactions cannot be ignored.

The main objective of this dissertation is to become aware of the several different methodologies used to the assess the seismic vulnerability in existing buildings, in particular the ones involving less computational efforts. This work aims to improve the knowledge about the behaviour of buildings within aggregates. Moreover, further calibration of hybrid methods is intended to be developed in order to improve the reliability of such approaches, which are known to be very helpful as they quickly assess the seismic vulnerability of a great amount of buildings. Moreover, this work aims to be considered as the first approach on building structural issues assessment, identifying priorities to further rehabilitation projects.

The framework preceding the present document has the goal of summarizing the most important developments regarding this thematic, recently undertaken in Europe, with particular focus to the Italian and Portuguese research.

Within the previous objectives, several tasks were intended to be developed in this dissertation, such as:

- Structural characterisation of a stone masonry buildings aggregate case study in

Italy;

- Numerical modelling through both non-linear static analysis and macro-elements based software, to globally assess the building aggregate;
- Perform fragility curves and estimate damage distribution by means of the Capacity Spectrum Method;
- Compare damage distribution with identified mechanisms and failures in the model, for further calibration;
- The usage of vulnerability index based methods to assess the seismic vulnerability of building aggregates.

1.4 Dissertation Outline

Part I is divided in two chapters, in which Chapter 1 presents a general overview of the dissertation, starting with an introduction to seismic engineering and the Portuguese building stock guesswork, followed by the dissertation motivation and the main established goals to attain. Finally in the current section the document outline is presented, where the author summarizes the contents of each chapter, useful for the reader's understanding of the organization of this document. Chapter 2 gathers the background of the building aggregates context and a reviewed of the most widespread literature regarding the seismic vulnerability evaluation of masonry building aggregates. Part II opens with Chapter 3 where it is presented the referred case study of a stone masonry building aggregate located in *San Pio delle Camere*, which was subsequently modelled through non-linear static analysis of macro-elements, adopting the 3muri® software. It was firstly introduced the historic and urban context of the village due to its importance to acquire the geographic characteristics of the village and earthquakes background knowledge throughout its history. Further on, the author will resume the urban development of *San Pio delle Camere* and describe the main features associated with existing stone masonry buildings typology, which prevails in this village. Then, a general review about the well-known *L'Aquila* earthquake will be made, with a description of the main conclusions of the micro mapping report of *San Pio delle Camere*, provided by the studies developed by the University of *Pisa*. Chapter 4 portrays all the features related to the Capacity Spectrum Method used to estimate the performance point of the structure. Moreover, it was described the most important features regarding the numerical modelling through 3muri® software, used to perform the non-linear static analysis of the structure. General considerations and assumptions regarding both the structure and seismic parameters were also presented in this chapter. In Chapter 5 it is described the elected hybrid and indirect techniques applied to assess the seismic vulnerability of building aggregate case study. While the hybrid technique took the advantage of the performance point to construct fragility curves and damage distribution, the indirect one evaluates the damage distribution through the estimation of the vulnerability index, either for individual buildings and buildings in aggregate. Part III covers the discussion and conclusions of the obtained results for building aggregate global seismic performance assessment, in terms of capacity, fragility and damage probabilistic distribution. At the end of Chapter 6 a final comparison is made between the hybrid and indirect techniques.

Chapter 7 indicates the most significant general comments and main conclusions drawn from the work developed. Finally there are pointed the future developments on the seismic vulnerability assessment of buildings in aggregates, which may be considered to improve the accuracy of the current comparison of results.

Chapter 2

Seismic Evaluation of Building Aggregates

2.1 Building Aggregates Context

Earthquakes may bring many hazards, from amplified ground shaking, landslides, liquefaction, surface fault rupture and tsunamis. There are a few changeable causes associated to city centres seismic risk, local hazard and vulnerability of buildings. The seismic vulnerability of a generic structure is the inherent predisposition of suffering damage due to seismic events, in which the damage is directly linked to the geometrical and structural design [Barbat 2003]. Thus, it is important to be conscious of the differences between the construction of new buildings and the existing ones since, on the one hand projects for new buildings must respect either National or European norms and seismic-codes, on the other hand regulations for the vulnerability assessment of existing buildings as well as the expectable damage grades are quite recent, which allied to the complexity of this matter, requires further specific investigation to prevent both human and economical losses.

Masonry buildings remain as one of the most common building typology and one of the most vulnerable too [Lagomarsino and Magenes 2009]. In Europe, over the last few years seismic codes and researchers are trying to establish an oriented trend to reach a simplified mechanical approach for the seismic vulnerability assessment of masonry buildings, using procedures based on non-linear static analyses and on the Capacity Spectrum Method (CSM) [Freeman 1998]. This method considers the non-linear behaviour of structures by means of their capacity curve, obtained reducing the pushover curve through the definition of an equivalent single degree-of-freedom (SDoF) system [Shibata and Sozen 1976]. In other words, the CSM uses the capacity and demand spectrum to obtain the performance point of the structure which corresponds to its maximum spectral displacement, and uses fragility curves to obtain the damage probability for the expected seismic input action [Barbat *et al.* 2008]. Recently, Galasco argued that the seismic demand was possible to estimate with reasonably accuracy, in terms of spectral displacement (performance point), intersecting the Capacity Spectrum with the earthquake response spectrum, plotted in (Acceleration-displacement response spectrum) ADRS and properly reduced taking into account the effects of energy dissipation related to the structural non-linear response [Galasco *et al.* 2006]. Accordingly, this method aims to predict the maximum horizontal displacement resulting from the envelope curve of a dynamic

analysis.

Is unanimous among researchers that the most common collapse mechanisms associated to the in-plane behaviour of recent (brick) masonry buildings are the tensile failure at the heal, the flexural failure at the toe and the shear failure, labelled as regions A, B and C, respectively, illustrated in figure 2.1, adapted from Lang [Lang 2002].

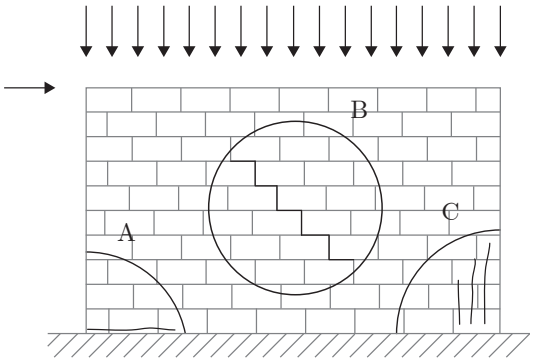

Figure 2.1: Different types of in-plane failure suitable to occur in masonry bearing walls. Adapted from [Lang 2002].

Technically a building aggregate is called a group of a non-homogeneous ensemble of two or more buildings arranged along the years and strictly linked to a historical planning system [Caniggia and Maffei 1979]. This arrangement means both alignments and structural connections. In other words, a building aggregate can be considered as a group of structural units, not necessarily homogeneous, interacting with each other by the mentioned structural connections. Generally, in historical centres, building aggregates match with the urban block [Ortolani *et al.* 2012]. The buildings constituting the aggregate, which have been submitted through generation processes, interact between themselves under a seismic or a general dynamic action giving the aggregate different characteristics from the individual element components. Over the years, this transformation process of the historical centres raised the need for a specific structural analysis to this particular structures. The aggregate response to a seismic action is strictly associated to distinct factors as the "confinement level", the quality of the connections between adjacent buildings and obviously factors regarding the properties of each structure, where the span between walls, the connection between floors and walls, the roof structure and both in-height and in-plan irregularities are considered crucial [Vicente 2008].

As mentioned before, on the one hand, the urban scale gathers a huge amount of data to manage, detailed and specific constructive characteristics of buildings and also information related to the spreading process of the aggregate over time, which logistics may result too impracticable. Nevertheless, this choice still depends on the objective and accuracy required for each situation. On the other hand, a scale at the individual building level could be considered inadequate, as it doesn't take into account those interactions between adjacent buildings reflecting an imprecise behaviour of buildings when subject to a seismic action. Hence, the need to adopt another scale, suitable for building aggregates emerges.

In order to make possible the seismic vulnerability assessment of buildings it is fun-

damental to have the knowledge over the structure under study. The level of knowledge clearly influences the engineer's way of facing each practical situation on seismic vulnerability assessment. Thus, different methodologies can be chosen according to the quantity and quality of the building survey. To achieve a thorough knowledge of the building aggregate, an approach on the following features is absolutely crucial [Carocci *et al.* 2010]:

- The formation and evolution in time of the aggregate itself;
- The morphological characteristics of the site and the environmental context in which the aggregate is located;
- The typologies of buildings and their variation during the evolution process;
- The analysis of the constructive technique and its workmanlike application.

The aggregate identification is meant to weigh both urban and environmental context. The geometrical survey is fundamental to perceive spatially the surrounding environment. Subsequently, comprehensive structural inspection should be done for each structural element of the aggregate (e.g. walls, floors and roofing systems). Finally, the detailed examination is considered complete after the damage assessment, which involves the individualisation of the collapse mechanisms, frequently associated in masonry buildings to the 1st and 2nd modes of collapse, both corresponding to in-plan behaviour of the buildings.

2.2 Literature Review

The seismic vulnerability is an inherent property of buildings reflecting the predisposition to suffer damages due to a determined seismic action which is associated with the physical and structural characteristics of such buildings [Barbat 2003]. This subject has been developed in various directions along the years hindering the possibilities of achieving a consensual classification involving all type of procedures. Although recent projects regarding risk mitigation for earthquakes and landslides [Pellegrini 2007] gathering several scientists and research groups all around Europe have concluded that these methodologies can be divided into three main groups, in this dissertation the author will use the classification proposal developed by Corsanego and Petrini, which divides the seismic vulnerability assessment techniques into four main groups, as a function of their results: direct, indirect, conventional and hybrid techniques [Corsanego and Petrini 1990].

Direct techniques estimate "directly" the damage caused in a structure by a seismic action and includes both typological and mechanistic methods. The first sub-group assigns a typological class to each structure, accounting inherent factors which influence the seismic response. The assessment of the damage probability of determined building class is made possible through post-event damage observation data. Starting from this information, damage probability matrices are developed for specific regions, representing a conditional probability for achieving a determined damage level, for different seismic intensities. Mechanistic methods can use both analytical or mathematical methodologies, representing the structure through simple or detailed models.

Indirect techniques often estimate the vulnerability index, establishing relations between the mean damage grade and the seismic intensity or another property capable to

describe the seismic action, as the peak ground acceleration (PGA) for example, being afterwards used to define vulnerability curves. One of the most well-known methodologies belonging to this class was developed by the GNDT-SSN, which brought an evaluation method appropriated for the assessment of a large number of buildings, based on observational and collected data from post-event damages in Italian historical centres building stocks [GNDT-SSN 1994]. Each building is classified with a specific vulnerability index value which can be directly related to expectable damage grade through vulnerability functions.

Conventional techniques use the vulnerability index or another parameter, characterising the vulnerability independently from the damage estimation. Such methods are used to compare different buildings within the same typology and geographical region, in which the seismic response and structure's performances are calibrated by experts [Vicente 2008]. Based on spectral displacements and acceleration, the HAZUS methodology classifies the damage in thirty-six different structural systems, defined by four levels of seismic-resistance quality design and describing four damage states [Reitherman 1999]. Capacity curves and spectral displacements related to each damage state are defined for each structural system and quality design requirement.

Finally, hybrid techniques combine distinct concepts and procedures from the previously mentioned methodologies. For instance, the macroseismic methodology, developed by Giovinazzi and Lagomarsino explores the potentialities of both typological and indirect techniques, using the same vulnerability methodology and classification proposed in the European Macroseismic Scale (EMS) by Grünthal [Grünthal 1998], improving the accuracy in the assessment of the vulnerability through an indirect methodology, allowing further damage estimations [Giovinazzi and Lagomarsino 2004].

During the past thirty years several methodologies have been developed in order to evaluate the seismic vulnerability both for individual and aggregate buildings [Calvi *et al.* 2006]. The extensive research developed by these authors led to the discussion of the advantages and disadvantages of various current procedures in order to find out a guideline for a hypothetical optimal methodology. In the following paragraphs the author will explain how this classification is organised.

Recent European research projects funded by the European Commission dealing with seismic risk and loss estimation [Mouroux and Le Brun 2006] [Erdik 2007] are consensual in dividing these methodologies in three main groups, accordingly to the scale intended to embrace in each project. Chever has recently summarised the most used methodologies for the seismic vulnerability assessment, arranging them by the analysis scale, as shown in the table 2.1 [Chever 2012].

Starting from 2004, a macroseismic method regarding the issues concerning historical centres and the role of building aggregates behaviour when submitted to a seismic event was introduced by Giovinazzi and Lagomarsino. Two parameters were added to the original observational method, one to evaluate the aggregate behaviour factor (the interaction between adjacent buildings with different heights and in-plan positions within the aggregate) and another to evaluate both historical centre traditional constructive typologies and the successive modifications that the aggregate suffered since early years. Also the existence of seismic constructive elements and their effects due to structural heterogeneity parameters were added beyond the performance modifiers for buildings considered as isolated [Giovinazzi and Lagomarsino 2004]. Applied in *Liguria* (Italy) historical centre, this method is based on a probabilistic interpretation of the content presented in EMS-98

Table 2.1: Damage assessment methodologies according to their analysis scale and objective [Chever 2012]. Methodologies assigned with star are those used out of their initial objective.

Analysis scale	Thousands of buildings	Few hundred to few dozens	Individual building
Objective	Large-scale vulnerability, earthquake scenario	Screening prioritising into a building stock	Rough first estimation of individual vulnerability
Methods	ATC 13 EMS98 DBELA GNDT level I GNDT level II HAZUS vulnerability model Risk-UE LM1 Risk-UE LM2 Vulneralp	AFPS (2001) ATC21 FaMIVE FEMA154 GNDT level II* IEB New Zealand JBDPA Japan NRC-CNRC OFEG level I Risk-UE LM1*	JBDPA Japan FaMIVE FEMA310 VC/VM procedure Italy VULNUS*

macroseismic scale. In order to test the method effectiveness the authors have compared it to other methodologies with the same purpose. Firstly, it was faced to a static limit method [D'Ayala and Speranza 2003] and secondly with a derivation of the level II of GNDT-SSN method [GNDT-SSN 1994] for historical centres analyses [Cella *et al.* 1994].

In the same year another methodology was developed in Italy [Valluzzi *et al.* 2004] taking into account the limitations of the analysis of existing masonry buildings in seismic areas concerning about the application of single or combined kinematics models involving the equilibrium of structural macro-elements [Bernardini *et al.* 1988] [Bernardini *et al.* 1990]. These different procedures were applied for the seismic analysis of both isolated and more complex masonry buildings. According to the authors, macro-elements were defined by single and combined structural components, considering their mutual bond and restraints, constructive deficiencies and the characteristics of constitutive materials. Both global and local level analysis were performed through VULNUS® procedure [Modena *et al.* 2009], being the last one also carried out through applying single kinematic mechanisms. The global analyses with VULNUS® showed that the lowest collapse coefficients were associated to the out-of-plane mechanisms. In order to avoid such simplifications authors alerted to the need of particular attention during both phases (method application and interpretation of results), specially when dealing with complex aggregates or irregular constructions.

In Portugal, Neves has developed a study regarding the structural seismic behaviour of a building aggregate localised in Horta, in Faial island, through numerical modelling using the CAST3M® FEM software. Among other conclusions this study has proved the influence of individual buildings over the building aggregate global behaviour, where higher vulnerability values were obtained for corner buildings and in the presence of in-height and in-plan irregularities.

Another research applied to building aggregates using the VULNUS® procedure was developed by Munari and Valluzzi, based on a limit state model for the assessment of the acceleration which activates the local collapse mechanisms of macro-elements (1 st and 2 nd modes of vibration) feasible to occur in historical masonry buildings [Munari and Valluzzi 2009]. The results obtained for the aggregate have shown conformity with the expected ones, as the building's façade of the masonry building aggregate is more vulnerable to out-of-plane than to in-plan mechanisms.

In 2008, Vicente brought an extensive research in the field of renewal and urban rehabilitation in Portugal [Vicente 2008]. The author has also developed a simplified mechanical model through non-linear static analysis to evaluate the vulnerability both for isolated and in aggregates masonry buildings, discussing aspects as the uncertainty of the structure capacity definition and its structural performance. These results were confronted to a vulnerability index based methodology, classified as an empirical approach. Further on, two numerical models were developed with the purpose of analysing different retrofitting and repair strategies and to confront the results obtained with both mechanical models. The first model was developed using Robot Millennium® software, described as a spectrum analysis of finite elements which considers the linear-elastic behaviour of materials [Millennium 2004]. The second model was carried out through 3muri® software, which performs non-linear static (pushover) analysis through macro-elements [STADATA 2007].

Two years later, Indelicato shown an interesting and complete theoretical review about the necessities of seismic vulnerability assessment to prevent unexpected damages and adequate reinforcement interventions to the damaged historical centres victimised by recent earthquakes in Italy [Indelicato 2010].

This Italian inter-university consortium in seismic engineering (ReLUIS) have been hardly researching in this matter over the last years and the result of their investigation was an exhaustive guideline with the knowledge, evaluation and design of intervention actions due to seismic post-events in masonry building aggregates rehabilitation [Carocci *et al.* 2010]. Moreover, this helpful guide advises for good practises in many branches regarding this particular type of structures such as materials and structure diagnostics, buildings behaviour interpretation, expectable failure modes and security evaluation. Lagomarsino and Magenes have synthesized the developments and outcomes of the *Linea 1* of the ReLUIS 2005-2008 Framework Project developed in Italy regarding the evaluation and reduction of the seismic vulnerability of existing masonry buildings [Lagomarsino and Magenes 2009]. According to the authors this study was focused in four particular objectives:

- Assessment and strengthening of structural units within building aggregates;
- Methods for the assessment of mixed masonry-reinforced concrete structures;
- Strategies and techniques of strengthening for masonry buildings, considering both horizontal and vertical structural elements;
- Methodologies for modelling the seismic response of masonry structural systems.

Nevertheless, the authors involved have recognized that more research is needed also on the interaction between adjacent building units in complex aggregates, in order to

unravel how to analyse a single building without discarding interactions and its position within the aggregate.

The constant effort made by the Italian research community in recent years have contributed to the development of the problematic of masonry buildings seismic evaluation, leading to its introduction into the Italian Seismic Code, published after revision as *OPCM 3431/05* [OPCM 2005] containing the new guidelines for the seismic safety assessment of existing masonry buildings. Another novelty related to building aggregates aroused with the Italian Seismic Code publication, in which it is suggested that the knowledge level of the structural behaviour of an aggregate should be ruled by the formation and historical evolution of the aggregate, the morphological site characteristics and the local environmental context, the differences between buildings typologies and the analysis of the constructive quality [Carocci *et al.* 2010].

An alternative simplified method based on cell subdivision of the aggregate was developed by Amadio *et al.*, which procedure comprehends the calculation of the stiffness for each cell considering in-plan and in-height irregularities [Amadio *et al.* 2011]. In this method two distinct analyses were made, one considering the torsional and translational stiffness of every component units, and the other in which the single component unit was consider separately. Some hypotheses were implemented in order to achieve reasonable results such as:

- Floors are considered rigid in their plan and over cross Structural Units (US);
- Materials are ruled by linear-elastic constitutive law;
- Centre of mass (CM_i) of each US match with the shear centre (CT_i);
- Each US has their own stiffness and mass per unit area, equally distributed inside the cell.

Continuing in the year of 2011 a four-building row aggregate of the old city centre of *Coimbra*, in Portugal, was modelled by Vicente *et al*, once again with the finite-element tool Robot Millennium®, in order to understand the dynamic behaviour of these old constructions. This numerical analysis intended to estimate the natural frequencies and vibration modes for the original structure and for different strengthening solutions. Furthermore, this analysis was used to understand the seismic behaviour and assess the seismic safety of the structure through global results both for horizontal displacements, drifts, and stresses [Vicente *et al.* 2011]. To assess the seismic behaviour of the building aggregate, a spectral analysis was performed considering the seismic action through a response spectrum, acting along the two independent horizontal directions, according to EC8 [CEN 2004] and also with the ground type and seismic zones defined as suggested in the national annex [Pinto 2007]. Retrofitting solutions were designed such as tie rods, applied at the floor and roof ridge levels, joists stiffeners and masonry walls consolidation. *In situ* dynamic identification tests were carried out with seismograph GSR-16 [Biro, T. 2009] to obtain the natural frequencies leading to numerical model calibration [Júlio *et al.* 2008]. The main conclusions from this research were:

- The higher number and dimensions of openings at ground floor greatly influence the deformation of wall façades and stress concentration for earthquakes acting in the longitudinal direction;

- Inter-story drifts are rather high at ground level, which can originate a soft-story mechanism;
- Enlargement of openings or suppression of masonry walls at ground floor is an inadequate practise in old buildings that should not be overlooked;
- The asymmetry of total area of openings between the front and posterior façades induces a global torsion of the buildings modelled, despite the global behaviour of the aggregate, which attenuates this effect;
- The linear elastic material assumption is a good first iteration to understand the global structural seismic behaviour;
- Non-linear dynamic analyses are necessary to understand cracking patterns that lead to energy dissipation, and also to improve the knowledge over the effectiveness of the retrofitting strategies proposed.

Pagnini [Pagnini *et al.* 2011] led another research using the old city centre of *Coimbra* as a case study, this time using a mechanical model for the vulnerability assessment of old masonry building aggregates, taking into account the uncertainties inherent to building parameters, seismic demand and modelling errors. According to the authors and starting from a non-linear mechanical model developed by Cattari *et al.* [Cattari *et al.* 2004] it was derived an analytical description of the capacity curve and damage threshold for row building aggregates which releases a certain number of geometrical, mechanical and constructive parameters. Moreover, the two well-known structural collapse mechanisms for this type of buildings (uniform and soft-storey mechanisms) were considered.

An alternative research [Formisano *et al.* 2011b] was developed in the University of Naples *Federico II* approaching an empirical procedure for the seismic vulnerability assessment of masonry building aggregates, based on several finite-element analyses performed through 3muri® software. This methodology derives from the well-known vulnerability form for masonry buildings integrated by five parameters accounting for the aggregate conditions among adjacent units. Starting from Benedetti and Petrini methodology [Benedetti and Petrini 1984] used in the past as a quick technique based on observational collecting data of each single structural unit of the aggregate, a new procedure was developed, considering the structural interaction among adjacent buildings, by adding five new additional parameters to the basic ten of the original form. These five parameters, derived from previous studies [Cattari *et al.* 2004], were:

- In-height interaction;
- In-plan interaction;
- Number of staggered floors;
- Structural or typological heterogeneity among adjacent structural buildings;
- Difference of opening areas percentage among adjacent façades.

Scores and weights were assigned in order to achieve a totally homogeneous form by means of numerical calibration. The final form is composed by fifteen parameters, in which both positive and negative scores were assigned, differently from the original form,

regarding a few beneficial effects of the aggregate condition on the seismic behaviour of a masonry building within a block. According to the authors, even though the results seemed to be reasonable further validation is needed implementing this procedure to alternative building aggregates case study located in important seismic areas.

The latest World Conference on Earthquake Engineering brought together several reputed researchers that have demonstrated to be very concerned about the seismic vulnerability assessment of building aggregates and historical centres, evidenced by the quantity of proceedings presented regarding this particular subject. Hence, in the next paragraphs, it will be made a brief reference to the most relevant research submitted in this conference.

Starting from a deterministic model developed by Monti and Vailati [Monti and Vailati 2009], a fully probabilistic procedure was developed to assess masonry building aggregates through non-linear analysis [Vailati *et al.* 2012]. The deterministic procedure is summarised, according to the authors, as follows:

- Definition of a constitutive bilinear law for each masonry wall in terms of three parameters (yield strength, yield and ultimate displacements);
- Derivation of a constitutive law for each floor, by summing each wall contribution, when rigid floor condition is assumed;
- Derivation of an equivalent bilinear constitutive law for each floor;
- Computation of the dynamic response by means of a simplified modal analysis;
- Computation of the inter-story drift;
- Comparison between capacity and demand for each inter-story (if the ratio of the two is larger than one for all inter-stories, the ULS is verified, otherwise it is not).

Once defined the uncertainty nature of each variable, the corresponding distribution model was assigned. Performed by means of Monte Carlo simulation, the results from the analysis have shown that the ultimate diagonal shear displacement d_{uv}, the compressive strength of masonry f_m, and the Young's modulus E, to estimate the damage effects, are the most influential parameters affecting the structural response of the masonry building aggregate.

Some researches have being developed with respect to confined masonry buildings. A case study located in *Reggio Calabria*, Italy, was assessed by Nucera *et al*, by means of a new macro-element based model analysis [Nucera *et al.* 2012]. In these seismic resisting structures, openings are confined by reinforced concrete frames, while wall intersections and floors slab-wall connections are achieved by means of reinforced concrete elements, which increases the global ductility of the structure. The seismic vulnerability of the structure was assessed according to the Italian Seismic Code NTC08 by using 3DMacro® structural analysis software [Gruppo Sismica srl 2009]. This new macro-element allows the study of the following collapse mechanisms:

- Rocking (flexural bending failure);
- Shear failure by diagonal cracking;
- Shear failure due to sliding.

As detailed finite element approaches requires large computational time during both modelling and in the results interpretation phase, a simplified analytical approach [Caliò *et al.* 2012] was applied to evaluate the seismic resistance of confined masonry structures. It was found that the influence of the confinement was verified by means of the deformed shapes of the structure and force diagrams at the collapse. Moreover, the shear strength on the global response of the structure has shown a strong influence in confined masonry buildings.

L'Aquila recent earthquake of April 2009 has been the support for the development of many seismic vulnerability researches in this area ever since. Ortolani, with the case study of *Castelnuovo* has shown the seismic response of masonry building aggregates regarding the qualitative classification of out-of-plane mechanisms. From the work carried out, the damaged level verified in *Castelnuovo* village was mainly related to the intrinsic vulnerability of the surveyed buildings (stone masonry type and poor mortar) and their severe conservation status [Ortolani *et al.* 2012].

In Portugal, a macroseismic approach for the vulnerability assessment of building aggregates was developed in the University of Aveiro by Vicente *et al.* [Ferreira *et al.* 2012], using a similar empirical methodology as previously mentioned in the work developed either by Vicente [Vicente 2008], Ferreira [Ferreira *et al.* 2010] or Formisano [Formisano *et al.* 2011a]. The seismic vulnerability of building aggregates was considered by the weighted mean value of five parameters, developed specifically to the assessment of building aggregates. In a first phase, buildings were assessed individually through a methodology suggested by Vicente [Vicente *et al.* 2011] and in a second one, the previous results were confronted by applying this new methodology to the aggregate scale. It was found that for the same particular conditions, individual assessment overestimates the global vulnerability of the building aggregate. Nonetheless, end buildings are very vulnerable due to their position and normally suffer damage by rotation and sliding phenomenon induced by inertial forces of the whole aggregate in one direction, which in this case building aggregate vulnerability is underestimated. Nevertheless, the results achieved with this procedure, comprehending only five parameters, are satisfactory when compared to more detailed and singular building assessment in terms of an overall value. Notwithstanding, further validation is need by means of masonry building damage post-seismic observation. In the future, this methodology should be compared to simplified mechanical methods, assessing the building on the two principal directions, leading to improvement or incorporation of new parameters.

Finally, Ulrich [Ulrich *et al.* 2012] has developed a simplified methodology based on the discretisation of walls into macro-elements through non-linear behaviour (rocking and shear cracking) of each masonry panel using plastic hinges. The simplified non-linear modified beam-column macro-element is coded into the open source finite-element software OpenSees® and it was developed for modelling the piers and spandrel beams of masonry façades. Globally, with the geometric configuration and mechanical properties considered, the weakest elements observed were the spandrel beams, which always fail due to shear mechanism. As a consequence of dynamic loads on the single building, spandrel beams were heavily damaged and piers of the ground floor underwent important rocking failure. The investigation around these topics found that in-height discontinuities between adjacent buildings affect the top floors of the higher structural unit, as its façade is not strengthened by the presence of adjacent buildings, increasing both deformation and damage. Moreover, the presence of a stronger unit within the aggregate influences

the damages occurred in the weakest ones. When walls between two adjacent buildings are not connected pounding effects are predictably expected which could damage these and nearby structural elements. Nevertheless, the macro-element needs to be improved in order to get higher reliability, considering out-of-plane failure mechanisms and improving the calibration accuracy by comparison to discrete element method models.

In order to perceive the scientific evolution regarding the seismic vulnerability of existing buildings and to construe an overall perspective among the reviewed literature, a chronological view is shown in table 2.2, in which it was included also the literature considered fundamental to the development of this dissertation.

Table 2.2: Literature review regarding the thematic of seismic vulnerability assessment of buildings, with particular attention to the assessment of old stone masonry buildings. The literature considered essential to this dissertation is assigned with star *.

Year	Authors	Research Topic
1977	[Murphy and O'Brien 1977]	Peak ground acceleration amplitude with seismic intensity and other physical parameters.
1979	[Caniggia and Maffei 1979]	Architectural and structural building typology.
1984	[Benedetti and Petrini 1984]	Hybrid method Vulnerability index methodology*.
1988	[Bernardini *et al.* 1988]	Kinematic models. Out-of-plan mechanisms.
1989	[Guarenti and Petrini 1989]	I–PGA correlation law for ancient buildings.
1990	[Bernardini *et al.* 1990]	Analytical models application.
	[Corsanego and Petrini 1990]	Seismic vulnerability of buildings.
1992	[Margottini *et al.* 1992]	Intensity versus ground motion: a new approach using Italian data.
1994	[GNDT-SSN 1994]	Composed damage index*.
	[Vidic *et al.* 1994]	Consistent inelastic design spectra: strength and displacement.
1997	[Gambarrota and Lagomarsino 1997]	Damage models for the seismic response of brick masonry shear walls: part II.
	[Magenes and Calvi 1997]	In-plan seismic response of brick masonry walls.
	[Riuscetti *et al.* 1997]	Seismic vulnerability assessment of masonry buildings in a region of moderate seismicity.

Year	Authors	Research Topic
1998	[Freeman 1998]	Development and use of capacity spectrum method*.
	[Grünthal 1998]	European macroseismic scale*.
1999	[Fajfar 1999]	Capacity spectrum method based on inelastic demand spectra*.
	[Reitherman 1999]	HAZUS earthquake loss estimation methodology*.
2000	[Fajfar 2000]	A non-linear analysis method for performance based seismic design (N2 Method).
2001	[Augusti *et al.* 2001]	Seismic vulnerability of monumental buildings.
	[Carocci 2001]	Historical constructions: guidelines for the safety and preservation of historical centres in seismic areas.
	[Ravara *et al.* 2001]	Reducing the seismic vulnerability of the building stock.
2002	[D'Ayala and Speranza 2002]	Integrated procedure for the assessment of seismic vulnerability of historic buildings based on a failure analysis of structures and identification of feasible collapse mechanisms.
	[Lang 2002]	Seismic vulnerability of existing buildings.
	[Marchetti 2002]	Vulnerability of historic centres and cultural heritage.
2003	[Corradi *et al.* 2003]	Experimental study on the determination of strength of masonry walls.
	[D'Ayala and Speranza 2003]	Definition of collapse mechanisms and seismic vulnerability of masonry historical buildings.
	[Dolce *et al.* 2003]	Earthquake damage scenarios of the building stock of *Potenza* including site effects.
	[FEMA 2003]	HAZUS methodology*.

Year	Authors	Research Topic
	[Spence *et al.* 2003]	Comparison loss estimation with observed damage: a study of the 1999 *Kocaceli* earthquake in Turkey.
2004	[Alexandris *et al.* 2004]	Collapse mechanisms of masonry buildings derived by the distinct element method.
	[Borri and Cangi 2004]	Vulnerability and anti-seismic interventions in *alta val tiberina*, *Umbria* Region.
	[Calderini 2004]	Constitutive model for complex masonry structures.
	[Cattari *et al.* 2004]	Mechanical model and damage scenario.
	[CEN 2004]	Design of structures for earthquake resistance*.
	[D'Ayala and Speranza 2004]	Fragility curves and damage scenarios formulation and calibration in *Nocera Umbra* (*PG*).
	[Galasco *et al.* 2004]	Non-linear seismic analysis of masonry structures.
	[Giovinazzi *et al.* 2004]	A vulnerability model for buildings in historical centres.
	[Giovinazzi and Lagomarsino 2004]	A macroseismic method for vulnerability assessment of buildings.
	[Mendes and Lourenço 2004]	Seismic vulnerability reduction of old masonry buildings.
	[Neves 2004]	Seismic behaviour analysis of an urban block localised in Horta - Faial island.
	[Oliveira *et al.* 2004]	Planning in seismic risk areas: the case of Faro, Algarve.
	[Ramos and Lourenço 2004]	Modelling and vulnerability of historical city centres in seismic areas: the case of Lisbon.
	[Valluzzi *et al.* 2004]	Seismic vulnerability methods for masonry buildings in historical centres: Validation and application for prediction analyses and intervention proposals.

Year	Authors	Research Topic
	[Restrepo-Velez and Magenes 2004]	Simplified procedure for the seismic risk assessment of unreinforced masonry buildings: MeBaSe procedure, kinematic model.
2005	[Giovinazzi 2005]	The vulnerability assessment and damage scenario in seismic risk analysis.
	[Vasconcelos 2005]	Experimental investigations on the mechanics of stone masonry.
2006	[Borri *et al.* 2006]	Building stock seismic vulnerability: the case of *Gubbio*.
	[Calvi *et al.* 2006]	Reflection over the past 30 years.
	[Dolce *et al.* 2006]	Vulnerability assessment and earthquake damage scenarios of the building stock of Potenza using Italian and Greek methodologies.
	[Galasco *et al.* 2006]	On the use of pushover analysis for existing masonry buildings*.
	[Giovinazzi *et al.* 2006]	Vulnerability methods and damage scenario for seismic risk analysis as support to retrofit strategies: an European perspective.
	[Lagomarsino and Giovinazzi 2006]	Mechanical models for the vulnerability assessment of current buildings.
	[Valluzzi *et al.* 2006]	Seismic vulnerability assessment of Pombaline cage buildings with a macro-element approach.
2007	[Bernardini *et al.* 2007b]	Vulnerability and damage prediction using a macroseismic methodology coherent with the EMS–98 scale*.
	[Bernardini *et al.* 2007a]	DPM through EMS–98 scale.
	[Calvi 2007]	Guidelines for seismic vulnerability reduction in the urban environment.
	[Carvalho 2007]	Seismic risk in Portugal.
	[Erdik 2007]	Earthquake disaster scenario prediction and loss modelling for urban areas.

Year	Authors	Research Topic
	[Pellegrini 2007]	European manual for *in situ* assessment of important existing structures.
	[Gallonelli 2007]	Dynamic response of masonry buildings with rigid or flexible floors.
	[Rush 2007]	Seismic evaluation of masonry building conglomerations of adjacent structures.
2008	[Barbat *et al.* 2008]	Vulnerability assessment of dwelling buildings.
	[Candeias 2008]	Seismic vulnerability assessment of masonry buildings.
	[Costa 2008]	Seismic vulnerability assessment of the building stock of Doctor Lourenço Peixinho avenue in Aveiro.
	[Crowley *et al.* 2008]	Comparison between DBELA and SP-BELA mechanical methods.
	[DM 2008]	Italian seismic code*.
	[Fusco *et al.* 2008]	Seismic assessment of historical natural stone masonry buildings through non-linear analysis.
	[Vicente 2008]	Strategies and methodologies for urban interventions and rehabilitation: vulnerability and seismic risk*.
2009	[Almeida 2009]	Retrofit interventions for stone masonry buildings.
	[Lagomarsino and Magenes 2009]	Evaluation and Reduction of the Vulnerability of Masonry Buildings.
	[Michel *et al.* 2009]	Vulnerability assessment of existing masonry buildings in moderate seismicity areas using experimental techniques.
	[Monti and Vailati 2009]	Non-linear static analysis for building aggregates.
	[Munari and Valluzzi 2009]	Building aggregates seismic vulnerability classification through macro-elements.

Year	Authors	Research Topic
	[Reitherman 2009]	Unreinforced masonry buildings and earthquakes.
	[Senaldi 2009]	Numerical investigations on the seismic response of masonry building aggregates.
2010	[Florio 2010]	Vulnerability of historical masonry buildings under exceptional actions.
	[Formisano *et al.* 2010]	A quick methodology for seismic vulnerability assessment of historical masonry buildings.
	[Lourenço *et al.* 2010]	Analysis of recent and ancient masonry structures.
	[Munari *et al.* 2010]	Mechanical analysis.
	[Munari 2010]	VULNUS, mechanical analyses.
	[Parisi 2010]	Non-linear seismic analysis of masonry buildings.
	[Pujades *et al.* 2012]	Seismic performance of a block of buildings representative of the typical construction in the eixample district of Barcelona.
	[Carocci *et al.* 2010]	Analysis and project guide for seismic interventions in masonry buildings aggregates.
	[Vicente *et al.* 2010]	Seismic vulnerability assessment, damage scenarios and loss estimation: the case of Coimbra (hybrid technique with 14 parameters)*.
2011	[Ademović 2011]	Structural and seismic behaviour of typical masonry buildings from Bosnia and Herzegovina.
	[Amadio *et al.* 2011]	Sub-division of building aggregates into structural units.
	[Bothara and Brzev 2011]	Improving the seismic performance of stone masonry buildings.
	[D'Ambra 2011]	Local mechanisms global analysis.

Year	Authors	Research Topic
	[Formisano *et al.* 2011b]	Hybrid method for the large scale assessment of seismic vulnerability of historical building aggregates (hybrid method with 15 parameters)*.
	[Formisano *et al.* 2011a]	Hybrid technique with 15 parameters*.
	[Ishiyama 2011]	Introduction to earthquake engineering and seismic codes in the world.
	[Marques and Lourenço 2011]	Possibilities and comparison of structural component models for the seismic assessment of modern unreinforced masonry buildings.
	[Pagnini *et al.* 2011]	Mechanical model masonry buildings.
	[Vicente *et al.* 2011]	Evaluation of strengthening techniques of traditional masonry buildings: case study of a four-building aggregate*.
2012	[Caliò *et al.* 2012]	New discrete element model.
	[Chever 2012]	Use of seismic assessment methods for planning vulnerability reduction of existing building stock.
	[Ferreira *et al.* 2012]	Hybrid technique for building aggregates (vulnerability index methodology) with 5 parameters *.
	[Marques *et al.* 2012]	Pushover analysis of a modern aggregate of masonry buildings through macro-element modelling.
	[Marques 2012]	Innovatory seismic calculation methodologies for both simple and confined masonry structures.
	[Mendes 2012]	Seismic assessment of ancient masonry buildings: shaking table tests and numerical analysis.
	[Nucera *et al.* 2012]	Confined masonry buildings through macro-elements modelling.
	[Ortolani *et al.* 2012]	Study of vulnerability and damage: the case of *Castelnuovo*.

Year	Authors	Research Topic
	[Spacone *et al.* 2012]	Safety assessment of masonry building aggregates in *Poggio Picenze*.
	[Ulrich *et al.* 2012]	Simplified methodology through macro-elements.
	[Vailati *et al.* 2012]	Probabilistic assessment method.

Part II

Analysis

Chapter 3

San Pio delle Camere Case Study

3.1 Historical and Urban Context of San Pio delle Camere

San Pio delle Camere is a small medieval village born in 1001, in the region of *Abruzzo*, about 25 km south from *L'Aquila* and elevated 800 meters above the sea level. This village was first hit by an earthquake in 1315 and later in 1348, destroying most of the buildings around *L'Aquila* province and causing around 800 deaths.

Followed by these natural disasters, the XV century was considered one of the most tragic periods of *San Pio delle Camere* history, on the occasion of Braccio of Montone's milestone invasion in 1424, which brought about the complete destruction of the village. Nevertheless, in late XIX century, as part of the Kingdom of Italy, the village rose due to an economic and social boom arising from agriculture, pastoralism and handicrafts activities [Attanasio *et al.* 2011].

The arrival of the industrial revolution increased both immigration and emigration, displacing workmanship to the brand new economic capital cities. Therefore, interior small village's economical activities decreased abruptly and *San Pio delle Camere* has increasingly become sparsely populated throughout the years [Attanasio *et al.* 2011].

As in most of medieval villages, *San Pio delle Camere* historical centre can be easily separated from recent constructions areas through the physical boundaries that it's possible to observe crossing the village. Historical village centres are obviously associated to a higher seismic vulnerability because ancient buildings, designed with no seismic purposes, are concentrated in this area. *San Pio delle Camere* historical centre, recently included in the European Cultural Heritage Protection Program, is located in the upper part of the village, as the majority of the medieval Italian villages. During the last century, several intrusive interventions were carried out, mischaracterising both the architecture and morphology of the village.

The historical centre was built along the main axis that crosses the entire village, *Via del Protettore* (see figure 3.1 on the next page). The buildings along this road are generally narrow, featuring low ceilings and often showing in-height irregularities. The presence of buildings sharing the same transversal load-bearing masonry walls arising of the row construction strategy along this longitudinal axis is significantly frequent [Attanasio *et al.* 2011].

Of a particularity architectonic interest of this village is the existence of innumerable interconnected underground pathways, known as *Ipogee* Cavities, just beneath the historical centre building stock, justifying the ancient name for which it was known, *San Pio*

Figure 3.1: *Via del Protettore*, the main axis of the village.

delle Grote [Cambri *et al.* 2011]. The dimensions of such cavities range between 10 and 20 meters long, 2 and 3 meters height and range in between 4 and 5 meters thick. Unlike what we might think, according to Favilli and Mamone [Favilli *et al.* 2011] the existence of these cavities didn't seem to have been significantly affected by the amplification of the seismic signal in *San Pio delle Camere* and so, during the numerical analysis it's possible effects were neglected.

3.2 Existing Stone Masonry Buildings

Stone masonry is a traditional building typology that has been practised for centuries all over the world. These type of constructions were erected both in urban and in rural areas. Typically in rural areas as the historical centre of *San Pio delle Camere*, stone masonry buildings are smaller in their overall size but they also have a smaller percentage between the volume of openings and the overall volume of the building, being the quality of construction lower than the one found in urban stone masonry buildings. The quality and heterogeneity of materials used for each single constructive typology, whose characteristics vary from country to country, depending on the culture, tradition and raw material available, made stone masonry building a special class of structure. Figure 3.2 on next page, shows different samples of the existing stone masonry quality collected in *San Pio delle Camere* historical centre.

Stone masonry buildings are constituted by the following key structural elements: floor and roof systems; walls and foundations. Starting by the horizontal structure, in this type of buildings floors and roofs show large number of constructive materials and structural systems, as vaults, timber joists and reinforced concrete slabs [Bothara and Brzev 2011]. This choice is often governed by the regional cost and material availability and also by the manpower skills and experience. Stone masonry walls are vertical elements that support floors and roof. They are usually built with stone boulders bonded together with mortar. Foundation elements support the global weight of the structure concentrated in walls and are responsible for spreading those loads through the underlying soil.

With respect to the mechanical behaviour of this natural non-homogeneous compound

(a) (b) (c)

Figure 3.2: Example of different preservation status of stone masonry quality in the building aggregate. (a) Recently intervened stone masonry. (b) Reasonable preservation state. (c) Disorganized multi-leaf stone masonry in a poor state of preservation.

material, it's known that stone masonry buildings have an extremely low tensile strength value, approximately 1/30 of the compressive strength one [Borgesa and Castagnone 2011]. Thus, their behaviour is inherently non-linear.

According to the Portuguese Association of Engineers research developed in 2001, the following deficiencies were appointed as usually observed in masonry buildings, which represent the majority of historical centres building stock [Ravara *et al.* 2001]:

- Deterioration of the properties of the structural materials;
- Highly weak construction, in some cases with insufficient bracing systems;
- Highly weak rehabilitation;
- Addition of floors and basements;
- Alterations, particularly regarding the lower ground floors, which have been defectively designed and/or executed, and which consequently decrease the strength of walls and foundations;
- Unplanned introduction of metallic and reinforced concrete elements without criterion;
- Walls with reduced thickness, lacking strength and in insufficient number;
- Defective foundations, in some cases;
- Use of heavy decorative elements.

Some of these deficiencies can not be extrapolated to *San Pio delle Camere* since the sample where the study was based is the historical centre of Lisbon. Nonetheless, stone masonry buildings still the most common typology present in *San Pio delle Camere*. They're generally built with irregular stone connected with poor quality mortar. Intrusive interventions as filling openings with completely different materials, such as hollow bricks, are frequently visible. Also cement blocks are commonly used in such interventions.

3.3 The L'Aquila Earthquake

3.3.1 Introduction

In order to evaluate the behaviour and damage distribution of buildings affected by earthquakes it is extremely important to understand the main characteristics of the real seismic event at its epicentre but also the local amplification of such event nearby the structure under analysis. Since the peak ground acceleration value used to estimate the performance point of the structure was a design PGA value, the following description only has an informative nature.

Italy and especially the region of *Abruzzo* have experienced a vast history of damaging due to seismic activity. *L'Aquila*, one of the largest urban centres in *Abruzzo*, considered a medieval treasure, is located in the middle of one of the most seismically dangerous zones in Italy [Hall 2011]. The seismic sequence that struck *L'Aquila* province took place between October and December 2008, with several thousands fore-shocks and aftershocks, some of them with significant values on the Richter magnitude scale. However, the main shock (lasting 20 seconds) was recorded at 1:32:40 UTC on 6^{th} April 2009, rating 5.8 on the Richter scale and 6.3 on the moment magnitude scale M_w. The epicentre, with the following coordinates Lat.42°34'76N and Long.13°38'00E, was about 10 Km west of the surface rupture, and the seismic shaking and ground subsidence were dominant mostly in between the epicentre and the surface of rupture, coinciding more or less with the morphology of the *Aterno* Valley [Salamon *et al.* 2010]. The pattern and intensity of damage were also function of the local site, basin and directivity effects, spread of the population and the lack or absence of anti-seismic properties in the built environment [Salamon *et al.* 2010]. The damage was mostly caused by ground shaking, followed by a couple of surface rupture events and slope failures, respectively, although on a smaller scale. Almost no liquefaction events were observed [Salamon *et al.* 2010]. The earthquake occurred along a NW-SE trending normal fault (between 15 and 20 Km long, dipping about 45° SW) and the damage was even more concentrated in the SE area, more precisely nearby the *Paganica* Fault, where the maximum level of damage $I_{MCS} = IX$ was identified [Sassu 2011]. Causing considerable loss of life and damage to man-made structures, expressed by 308 casualties and large damage in the town and surrounding villages, it was considered the third largest earthquake recorded by strong motion instruments in Italy (after the 1980, M_w 6.9, *Irpinia* and the 1976, M_w 6.4, *Friuli* earthquakes) and the second deadliest one in the Italian history. [Ameri *et al.* 2012]. Over 1500 people were injured and more than 65000 people were forced to leave their houses [Hall 2011]. Roughly 20000 buildings were destroyed and the global damage relative to buildings was estimated to be between 2 and 3 billion euros [Bazzurro *et al.* 2009]. Further information about the collected records and geotechnical aspects of *L'Aquila* earthquake can be consulted in the researches of Ameri *et al.* [Ameri *et al.* 2012], Pallazzo and De Iuliis [Palazzo and De Iuliis 2011], Monaco *et al.* [Monaco *et al.* 2009] and Pacor *et al* [Pacor *et al.* 2010]. The destruction caused by this earthquake surprised experts and generated discussions about the anti-seismic building standards adopted in Italy, since modern buildings surprisingly suffered greater damages. Most alarming were the legal repercussions of the earthquake on science. Due to a general lack of understanding of science both by the public and authorities, six scientists were accused and convicted of manslaughter [Hall 2011] for having "ignored premonitory signs of the earthquake in form of pseudo-scientific

claims of dubious veracity and warnings mostly published by individuals on the internet".

The damage verified in *San Pio delle Camere* was not as severe as in other surrounding villages like *Castelnuovo* (see figure 3.3), due to the soil quality upon *San Pio delle Camere* was built [Sassu 2011]. Unlike what happen in *Castelnuovo*, where the presence of sedimentary soil stratum allowed the amplification of the seismic waves, in *San Pio delle Camere* the rocky soil reduced this amplification and subsequently brought both lower material damages and deaths.

Figure 3.3: Damage found in a building aggregate in *Castelnuovo* village, belonging to *San Pio delle Camere* municipality.

According to the *Schede AeDES*, that gathers the first post-event information regarding the typological characteristics of the village's buildings, the level of damage and the usage condition classification of the built environment in *San Pio delle Camere* were estimated. The results are reported in table 3.1 and in figure 3.4, both adapted from *Schede AeDES* [Sassu 2011]. This practical report was filled to allow the collection of an overall view over the village in terms of building heritage immediate damage. These evaluations were based on the assigned structure vulnerability classification.

Table 3.1: Usage condition classification of the built environment in *San Pio delle Camere*, adapted from [Sassu 2011].

	Usage condition classification from *Schede AeDES*	Nº of Building Aggregates
A	Usable building	88
B	Temporarily unusable building	19
C	Partially unusable building	9
D/E	Unusable building	29
F	Unusable with external risk	3

The micro mapping research refers to the assessment of the seismic hazard through the individualisation of regions with homogeneous seismic behaviour [Favilli *et al.* 2011]. The municipal area of *San Pio delle Camere*, 30 km from the earthquake epicentre, is the most eastern inhabited village located in the macro-area 4, which includes the villages

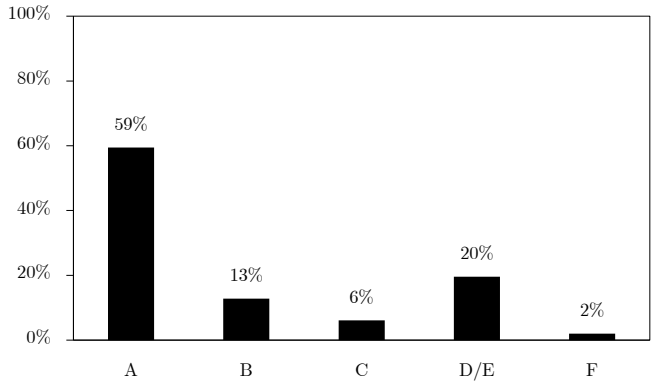

Figure 3.4: Usage condition class percentage.

of *Poggio Picenze*, *Barisciano*, *San Martino*, *Petogna Picenze* and *Castelnuovo*. The damage intensity in *San Pio delle Camere* was evaluated as $I_{MCS} = V - VI$ class on the MCS (Mercalli-Cancani-Sieberg) scale. By comparing to the classification made by the civil protection authority it is possible to conclude that the damage level evaluated for *San Pio delle Camere*'s built environment is not as severe as in other surrounding villages.

3.3.2 Seismic Micro Mapping Report

Favilli and Mamone have summarized the site effects during the seismic event. The damage level observed in structures caused by ground motions depends not only on the construction quality but also from site to site, as seismic waves have different modes of propagation. In this sense, seismic hazard should be treated independently for distinct sites.

The micro mapping process of a seismic area consists in the evaluation of the local hazard by the individualisation of the territory areas with homogeneous seismic behaviour. This way it is possible to distinguish stable zones, with or without local amplification, from the unstable ones (areas where amplification effects shouldn't be ignored). The basis standard soil condition used in these type of evaluations have considered the soil as an outcropping bedrock with horizontal topographic surface. With the necessity of evaluating the seismic hazard under different geological, geomorphological and geotechnical conditions, additional factors were added to the basic standard soil conditions, which in recent codes are represented by the topographic and stratigraphic amplification coefficients, S_T and S_S, respectively. The local soil conditions affects both amplitude, frequency and period of the design seismic action.

The detailed mapping developed in *San Pio delle Camere* was intended to be a useful help for drawing the priorities and strategies to emergency plans and also for post-earthquake re-construction. This work is a part of an extended research on seismic micro mapping of macro-area 4 [Favilli *et al.* 2011]. According to the village geological map, the ground soil beneath the building aggregate under study is identified as rubble debris and heterogeneous deposit thickly layered, sometimes laminated, composed by cement-less debris, sub rounded and angular, sometimes overlapping with sandy matrix, debris fill

watersheds and alluvial fans at the mouth of the valley. It's geometry is strongly lenticular and the maximum thickness of a few meters. From *in situ* tests carried in *San Pio delle Camere*, Favilli and Mamone presented the main physical and mechanical properties of ground soil in *San Pio delle Camere* in table 6.2 of the corresponding document [Favilli *et al.* 2011]. Rubble debris, given its shear wave velocity value $v_{s,30} = 300m/s$, is considered a ground soil type C, according to EC8 [CEN 2004]. Generally, soils in this range have values of $v_{s,30} < 800m/s$. The damage observed in *San Pio delle Camere* is not as severe as for example in *Castelnuovo* due to low amplification effects, which were evaluated between 1–1.2 [Favilli *et al.* 2011].

3.4 The Building Aggregate

In this section all considerations and fundamental characteristics regarding this particular case study will be presented. Initially there is going to be introduce the building aggregate and its location within the village of *San Pio delle Camere* (on figure 3.5). Later on, based on the *Scheda di Aggregato* developed by the University of Pisa, the author will clearly identify the main properties of the aggregate building. Finally, the historical evolution hypothesis of the building aggregate is presented.

(a) (b)

Figure 3.5: (a) South and (b) north façade of the building aggregate environment, along *Via del Prottetore*.

The generalized characteristic of historical centres layout is the structural continuity of buildings [Carocci 2001], frequently ensured when adjacent buildings are structurally connected to each other being capable to induce or constraint vertical loads or horizontal thrusts among themselves [Binda *et al.* 2010]. These blocks generally have the configuration and size defined by the urban layout of the village.

The building aggregate number in figure 3.6 is located in *Via del Prottetore* nº44–42 (geographic coordinates Lat.42º28'51 and Long.13º65'91), *San Pio delle Camere*. The urban delimitation of this row building aggregate, as most of the common typologies

within Italian historical centres, is bounded by streets layout, in this case *Via del Prottetore* at north and one secondary street at south. From the west side, is delimited by a flight of stairs providing the discontinuity between the structural unit *US F* and the adjacent building.

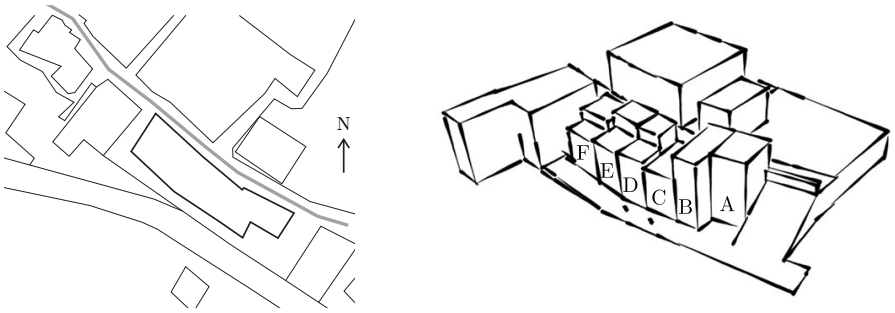

(a) (b)

Figure 3.6: Building aggregate environment.

As the author has argued, in order to carried out the study of the seismic vulnerability assessment of any type of building possible, engineers need a certain survey accuracy level. It is obvious the more detailed the survey level is the more feasible results are. In this sense, the University of Pisa has developed a detailed survey of the building aggregate. In July 2010, the final standard report called *Scheda di Aggregato* was summarised, containing the main input information needed for further seismic vulnerability assessment and evaluation such as the aggregate typology and dimensions, conservation state, damage survey, plants and explanatory pictures, as suggested by ReLUIS [Carocci *et al.* 2010]. It was given particular attention to the following constructive elements:

- Vertical structures (walls);
- Horizontal structures (floor diaphragms);
- Roof structure;
- Relevant restructuring;
- Stairs;
- Non-structural elements with high vulnerability to acceleration or displacement.

During the following paragraphs there is going to be described the main geometrical properties of the stone masonry building aggregate under study. With a total planar area of 319.5 m^2 and a total volume of 4535 m^3 the wall's thickness of the building aggregate varies approximately between 0.50 and 1.10 meters, while floors height varies between 2.60 and 3.20 meters. In a general manner, openings are not distributed evenly and their sizes vary widely. The north façade has two underground floors, representing approximately 15.5% of the total volume of the aggregate, accounting higher stiffness when compared with the opposite façade. Moreover, openings represent approximately 7% of the aggregate total volume.

The building aggregate was divided in three minimum liable intervention units (UMI) as illustrated in figure 3.7. Each UMI is divided in two distinct structural units from A to F (US). The majority of these buildings are used as dwellings. According to the *Scheda di Aggregato* the survey quality acquired for each UMI was considered complete, which means that all structures were made available for extensive inspection. The same figure 3.7 goes further with the individualisation process undertaken in the building aggregate, dividing each UMI into structural units US.

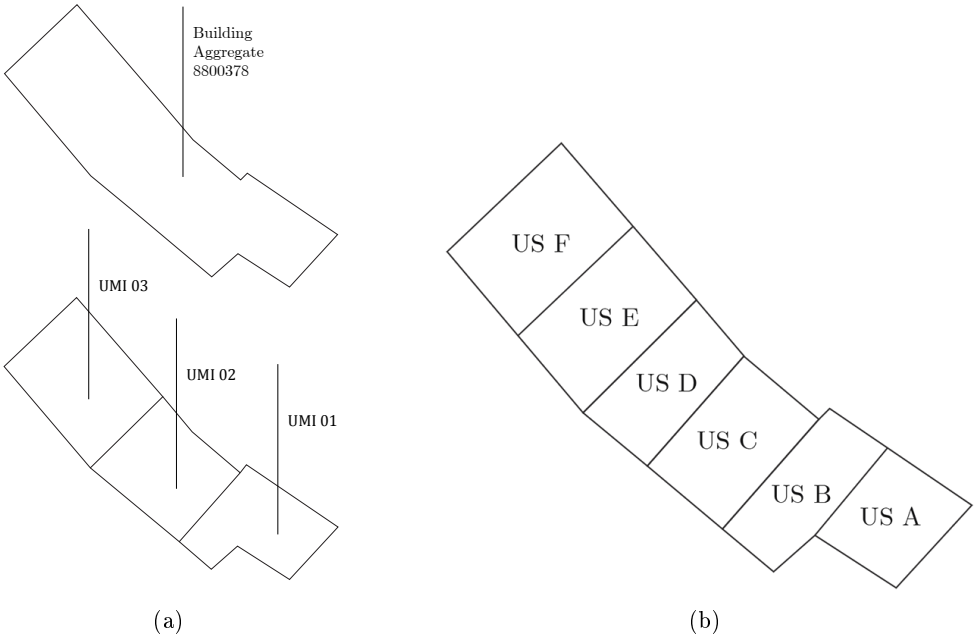

Figure 3.7: Building aggregate divided into (a) minimum liable intervention units and (b) into structural units, from A to F.

The principal elevations and plans of each structural unit, adapted from [Scheda di Aggregato 2010], are presented at the end of the current section (see figure 3.11). At first sight it is evident the irregularity in height and also an non-homogeneous distribution of openings on both façades that was previously explained.

The reconstruction process of the row building aggregate evolution is a key point in the vulnerability evaluation since it can clarify the effectiveness of the restraints between the walls and locate discontinuity between masonry walls [Binda *et al.* 2010]. Figure 3.8 explains the most probable hypothesis for the evolution of the row aggregate building along the years.

Although the lack of information on the structural units construction dates it is easy to understand that the aggregate was built from structural unit F to A, following the village growth direction along *Via del Prottetore*. According to the *Scheda di Aggregato*, the first phase corresponds to a higher percentage of the built aggregate, about 74% with the complete construction of the stone masonry structural units USF, USE and USD. Structural units USC and USB, in stone masonry, were partially built in this first phase. The second phase is marked by the amplification in height of USC (second floor). The third phase, believed to have been carried out right after the Second World

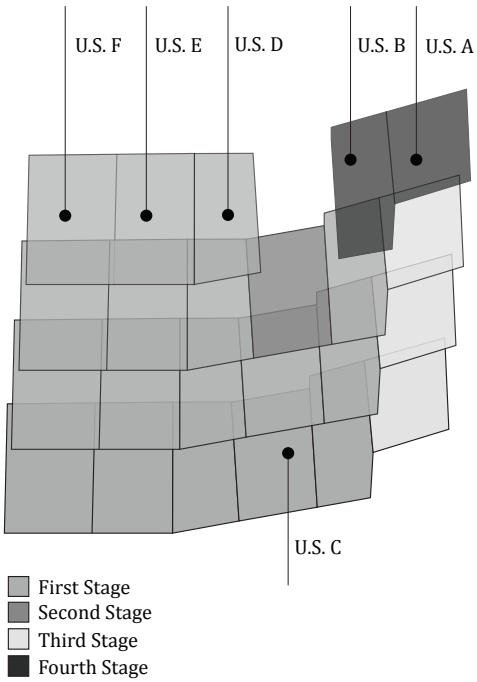

Figure 3.8: Historical evolution hypothesis of the aggregate under study.

War, brought the mixed and intrusive structure USA built in different materials (stone masonry, concrete blocks and massive concrete), changing the global stiffness and the behaviour of the building aggregate. Later on, during the fourth stage, the last floor of both structural units USA and USB was built.

According to the available pictures and drawings from *Scheda di Aggregato* some of the structural units were structurally reinforced with tie-rods and concrete jacketing (reinforced plaster). USF and USE outside appearance led to think they were recently restored, due to the existence of vertical-horizontal efficient connectors, tie-rods and well-arranged stone masonry, with voids filled with mortar, with some interventions apparently suggested in Mannari *et al.* [Mannari *et al.* 2011]. Moreover, some data from *Scheda di Aggregato* shows some inconsistency, namely the usage status of each structural unit in which the only units that seem to be occupied USE and USF are exactly the ones that the report considers abandoned. In this sense it was found reasonable to conclude that these structural units $US\ E$ and $US\ F$ were rehabilitated after the report was made, but obviously before these pictures being attached to the report. Thus, the conditions considered for the model were the ones only based on the written report, considering those structural units effectively abandoned.

The following figure 3.9, adapted from the *Scheda di Aggregato* shows the damage level and the serviceability classification achieved for each structural unit, respectively. Damage level $D2$ is associated to the presence of damages in many walls, where the majority of the covering mortar has fallen and a partial collapse of chimneys occurred. The damage level $D3$ means a widespread damage in most of the walls with both roof tiles and chimneys destroyed. Finally, the damage level $D4$ is related to walls collapse

and partial collapse of the roof structure and floors. Class E is assigned to unserviceable buildings while Class F is for more severe cases of unserviceable buildings due to the external collapse risk.

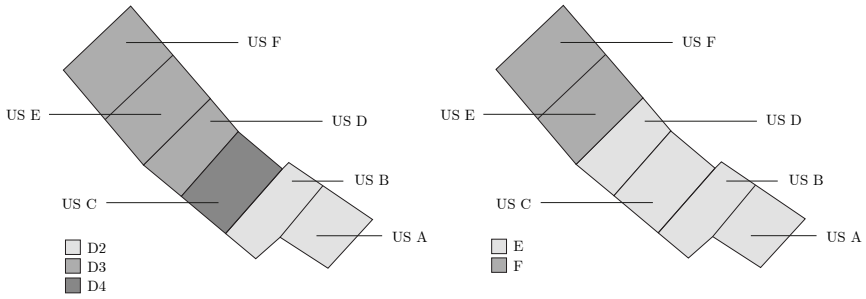

Figure 3.9: This figure portrays, from the left to the right, the damage level and serviceability classification for each structural unit, adapted from [Scheda di Aggregato 2010].

With respect to structural materials this building aggregate is mainly built in stone masonry but also has other materials, which added to its intrinsic geometry and quantity and distribution of openings and storeys, raised some structural complexity. While structural units *US C*, *US D*, *US E* and *US F* are mainly in stone masonry, the structural units *US A* and *US B* have different materials varying in height such as stone masonry, reinforced stone masonry, masonry in cement blocks and concrete. While appendix A, illustrates how such different materials are distributed within the building aggregate, for each reference level, figure 3.10 illustrates samples of each structural material present in the aggregate. More information regarding this building aggregate can be found in appendix A at the end of this dissertation, in which it is summarised the main aspects relative to each structural unit, adapted from *Scheda di Aggregato* report.

(a) (b) (c) (d)

Figure 3.10: From the left to the right, (a) a sample of irregular fabric of stone of masonry, (b) concrete, (c) cement blocks and (d) reinforced stone masonry.

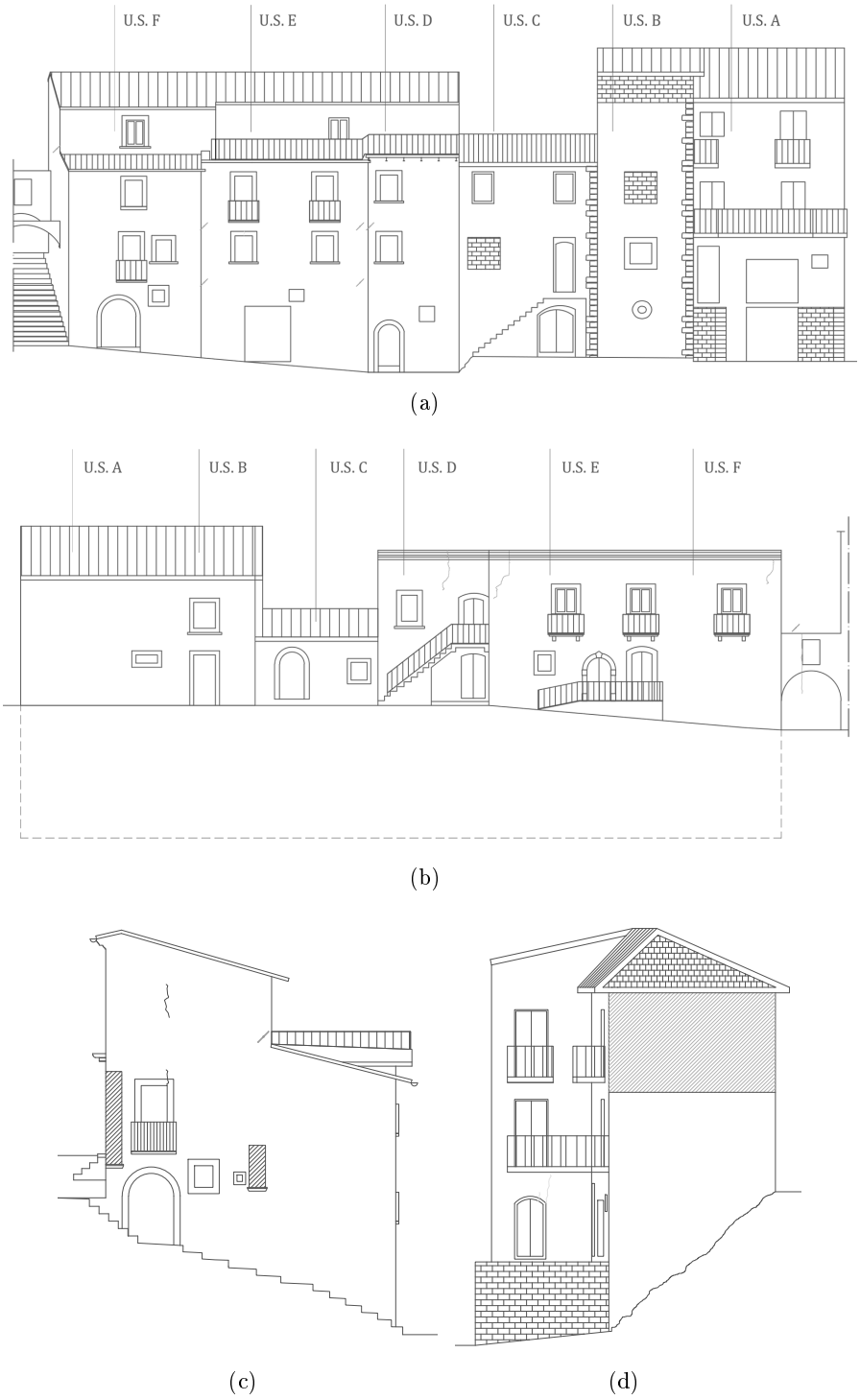

Figure 3.11: Building aggregate elevations given by *Scheda di Aggregato* [Scheda di Aggregato 2010]. (a) South façade. (b) North façade. (c) West side elevation. (d) East side elevation.

Chapter 4

Capacity Spectrum Method and Numerical Modelling

4.1 Capacity Spectrum Method

In the present dissertation it was used the Capacity Spectrum Method procedure to assess the seismic vulnerability of the building aggregate by evaluating the performance point of the structure, in order to use fragility curves on the prediction of damage distribution due to the seismic action installed in the structure. Further information regarding this method is presented in annex B at the end of this dissertation. Considered one of the most widespread graphical procedures for the seismic vulnerability assessment of structures, the CSM, developed by Freeman [Freeman 1998], is a non-linear static analysis method, which compares the capacity of a structure with the demands of earthquake ground motion acting on it. The lateral force resisting capacity represented by a force-displacement curve obtained by a pushover analysis, called capacity curve, is converted into spectral acceleration S_a and spectral displacement S_d (ADRS format) through the graphical transformation into an equivalent SDoF system, resulting in the Capacity Spectrum. This trial and error procedure estimates the performance point, which describes the spectral displacement of the building due to the given earthquake. Used in combination with fragility curves it is possible to predict the damage distribution over the building [Schnepf *et al.* 2007]. From this plot it is possible to understand how the structure will behave when subjected to that seismic action. Hardening and softening phenomenons were not considered in the used simplified capacity curve, being the yielding and ultimate capacity considered equal ($A_y = A_u$).

4.2 Non-linear Static Analysis

Static pushover analysis is becoming a widespread tool to perform the seismic assessment of both existing and new structures, since provides adequate information on seismic demands imposed by the design ground motion on the structural system, where "Static" means that the force is applied to the structure statically and "non-linear", the behavioural model used for the structure resistance elements. As seismic design code requirements are a relative recent matter and once they have been constantly upgraded over the years, as well as the engineering knowledge, buildings can become seismically unsafe. According

to EC8 this analysis was performed for the purpose of estimating the expected plastic mechanisms and the distribution of damage and also to assess the structural performance of existing buildings. The following paragraphs will summarise the basis concepts on which pushover analysis is based.

Briefly, pushover curves are a plot of the total base shear strength versus top displacement of the structure [Varum 2003], resultant from carrying the analysis up to failure, from which both ultimate load and ductility capacity are calculated. This enables to indicate premature failure or weakness in the structure from which retrofit interventions could be based on. Pushover analysis includes the CSM [Freeman 1998] and the N2 Method ([Fajfar 1999], [Fajfar 2000]) simplified methodologies, in which the assessment of the maximum expected response of the structure under a specific seismic action is accomplished by means of an equivalent non-linear SDoF system, considered representative of the real MDoF structure [Shibata and Sozen 1976]. Graphically these curves result as an envelope of the hysteresis cycles produced during the seismic event and can be considered as an indicator of the post-elastic behaviour of the structure.

According to the foregoing, the building aggregate response to a determined seismic event is characterised by the corresponding capacity curves, describing the pushover displacement of the global structure and the seismic design level as a function of laterally-applied earthquake load [FEMA 2003]. The pushover analysis is performed applying to the structure a monotonically increasing pattern of lateral forces, simulating the real ground shaking action. As loads are incrementally increasing several structural elements start sequentially yielding. Thus, at each event, the structure experiences a loss in stiffness [Fajfar 2000]. The first yielding elements are then relaxed to form plastic hinges and simultaneously incremental lateral loading is applied until a non-linear static capacity curve is created [Freeman 1998].

In figure 4.1 is illustrated the interpretation of a general pushover curve example. During event ①, the first elements start to fissure. Phase ② corresponds to the first signs of yielding on structural elements. Subsequently event ③ is characterised by the collapse of some of those elements, already yielded. Finally, phase ④ corresponds to the ultimate displacement of the structure for the global collapse situation.

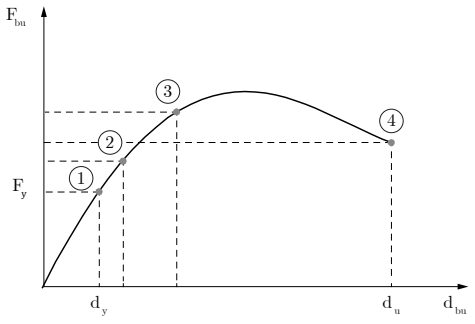

Figure 4.1: Example of a pushover curve.

At an initial phase, after selecting the node control for the analysis, the forces are applied step-by-step. As forces are increasing, some elements start to suffer the first damages, which means that those elements are no longer in the elastic field. In this sense, elements will behave in the plastic field until the collapse condition is reached. The

verification through pushover analysis is possible comparing different capacity curves for each expectable situation to the demand displacement. According to the Italian code NTC08 [DM 2008], capacity curves are required to be bilinear and representative of an equivalent SDoF system. With the capacity curve of the equivalent system it's possible to determine the corresponding period for the maximum displacement required for the system, in accordance with the elastic horizontal response spectrum. Once the ultimate displacement is exceeded, the structure is considered to have collapse. A plot of the base shear force versus horizontal displacement can be computed, which represents the capacity curve, or, in other words, the behaviour of the structure face to the horizontal seismic loads. This curve is independent of the seismic action, as it is an intrinsic characteristic of the structure, a function of the geometry and resistance characteristics of the materials [STADATA 2011]. Two load distributions were taking into account for the loading conditions requirements, one proportional to the masses and another proportional to the product between masses and the corresponding deformed shape of the first mode of vibration. The stop condition, meaning the collapse of the structure, is achieved when the base shear force has a decay of 20% of its peak value, where the maximum reached displacement is calculated automatically. These displacements, used to plot the capacity curve, are relative to a specific control node, carefully chosen due to its influence over the pushover analysis. Generally, for regular and homogeneous structures this control node is located at the higher level of the structure and is taken as a reference point for tracing the force-displacement curve.

4.3 Numerical Modelling with 3muri

The program 3muri® was the selected tool to perform pushover analysis in the stone masonry building aggregate enabling the assessment of the building seismic global response. This program performs non-linear static analysis of masonry buildings and it was developed by the University of Genoa under the leadership of Sergio Lagomarsino, being nowadays one of the most widespread software within it's category for the seismic vulnerability evaluation of masonry structures. Although in Portugal this software is not widely known, there are a few researches developed in University of Aveiro and University of Minho which used 3muri® to perform pushover analysis in masonry buildings [Vicente 2008] [Ademović and Oliveira 2012] [Marques *et al.* 2012] [Marques 2012].

4.3.1 General Description of the Software

Inspired by the "equivalent frame" method 3muri® analyses masonry or mixed structures (with RC and steel elements, timber beams and columns) enabling the possibility of the application of intervention and reinforcement solutions as reinforced masonry, FRP or even designing new linear elements in RC, steel or timber, both for the design of new structures or for examination of the existing ones [Ademović and Oliveira 2012]. This software uses the frame by the macro-elements (FME) method [STADATA 2011], in which macro-elements dimensions are a function of the global geometry of the aggregate, the dimensions of the storeys, openings and the distances between openings [Pujades *et al.* 2012]. The FME approach reduces the number of degrees of freedom to represent the seismic response of complex masonry structures with a very interesting computational demand. Figure 4.2, adapted from [STADATA 2011], resumes a scheme of a basis

calculation procedure of the software.

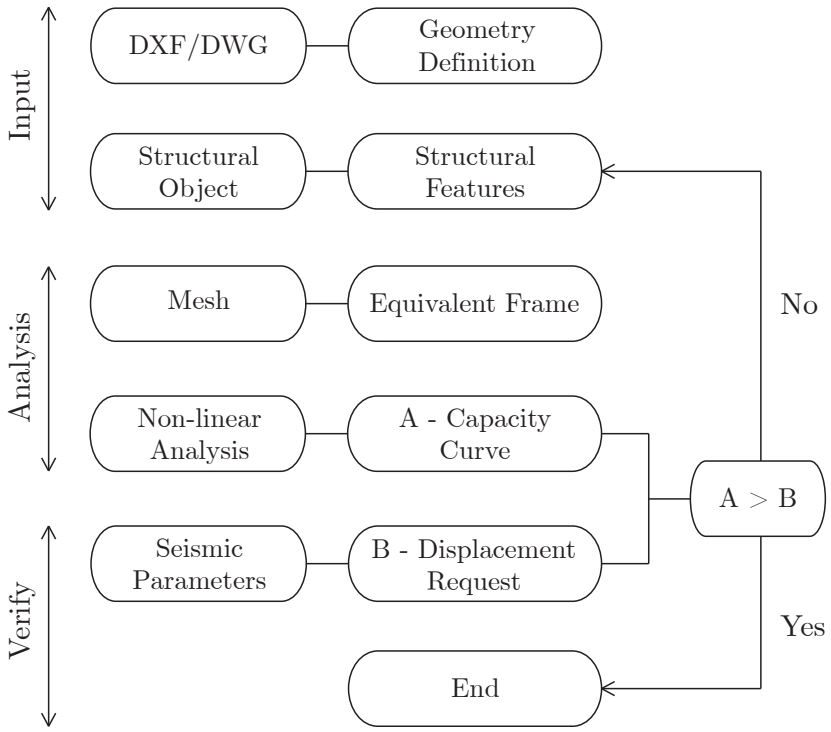

Figure 4.2: General scheme of the program, adapted from [STADATA 2011].

4.3.2 Masonry Macro-elements

The formulation of masonry macro-elements emerged by observing the post-event effects in structures. Along the years, closely analysis done by scientists of the damages induced by earthquakes in masonry buildings allowed to found a trend to determined failure mechanisms occurrence, which has led to the individualisation of the structure into macro-elements. 3muri® considers that structures can be efficiently represented as a combination of masonry panels constituted by spandrels beams and piers, subsequently represented by macro-elements with non-linear behaviour, connected by rigid nodes [Vicente 2008]. This formulation reproduces the three principal in-plan collapse modes of a masonry panel, the bending-rocking, shear-sliding and diagonal shear cracking, distinguished in figure 2.1, in chapter 2, section 2.1, with a limited number of degrees of freedom. These mechanisms are inserted in the model, based on a maximum acceptable deformation (drift) of the panel, due to shear and flexural mechanisms (see figure 4.3). If this value is exceeded, the panel is considered unable to withstand the horizontal actions. Once happening this reduction of resistant capacity, the element is replaced by a connection rod which ensures only the transmission of normal forces [STADATA 2011]. The formulation behind this macro-element is partially described in appendix C, at the of this dissertation.

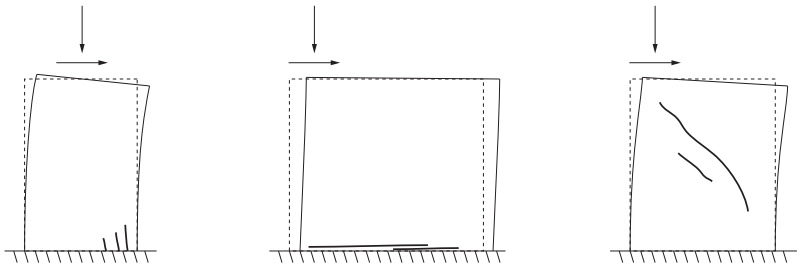

Figure 4.3: Collapse mechanisms in masonry walls, adapted from [STADATA 2011]. From left to the right the flexural-rocking, shear-sliding and diagonal shear cracking failures.

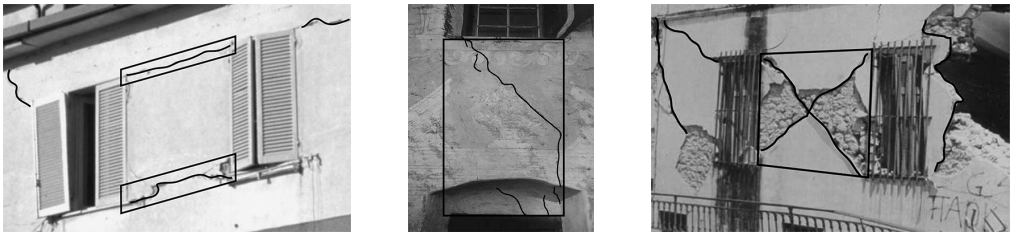

(a) (b) (c)

Figure 4.4: Theoretical formulation of macro-elements. (a) Compression-bending failure [STADATA 2007], (b) and (c) shear failure observed in damaged buildings in Greece and Switzerland, adapted from [Grünthal 1998].

4.3.3 The Italian Seismic Code

In the following paragraphs there is going to be briefly expose the historical and technological evolution of the Italian seismic codes, until the recent italian code NTC08.

The identification and individualisation of seismic zones in Italian territory has begun in the early twentieth century, after the 1908 catastrophic earthquake, occurred in *Reggio Calabria and Messina*. Nevertheless, this effort was not efficient since it was focused only on account recently affected zones and thus, the majority of the Italian seismic zones turned out not being classified properly, as seismic zones. Subsequently there were no apparently reasons to build pursuant to anti-seismic codes. Actually, only in between 1980 and 1984, several laws were approved, sustained on seismological studies developed after the 1976 *Friuli Venezia Giulia* and the 1980 *Irpinia* earthquakes, constituting the Italian seismic classification until the arising of the *OPCM 3274 20/03/2003*.

After the 2002 *Molise* earthquake, Civil Protection has adopted the *OPCM 3274 20/03/2003* to provide a proper response to the urgent updating necessity relative to seismic classification and anti-seismic codes in Italy. As expected in such a difficult duty, this first attempt contained significant inaccuracies [Galasco *et al.* 2006]. In this sense, Italian scientists and experts made a detailed review over this ordinance, identifying incongruities and suggesting amendments by the application in several case studies, which were afterwards gathered in *OPCM 3431 03/05/2005*. In 2005 a draft version of the NTC08 *DM 14/01/2008* has clashed with the previous ordinances, raising several doubtful aspects, until finally being published in 2008.

The seismic safety assessment is based on the seismic performance of the structure, in terms of spectral displacements, comparing the demand displacements with the one allowed for the building, with respect to the ULS (equation 4.1) and the DLS (equation 4.3) limit states, verifying the following equations:

$$D_{max} \leq D_u \tag{4.1}$$

$$q^* < 3 \tag{4.2}$$

where,

- D_{max} is the maximum spectral displacement for ULS, demanded by the NTC08, according to the elastic response spectrum formulation;
- D_u is the maximum displacement offered by the structure, corresponding to a decay of 20% on the pushover curve maximum base shear value;
- q^* is the relation between elastic and the equivalent system yielding force.

$$D_{max_{DLS}} \leq D_d \tag{4.3}$$

where, $D_{max_{DLS}}$ is the demand displacement for DLS, assuming a PGA value equal to $a_{g_{DLS}} = \frac{a_g}{2.5}$ and D_d is the maximum displacement of the structure for this limit state, corresponding to the minimum value between the respective displacement value of the maximum base shear force and the limit of inter-storey maximum drift (usually equal to 0.3%) [Marques 2012].

The Italian code (NTC08) aims to control the damage level of existing structures due to the presence of a determined seismic action, which is evaluated based on the

seismic basis hazard, considering ideal site and topographical conditions (classified has ground type A). This code provides in its Annex B the values of a_g, F_0 and T_c^*, for 9 different return periods T_R (30, 50, 72, 101, 140, 201, 475, 975 and 2475 years) used to define the seismic action. These values were calculated for 10751 specific sites distributed along the Italian territory and represented by their geographical coordinates, latitude and longitude.

The program 3muri® is prepared to work pursuant different codes due to add-in modules (covered by licence). The Standardisation European Committee has released the EC8, a reference seismic code that is used by European countries [Marques *et al.* 2012]. This software contemplates also add-in modules for Italian and Switzerland national seismic codes. With respect to Italy, where the case study is located, the following codes are considered:

- *DM* 16/01/1996 [DM 1996];
- *OPCM* 3274 20/03/2003 [OPCM 2003];
- *OPCM* 3431 03/05/2005 [OPCM 2005];
- *DM* 14/09/2005 [DM 2005];
- NTC08 *DM* 14/01/2008 [DM 2008].

The version made available for this dissertation only had the possibility to work pursuant Italian code NTC08 which is based in the EC8. The most significant difference between them relies upon the values which defines the seismic action (mentioned above) being the EC8 more conservative than the NTC08.

4.4 Modelling Considerations and Assumptions

As suggested by the NTC08, several pushover analysis should be performed in order to recognize the most unfavourable seismic loading condition. Thereafter, the structure should be analysed for different global longitudinal and transversal directions (U_x and U_y), in both positive and negative directions, for different forces distribution (uniform or modal) and also considering accidental eccentricity of the center of mass equal to 5% of the maximum length of the building aggregate (with the direction perpendicular to the seismic action), to account possible torsional effects on the structure, amounting a total of twenty-four possible analysis.

Modelling a building requires an efficient knowledge of both horizontal and vertical resistant structure with respect to the mechanical and geometrical properties, fundamental to predict and understand expectable behaviours under a seismic action. In the next section the author will expose the main considerations regarding the software three-dimensional modelling phase.

4.4.1 Geometry Concerns

As described before, the aggregate building was modelled through the discretisation of walls into macro-elements, represented by piers and spandrels beams, which are normally aligned with the openings of the structure. The more irregular the global structure and

its openings, the more irregular will be the mesh generated. Rigid nodes are generated in areas usually less vulnerable to seismic damages representing the element that provides the connection between piers and spandrels beams. The horizontal structure is constituted by floors which are responsible for the transmission of the vertical loads and the horizontal seismic action to walls. Since vertical loads cause flexural deformations on floors, which for seismic purposes can be neglected, 3muri® considers floors as surface finite elements with diaphragm behaviour, ideal for these approaches, allowing the transmission of loads in the floor's plane. Thus, the stiffness of these elements is assigned according to the most common floor typologies.

Walls are considered the resistant element, both for horizontal and vertical loads. To horizontal structures is given the responsibility of distributing the vertical load to walls and then diving, as part of the floor's stiffening elements, the horizontal action on the respective walls. The collapse mechanisms outside floors are not modelled, once the resistance contribution of walls along the orthogonal direction to floors is neglected. Similarly, the flexural response on the floors is not simulated. Although it is significant in the local resistance checking, it can be neglected studying only the global response. Loads on the floor are divided by the adjacent walls as a function of the influence area and warping direction. The floor is considered as a resistant slab [STADATA 2011].

During the modelling phase, walls are divided vertically per floor level, taking into account the position of openings, identifying both masonry piers and spandrel beams elements, in which deformability and damage are concentrated. In this way, the structure is modelled by assemblage of the different floor levels. These two areas, representing the masonry walls, are modelled through a finite two-dimensional macro-element of two nodes, each one with three degrees of freedom (u_x, u_z, rot_y) and two more additional internal degrees of freedom [STADATA 2011]. The resistant portions of walls are considered as two-dimensional rigid nodes with finite dimensions to which macro-elements are connected. This division of elements into nodes enables the model association to a equivalent frame.

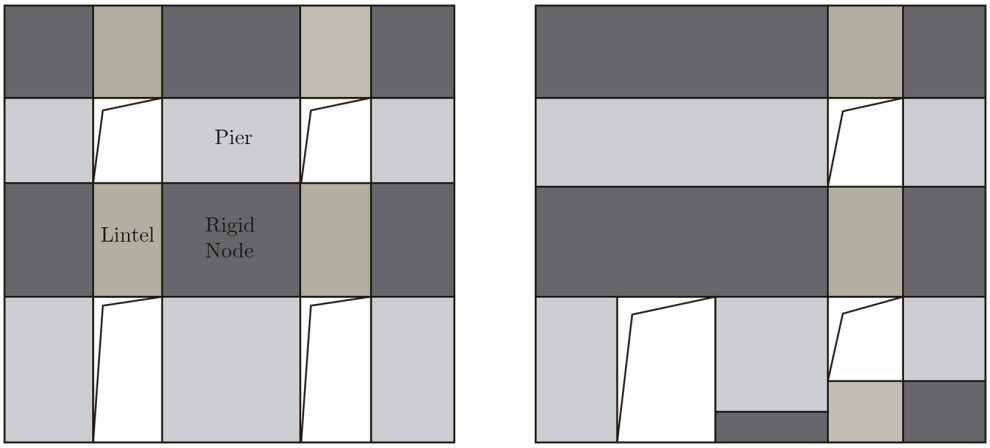

Figure 4.5: Examples of macro-element modelling of masonry walls, with the identification of piers, rigid nodes or spandrel beam. The picture from the right illustrate the corresponding procedure for the in height differences of openings [STADATA 2011].

In order to overtake some limitations of the software and to have more feasible re-

sults, some adjustments and assumptions in the original data provided by the *Scheda di Aggregato* report were made [Scheda di Aggregato 2010]. Due to some plant design irregularities in height, the ground floor level was assumed as the guiding plan. Thus, slightly skewed lines belonging to different structural units were approximated as a unique line, as suggested by the software. The planar dimensions of the aggregate building were performed through AutoCad®, drawing lines at the central axis of the structural elements and, in the presence of a wall element without a uniform thickness, a mean thickness value between the two ends of that wall was considered. Figure 4.6 illustrates the difference between the original structural geometry and the simplified one, used as the model. It is important to refer that the x-axis considered in the model is aligned with the *Via del Prottetore* and the corresponding longitudinal direction.

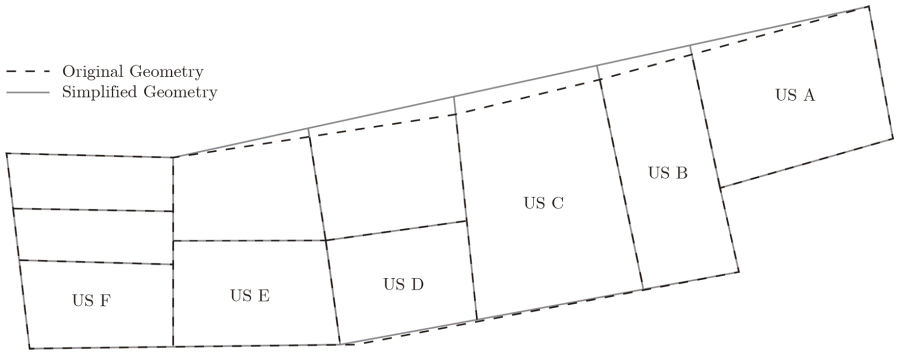

Figure 4.6: Differences between the original and the simplified geometry.

Storeys height was adjusted in order to simplify the quantity of horizontal levels within the model and its values were measured starting from door base. Doors and windows irregular distribution led the author to perform some adjustments in their general dimensions in such a way to obtain the more uniform mesh as possible, keeping unchanged the global aspect of the building aggregate. Accordingly, window's height h_1 was also measured starting from doors base. Moreover, differences between floor levels equal or smaller than 50 cm were approximated, considering the pounding effect negligible, simplifying the structural model whose geometry is somewhat complex. Considering this effects would lead to the definition of small macro-elements with potential to compromise the numerical computational process.

4.4.2 Structural and Mechanical Properties

Once described the general assumptions taken into account during the modelling process, the following paragraphs will resume the different structural elements of the building aggregate.

The vertical structure is represented mainly by disorganised stone masonry walls. Due to the absence of experimental tests, the author researched several articles related to *in situ* tests in similar stone masonry. Candela *et al* [Candela *et al.* 2011] carried out experimental double flat-jack *in situ* test for a stone masonry panel of a building in *L'Aquila* which have resulted somewhat approximated to the ones suggested by the NTC08. After some deliberation and acknowledging the extremely high rigidity of the building aggregate understudy, the author has opted to assume a lower stone masonry

Young's modulus value E given by the NTC08. The remaining materials were assigned with values given by the software for similar structural materials. Table 4.1 resumes the input mechanical properties of each structural material of the vertical structure.

Table 4.1: Mechanical properties values of the vertical structural materials used in the model.

Materials	E [N/mm^2]	G [N/mm^2]	γ [kN/m^3]	f_m [N/cm^2]	τ [N/cm^2]	f_k [N/cm^2]	γ_m [–]
Irregular and rubble stone disorganised masonry	690	230	20	100.0	2.0	210.0	3.0
Cement block masonry	1400	350	12	111.1	7.0	77.8	3.0
Concrete C16/20	24167	11920	25	24.0	10.0	16.0	1.5
Reinforced masonry with irregular and disorganised stone	2175	725	20	185.2	3.7	129.6	3.0

The foundation elements, of which the author has no detailed information, were assigned, with the same material as the main vertical structure (masonry in disorganized stone) and with the following dimensions: base b with the double of the ground floor level wall thickness and height h equal to 0.50 meters.

The horizontal structure is composed by the floor and roof systems. Starting from the roof simulation, despite latest versions of 3muri® brought significant improvements relative to roof assignments, the version available for this dissertation doesn't include such possibility. Therefore, roofs were assigned as flat roofs, in which the equivalent load was vertically and equally distributed on the upper floor for each structural unit. In other words, flat roofs were assigned considering only the vertical component of the load provided by the original gable roof system. These elements, connected to the three-dimensional nodes, are loaded perpendicular to its plane both by accidental and live loads. Finite elements are defined only with axial rigidity, with no flexural rigidity, as the mechanical behaviour that is intended to evaluate is the one induced by the horizontal loads that represent the seismic action.

Once the *Scheda di Aggregato* is not always supported by pictures there were no possibilities to evaluate and have a complete knowledge of the properties of each type of floor. Thus, floors were assigned with estimated values based only on scarce information provided by *Scheda di Aggregato*. Accordingly to this report the author has chosen the following floor typologies given by the software to simulate the behaviour of the real floor systems founded in the building aggregate:

- Barrel and cloister vaults;
- Masonry-RC composite floor;
- Steel-Beam, Hollow flat block and RC slab;
- One-way timber floor with over lapped wood planks.

Mass loading was considered unidirectional and the support length input value was calculated according to the following equation 4.4, where t_{min} and t_{max} are the minimum and maximum thickness value of the walls supporting the horizontal structure,

respectively. Figure 4.7 shows the final aspect of the building aggregate model.

$$s_l = min\{t_{min}; \frac{t_{max}}{2}\} \tag{4.4}$$

The tie-rods assigned for the respective walls with steel class S235 and diameter $\phi = 24\ mm$, simulate a passive mechanical behaviour, meaning the pre-stressed value equal to zero. It was considered a steel yield strength mean value given by Karmazínová [Karmazínová and Melcher 2012] equal to $f_{ym} = 327,5\ N/mm^2$.

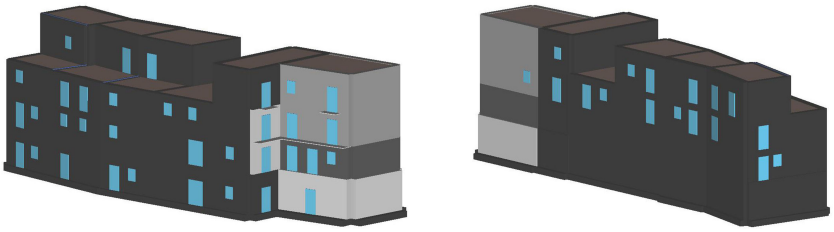

(a) (b)

Figure 4.7: The picture portrays the south (a) and north (b) façades of the building aggregate, modelled with 3muri®.

4.4.3 Seismic Action

The elastic horizontal response spectrum is defined according to the spectral parameters attached in table 1 of Annexo B of the NTC08 by means of the following three required parameters a_g, F_0 and T_c^*, a function of the site geographic coordinates of the aggregate building (presented in chapter 3) [DM 2008]. Equation 4.5 describes the elastic response spectrum in a ADRS format, representing the spectral acceleration S_a, versus the spectral displacement S_d [Chopra and Goel 1999].

- a_g - design peak ground acceleration (horizontal acceleration) on ground type A;
- F_0 - peak value of the amplification factor of the horizontal acceleration spectrum on ground type A;
- T_c^* - period that marks the beginning of constant velocity in the horizontal acceleration spectrum.

These three values were estimated for a return period T_R equal to 475 years, and calculated for each limit state (ULS, DLS and SLS). In this way, for the geographical coordinates of *San Pio delle Camere* it were considered the following values: $a_g = 0.26g$, $F_0 = 2.37$ and $T_c^* = 0.35$. To complete the response spectrum two additional factors are needed, the subsoil factor and the topographic category. The elastic response spectrum is defined by equation 4.5 for different period ranges, as mentioned in the Italian seismic code NTC08 [DM 2008] in a traditional format. The period ranges were calculated

according to equations 4.7, 4.8 and 4.9, presented in the NTC08 code.

$$\begin{cases} S_e(T) = a_g S \eta F_0 \left[\frac{T}{T_B} + \frac{1}{\eta F_0}\left(1 - \frac{T}{T_B}\right)\right] & \text{if} \quad 0 \leq T < T_B \\ S_e(T) = a_g S \eta F_0 & \text{if} \quad T_B \leq T < T_C \\ S_e(T) = a_g S \eta F_0 \frac{T_C}{T} & \text{if} \quad T_C \leq T < T_D \\ S_e(T) = a_g S \eta F_0 \frac{T_C T_D}{T^2} & \text{if} \quad T_D \leq T \end{cases} \tag{4.5}$$

The software in use (3muri®) calculates automatically the performance point of structures, only with the site and the soil ground type input values. The elastic response spectrum is then calculated for a damping coefficient $\beta = 5\%$, which means, according to equation 4.6 the damping corrector factor η is equal to 1.

$$\eta = \sqrt{\frac{10}{(5+\xi)}} \geq 0.55 \tag{4.6}$$

$$T_c = C_c T_c^* \tag{4.7}$$

$$T_B = T_C/3 \tag{4.8}$$

$$T_D = 4.0\frac{a_g}{g} + 1.6 \tag{4.9}$$

The soil factor value S, is obtained by multiplying the stratigraphic and topographic amplification coefficients, S_S and S_T, respectively. The coefficient C_c, also depending on the ground category, was calculated using the following table 4.2. For a ground type A, these values are assumed equal to 1.

Table 4.2: Stratigraphic amplification coefficient S_S and C_c values given by NTC08.

Ground type category	S_S	C_c
A	1.00	1.00
B	$1.00 \leq 1.40 - 0.40F_0\frac{a_g}{g} \leq 1.20$	$1.10(T_c^*)^{-0.20}$
C	$1.00 \leq 1.70 - 0.60F_0\frac{a_g}{g} \leq 1.50$	$1.05(T_c^*)^{-0.33}$
D	$0.90 \leq 2.40 - 1.50F_0\frac{a_g}{g} \leq 1.80$	$1.25(T_c^*)^{-0.50}$
E	$1.00 \leq 2.00 - 1.10F_0\frac{a_g}{g} \leq 1.60$	$1.15(T_c^*)^{-0.40}$

Figure 4.8 (a) shows the elastic horizontal response spectrum plotted for *San Pio delle Camere*, considering a ground type C. The spectral acceleration response S_{ae}, is presented as a function of the gravity acceleration g.

In order to have a ADRS plot format, the elastic displacement response spectrum is constructed, using equation 4.10. The final result is the elastic response spectrum presented in figure 4.8 (b), which represents the spectral acceleration S_{ae}, versus the spectral displacement S_{De} [Chopra and Goel 1999].

$$S_{De}(T) = S_{ae}(T)\left(\frac{T}{2\pi}\right)^2 \tag{4.10}$$

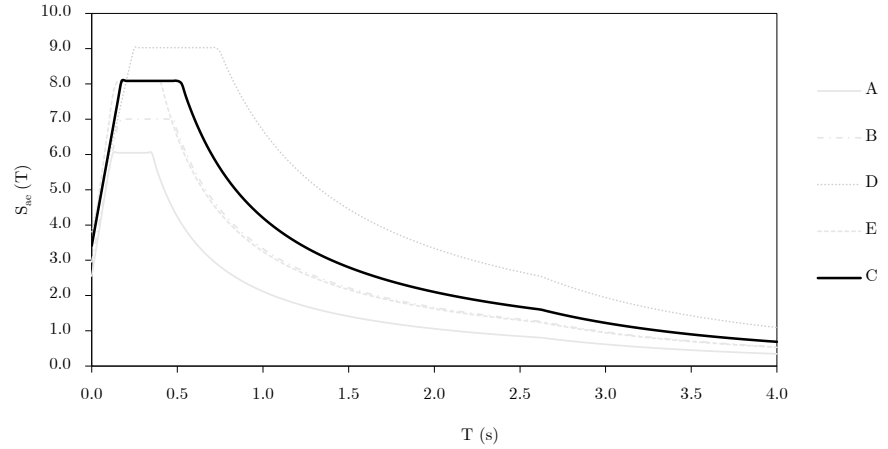

(a)

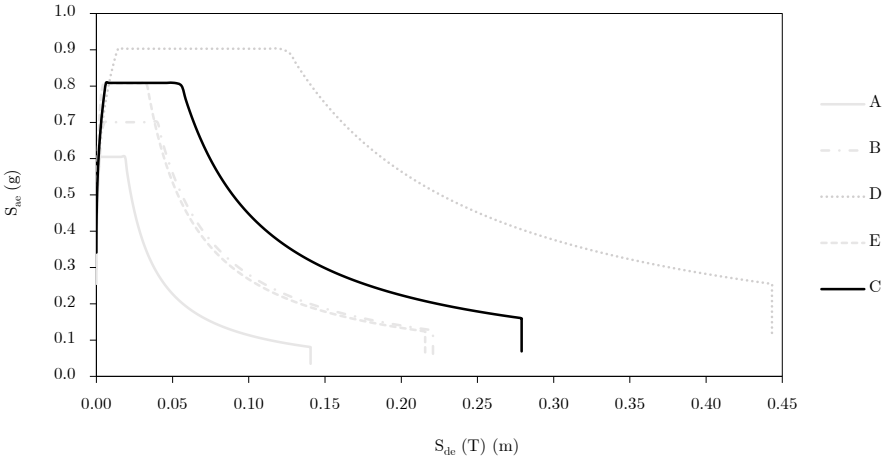

(b)

Figure 4.8: Elastic Horizontal Response Spectrum according to the NTC08 for $a_g = 0.2552\ g$ and ground type C. (a) Traditional format (S_{ae}–T). (b) ADRS format (S_{ae}–S_{De}).

Chapter 5

Seismic Vulnerability Assessment of Building Aggregates

5.1 Seismic Vulnerability Assessment Introduction

Building's vulnerability is defined as an inherent characteristic of buildings, which is a function of the constructive process and the quality of such construction [Vicente 2008]. Therefore, seismic vulnerability emerge with the intrinsic predisposition of buildings to suffer damages caused by earthquakes and it is strictly connected to physical and structural properties of structures [Barbat 2003]. The assessment of the seismic vulnerability of buildings through indirect methodologies such as the vulnerability index based method, must be performed considering their importance in terms of cultural heritage and constructive typology. This way the quality of the results are proportional to the know-how of the building under study. As described before in section 2.2, presently several methods were developed according to different ranges, from the single unit building and individual façade walls to buildings within aggregates (see table 2.1 in section 2.2). Since this dissertation regards the study of a single building aggregate, the assessment methods were chosen taking into account this specific scale. Hence, both hybrid and indirect techniques were used to assess and predict fragility and damage distribution on the building aggregate. With respect to the hybrid techniques fragility curves were defined using the well-known damage limit states methodology which associates the bilinear capacity curve to the damage grade definition of the EMS–98 macroseismic scale [Grünthal 1998] and through the HAZUS–MH–MR3 methodology values for a URMM low-code building class, developed by FEMA [FEMA 2003]. Two different formulations of indirect methods were applied based on individual buildings vulnerability index evaluation, firstly proposed by GNDT [GNDT-SSN 1994]. These recent formulations were developed by Vicente [Vicente 2008] and Formisano *et al.* [Formisano *et al.* 2011b], from which mean vulnerability index were obtained to estimate the vulnerability of the building aggregate. Thus, fragility curves and damage distributions were estimated for different seismic intensities, according to EMS–98 scale [Grünthal 1998]. Finally, a similar procedure developed by Vicente designed specifically for building aggregates was applied with the same assessment purpose [Ferreira *et al.* 2012].

5.2 Hybrid Techniques

As the author has been arguing, hybrid techniques assembles different classes of methodologies. The technique used in this dissertation is an association between mechanical and conventional techniques. The direct mechanical technique used is considered an analytical methodology based on numerical detailed models, in this work performed through 3muri® software capabilities. Thus, this mixed technique takes the advantage of pushover analysis and the CSM (see section 4.1) to estimate the performance point of the structure, for then, by means of a conventional technique based on expert's knowledge, evaluate fragility curves and the corresponding damage distribution in the structure. With respect to this conventional technique it were considered two distinct approaches.

Firstly, it was applied the HAZUS–MH–MR3 earthquake model methodology, developed by FEMA [Reitherman 1999] [FEMA 2003], which is defined as the conditional probability $P\left[d_S|S_d\right]$ of reaching or exceeding a given damage state d_s for a determined spectral displacement S_d.

$$P\left[d_s|S_d\right] = \Phi\left[\frac{1}{\beta_{ds}} ln\left(\frac{S_d}{\overline{S_{dds}}}\right)\right] \tag{5.1}$$

where, Φ is the standard normal cumulative distribution function, $\overline{S_{dds}}$ is the median value of spectral displacement at which the building reaches the threshold of damage state d_s and β_{ds} is standard deviation of the natural logarithm of spectral displacement for damage state d_s. Secondly, it was used the widespread damage limit states formulation developed by experts and technicians, which depends directly on the capacity curve obtained through pushover analysis. In order to predict damage, this methodology is associated to the EMS–98 macroseismic classification of such damage grades, dividing the damage into six different grades, as shown in table 5.1. Each damage limit state S_{d_i} is associated to a spectral displacement value relative to the yielding and ultimate capacity, D_y and D_u, which in turns is related to the seismic action deformation response from the elastic behaviour range until reaching the collapse.

Table 5.1: Damage grades definition for masonry buildings [Grünthal 1998].

Damage grade D_{k_i}	Description
D_{k_0}: No damage	No damage evidences
D_{k_1}: Despicable or slight damage (no structural damage, slight non-structural damage)	Small cracks in wall's covering and eventual detachment.
D_{k_2}: Moderate damage (slight structural damage and moderate non-structural damage)	Non widespread cracking in walls. Weakening and detachment of coverings and non-structural elements.
D_{k_3}: Extensive damage (moderate structural damage and severe non-structural damage)	Extensive and generalized cracking in walls. Collapse and weakening of non-structural elements.
D_{k_4}: Severe damage (severe structural damage and extremely severe non-structural damage)	Partial collapse of structural elements such as walls, floors and roofs.

D_{k_5}: Destruction (Extremely severe structural damage or collapse)	Collapse or in imminent collapse condition.

The damage state values definition have been studied by the research community through both experimental and non-linear analyses tested in type buildings, assuming different values according to the structural deformation demand. With respect to hybrid techniques it were used two different approaches to estimate fragility curves. The first uses the following nominal mean values to determine the damage limit states, as shown in equation 5.2 a function of D_y and D_u [Vicente 2008].

$$\begin{cases} S_{d_1}^{NV} = 0.7D_y \\ S_{d_2}^{NV} = 1.5D_y \\ S_{d_3}^{NV} = 0.25(D_u + D_y) \\ S_{d_4}^{NV} = D_u \end{cases} \tag{5.2}$$

Once obtained these fragility curves through its fundamental parameters founded in literature [Reitherman 1999] [FEMA 2003], for both longitudinal and transversal direction U_x and U_y, further damage probability histograms of the mean values can be obtained for different damage states, using equation 5.1 for the spectral displacement value S_d^* relative to the performance point of the structure.

$$P\left[d_{s_k}|S_d^*\right] = \Phi\left[\frac{1}{\beta_{ds}} ln\left(\frac{S_d^*}{\overline{S}_{dds_k}}\right)\right] \tag{5.3}$$

where k can assume the values corresponding to each damage state ($K = 1, 2, 3, 4$ and 5). The damage probability values are obtained by the following equations:

$$\begin{aligned} P(D_0) &= 1 - P\left[d_{s_1}|S_d^*\right] \\ P(D_k) &= P\left[d_{s_k}|S_d^*\right] - P\left[d_{s_{k-1}}|S_d^*\right] \quad \text{with } k = 1, 2, 3, 4 \text{ or } 5 \\ P(D_5) &= 1 - P\left[d_{s_5}|S_d^*\right] \end{aligned} \tag{5.4}$$

where D_k represents each structural damage limit state, described in the table 5.1.

5.3 Indirect Techniques

5.3.1 Vulnerability Index for Individual Buildings

Within this methodology the author applied two different proposals regarding the assessment of the seismic vulnerability of individual buildings, both based on the original GNDT level II methodology [GNDT-SSN 1994] [Giovinazzi 2005]. Benedetti and Petrini have developed the vulnerability function definition which implied a deterministic correlation between the seismic action and the damage level [Benedetti and Petrini 1984].

This binomial was reached through extensive and detailed research and recent post-event observation of masonry buildings in the Italian territory. The characteristics which governs the seismic behaviour of masonry old buildings are treated as parameters, which must be evaluated in order to assess the vulnerability index value.

The methodology proposed by Vicente has advanced with the vulnerability index I_V^* varying between 0 and 650, obtained by means of fourteen weighted mean structural parameters (see equation 5.5), being each one of them classified into four classes, from A to D, with independent class values C_{vi} [Vicente 2008]. As shown in table 5.2 these parameters evaluates fourteen different aspects considered fundamental to describe the seismic behaviour, weighted by means of the p_i values, from 0.5 up to 1.5, representing the less or more importance in the building's vulnerability. I_V, varying from 0 to 100, results as the normalised value of the previous vulnerability index I_V^*. With this value damage distributions were predicted to different seismic represented through the European Macroseismic Scale intensities, I_{EMS-98}. A mean vulnerability index value I_{V_m} was calculated from the individual normalised vulnerability index I_V estimated for each structural unit, for further confrontation.

$$I_V^* = \sum_{i=1}^{14} C_{vi} p_i \tag{5.5}$$

Table 5.2: Vulnerability index for individual buildings proposed by Vicente [Vicente 2008].

	Parameter	Class C_{vi}				Weight p_i
		A	B	C	D	(pi)
1	Type and organisation of the structural system	0	5	20	50	0.75
2	Quality of the structural system	0	5	20	50	1.00
3	Conventional resistance	0	5	20	50	1.50
4	Maximum distance between walls	0	5	20	50	0.50
5	Building height	0	5	20	50	1.50
6	Position of the building and type of foundations	0	5	20	50	0.75
7	Site and interaction	0	5	20	50	1.50
8	Plain irregularity	0	5	20	50	0.75
9	Height irregularity	0	5	20	50	0.75
10	Openings disalignement	0	5	20	50	0.50
11	Horizontal diaphragms	0	5	20	50	1.00
12	Roof system	0	5	20	50	1.00
13	Structural damage identified	0	5	20	50	1.00
14	Non-structural elements	0	5	20	50	0.50

Formisano *et al.* has also developed a vulnerability index methodology based on the same original methodology above mentioned but accounting for fifteen parameters (see table 5.3), wherein the last five parameters evaluate the influence of adjacent buildings upon each structural unit behaviour [Formisano *et al.* 2011b] [Formisano *et al.* 2011a].

Similarly to Vicente's methodology, the vulnerability index I_V^* were estimated for each structural unit according to the following equation 5.6. Moreover, the normalised vulnerability index mean value I_{V_m} was calculated to further confrontation with the remaining methodologies (see also subsection 5.3.2).

$$I_V^* = \sum_{i=1}^{15} C_{vi} p_i \tag{5.6}$$

Table 5.3: Vulnerability index assessment proposed for buildings in aggregate, adapted from [Formisano *et al.* 2011b].

	Parameter	Vulnerability Class A	B	C	D	Parameter Weight (p_i)
1	Organisation of vertical structures	0	5	20	45	1.00
2	Nature of vertical structures	0	5	25	45	0.25
3	Location of the building and type of foundation	0	5	25	45	0.75
4	Distribution of plan resisting elements	0	5	25	45	1.50
5	Plain irregularity	0	5	25	45	0.50
6	Vertical irregularity	0	5	25	45	$0.50 \div 1$
7	Type of floor	0	5	15	45	$0.75 \div 1$
8	Roofing	0	15	25	45	0.75
9	Details	0	0	25	45	0.25
10	Physical conditions	0	5	25	45	1.00
11	Presence of adjacent buildings with different height	-20	0	15	45	1.00
12	Position of the building in the aggregate	-45	-25	-15	0	1.50
13	Number of staggered floors	0	15	25	45	0.50
14	Structural or typological heterogeneity effect among adjacent structural units	0	-15	0	45	1.20
15	Percentage difference of opening areas among adjacent façades	-20	0	25	45	1.00

Adopting the principles of a macroseismic methodology it is possible to obtain the mean damage grade, μ_D, by the following equation 5.8 for different macroseismic EMS–98 intensities [Grünthal 1998]. Once defined the vulnerability index V (see equation 5.7) varying between 0 and 1, and the ductility coefficient Q of a determined building typology, which represents the ratio between the growth of damage and the seismic intensity, mean damage grade curves can be obtained.

$$V = 0.58 + 0.0064 I_V \tag{5.7}$$

$$\mu_D = 2.5 \left[1 + tanh \left(\frac{I + 6.25V - 13.1}{Q} \right) \right];\ 0 \leq \mu_D \leq 5 \tag{5.8}$$

where, the ductility coefficient Q, can be assumed in between 1.5 and 3.0 for masonry buildings, according to Vicente [Vicente 2008]. With the mean damage grade μ_D it is

possible to predict the damage distribution through histograms for different seismic intensities and vulnerability values. In this dissertation binomial and beta probability functions were used to construct these histograms of damage distribution [Spence *et al.* 2003], which formulation can be consulted in appendix D, at the end of this dissertation.

5.3.2 Vulnerability Index for Building Aggregates

The seismic vulnerability of building aggregates is becoming widely recognised since the influence of adjacent buildings is considered fundamental when interpreting post-event damages. The present methodology was developed by Vicente *et al.* and it is analogue to the previous vulnerability index methodology, based in the GNDT [GNDT-SSN 1994] but specifically developed for buildings in aggregate structural seismic assessment [Ferreira *et al.* 2012]. The vulnerability index is calculated as the weighted sum of five parameters related to four classes C_{vi} of growing vulnerability (from A to D). As shown in table 5.4 each parameter evaluates one aspect regarding the seismic response of the building aggregate assigning the vulnerability class through the analysis of different properties associated with mechanical, geometrical and inherent characteristics. Subsequently, for each one of these parameters a weight p_i is assigned, varying between 0.5 and 1.75, depending on the importance considered for each parameter. The value of the building aggregate vulnerability index $I^*_{V_a}$ (equation 5.9) ranges between 0 and 225. Finally, normalising the previous value, by means of a weighted sum, allows obtaining the vulnerability index I_{V_a} of the building aggregate.

$$I^*_{V_a} = \sum_{i=1}^{5} C_{vi} p_i \tag{5.9}$$

Table 5.4: Vulnerability index assessment parameters and weights [Ferreira *et al.* 2012].

	Parameter	Vulnerability class, C_{vi} A	B	C	D	Parameter weight (p_i) [-]	Vulnerability index $I^*_{V_a}$ [-]
P1	Quality of the masonry fabric	0	5	20	50	1.50	
P2	Misalignment of openings	0	5	20	50	0.50	
P3	Irregularities in height	0	5	20	50	0.75	$0 \leq I^*_{V_a} \leq 225$
P4	Plan geometry	0	5	20	50	0.75	
P5	Location and soil quality	0	5	20	50	0.75	

The methodology applied to construct the corresponding fragility curves and damage distribution histograms were the same as for the vulnerability index of individual buildings, already described in the previous subsection 5.3.1.

Part III

Discussion

Chapter 6

Global Analysis and Damage Assessment

6.1 Global Analysis Introduction

Global analysis assessment of buildings are extremely useful for the knowledge of the structure's behaviour subjected to seismic actions. From here, it is possible to detect structural deficiencies and important collapse mechanisms to then construct fragility curves and damage distribution estimations to further calibrate more simplified vulnerability assessment procedures.

Due to the structural complexity reflected by its irregularity and heterogeneity of the model under analysis, it was performed different trial and error combinations to understand the influence of some parameters over the global behaviour of the building aggregate.

Beyond the combinations provided by the NTC08, such as direction, eccentricity and pattern of pushing forces, it was assessed the effect of the variability of the masonry Young's modulus E, the control node location within the building, connection efficiency among structural elements and the presence of lateral constraints, which were considered and modelled to simulate the lateral support existing condition provided by the slope between the north and the south façade.

The massive stiffness of building aggregate in both directions is mainly given by huge wall thickness and overall dimensions since, as mentioned in section 4.3, the Young's modulus E considered for disorganized stone masonry was $E = 690\ N/mm^2$. In order to overcome some convergence issues during the running of the model, it was studied the effects of increasing this value up to the maximum value allowed by NTC08 [Candela *et al.* 2011] equal to $1440\ N/mm^2$. For values larger than $E = 690\ N/mm^2$ these attempts led to computational convergence issues.

The selection of the control node usually performs a crucial role in the analysis results and is motive of discussion among researchers. The author shares the hypothesis of the non-existence of a perfect control node, but nodes which represent with more accuracy the building behaviour when subjected to a seismic action in different directions. Firstly, on the contrary of regular buildings where these nodes are located in the higher storey of the structure, in this model the reference storey level of the control node is at the third storey. Secondly, a mass weighted displacement of all nodes at this storey was

assigned to face in-plan irregularities. As illustrated in figure 6.1, control node $N70$, located in between the most rigid structural units, has shown the more feasible and reliable behaviour. The 3muri® software has the ability to consider different connection

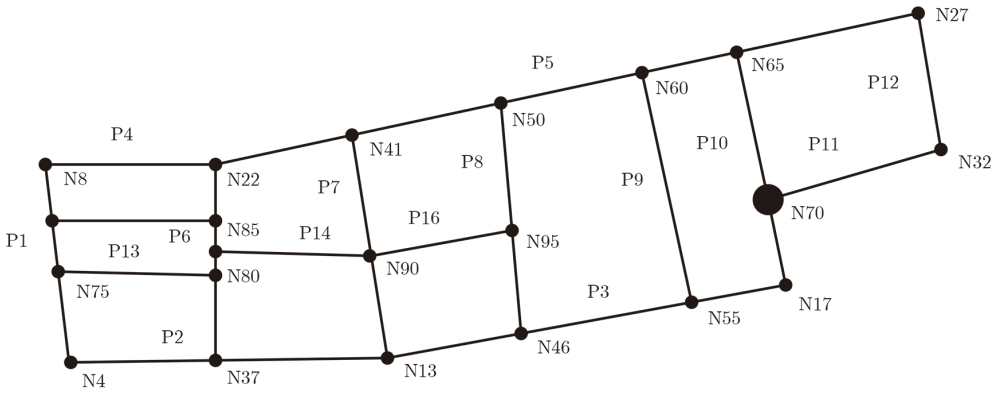

Figure 6.1: Nodes distribution upon the third storey and the chosen control node N70.

efficiency between horizontal and vertical structural elements, which directly affects the deformed shape of the structure. The total absence of any sort of information regarding this specific aspect led the author to evaluate the global behaviour in both situations. It was found reasonable considering the software default connectivity state, which leads to the most unfavourable analysis.

According to side elevations presented in section 3.4 it is possible to observe the existing slope acting passively on the north façade up to the second storey level, which behaviour can be idealised as a lateral spring support with infinite deflection along the slope direction. East and west elevations are also somehow constrained due to the presence of a flight of stairs. Although 3muri® is not prepared to represent properly the passive behaviour of this slope the author found interesting to change the supporting conditions in those walls constraining the node displacement in the respective direction. However, as expected, demand displacements resulted even smaller. Nevertheless, the mass participation factor, Γ, for each direction obtained through this specific analysis has become a key factor in the choice of the final analysis. Contradicting the majority of the analyses performed, in this analysis this value was considered feasible ($\Gamma < 1$), which allied with the more reliable representation of the structure supporting condition led the author to take into account this effect.

Combining the chosen particularities it was selected the most relative unfavourable analysis, which gathers feasibility and accuracy at the same time. Generally speaking this analysis includes a mass weighted displacement at the third storey control by node $N70$, accounting for the lateral constraints effect on the north façade inferior walls and considers the default wall-storey connectivity effect.

6.2 Capacity and Fragility

In this section it will be discussed the results related to the hybrid technique described in Chapter 4, from the pushover curves to the corresponding fragility curves and damage distribution.

6.2.1 Pushover and Capacity Curves

Pushover analysis was performed according to the modelling considerations already explained in sections 4.3 and 4.4. From the twenty-four different analyses performed using 3muri® for the "principal" analysis, it were distinguished the two most unfavourable pairs of analyses. The first one was performed considering the longitudinal and transversal negative directions for a modal load distribution with no accidental eccentricity, which will be referred hereinafter as *analysis 1*. This analysis has verified the safety verification with respect to ULS limit state. Subsequently *analysis 2* was performed in the U_x and U_y positive direction for the same load pattern but accounting for accidental eccentricity effects. In the next paragraph the author will discuss the general results obtained through this analysis. Later, *analysis 1* and *analysis 2* will be discussed with more detail.

Figure 6.2 illustrates separately the pushover curves for the longitudinal U_x and transversal U_y directions, plotting the mentioned *analysis 1* and *analysis 2*, but also U_xMass and U_y1stM, which grouped the remaining analyses into uniform and modal load distribution type. It is possible to observe a lower base shear force F_b value for the transversal direction U_y, being the most vulnerable direction of the structure. This foreseen statement was founded by the percentage of resistant elements which is significantly lower along this direction. In terms of base shear force, F_b, these values vary between 3000 and 6000 kN for the U_x direction. In the U_y direction, F_b varies between 2000 and 4000 kN, approximately. With respect to the control node ultimate displacements d_n, these values range between 0.4–1.6 cm and 0.4–1.0 cm for the U_x and U_y directions, respectively. The bilinear capacity curves were automatically generated by 3muri® software according to the methodology exposed in section 4.2.

From figure 6.3 it is observed that the base shear force of the equivalent SDoF system, F_y^*, varies roughly between 4000 and 6000 kN for both directions. The difference between yielding d_y^* and ultimate d_u^* displacements of the equivalent SDoF system was larger in the U_x direction varying from 0.4 cm to 1.8 cm. The mass participation factor Γ was numerically estimated at 0.65 and 0.86 for the U_x and U_y directions, accordingly.

The observed base shear force values are quite unusual and extremely high for traditional stone masonry structures. A simple relation between the total base shear force and gravity loads has proven this extremely high value, with this ratio varying between the impressive 26% and 60%, when for typical masonry buildings is estimated around 10%. Such value is likely to be justified by the small ratio between the volume of openings and the total volume of walls. Moreover, the large thickness of masonry walls, sometimes reaching a meter thick and the short span between structural walls increased the stiffness and subsequently, F_b. Figure 6.2 highlights the difference between both uniform and modal load distribution, in which the modal load distribution was estimated roughly 2000 kN below the uniform one. According to the bilinear capacity curves illustrated in figure 6.3, the ductility coefficient μ, unlike the U_y direction, varies significantly, from 1.00 up to 10.86.

The results obtained for *analysis 1* and *analysis 2* are highlighted in figure 6.2 and figure 6.3 and they are the two most unfavourable series from the "principal" analysis. Table 6.1 resumes the main parameters achieved for the referred pushover analysis, summarising both yielding and ultimate capacity, ULS spectral displacements and also another fundamental output values, allowing the confrontation of the building aggregate response in both planar directions. It is relevant to underline that the performance

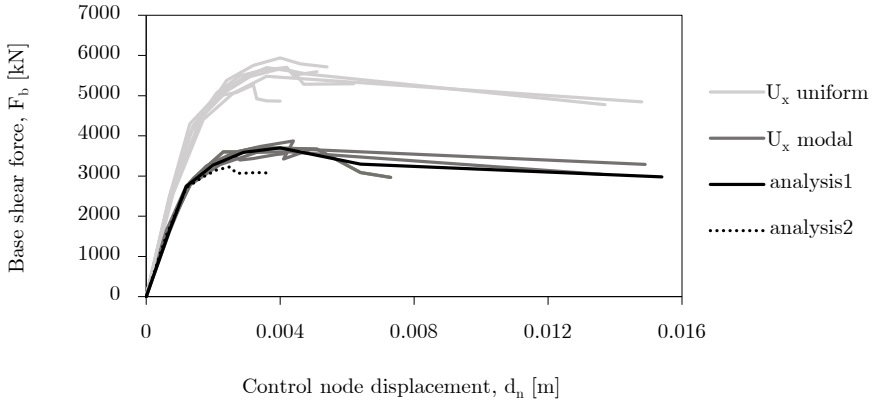

(a)

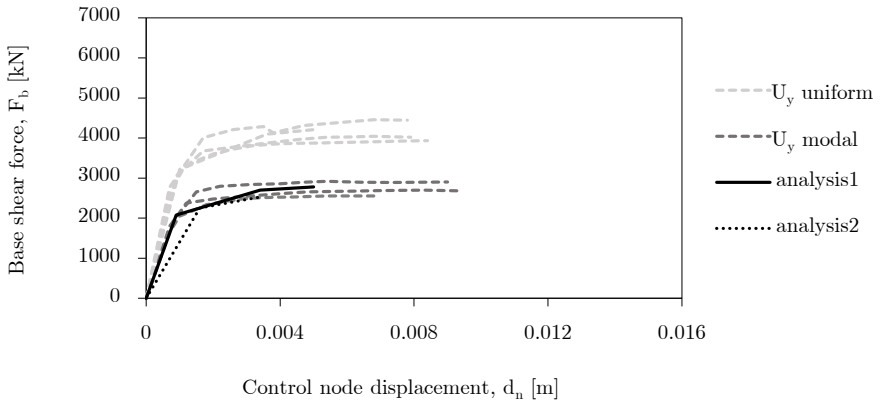

(b)

Figure 6.2: Pushover curves results. (a) U_x direction. (b) U_y direction.

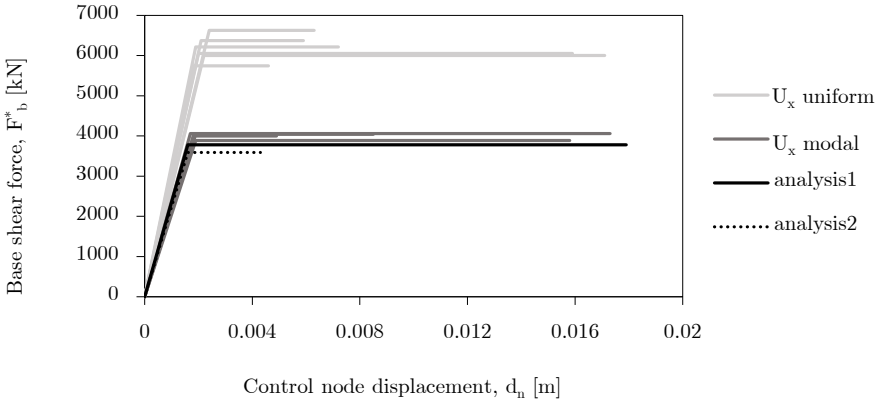

(a)

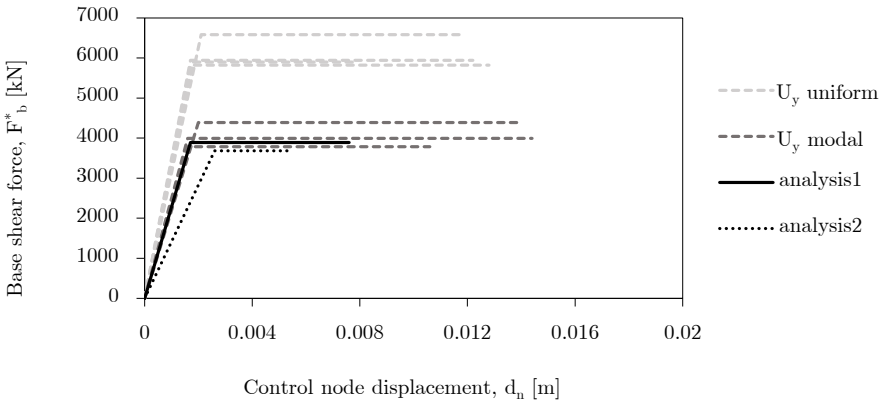

(b)

Figure 6.3: Bilinear capacity curves results. (a) U_x direction. (b) U_y direction.

point d_{max} values (also known as structural demand displacement), are used to estimate fragility curves. Thus, for *analysis 1*, d_{max} was evaluated as 0.33 cm for the longitudinal direction U_x and in 0.62 cm for the transversal direction U_y. Moreover, the displacement capacity of the structure d_u was equal to 0.50 cm and 1.54 cm for the U_x and U_y directions, respectively. The period T^* relative the equivalent SDoF system was evaluated as 0.12 s and 0.13 s for the U_x and U_y directions, respectively, being in accordance with the previous results since lower periods means lower displacements values. The first row of the table corresponds to *analysis 1* parameters while the second one is related to *analysis 2*.

Table 6.1: Overall output values achieved through the application of the CSM procedure.

Pushover curve direction	d_{max} [m]	d_u [m]	α_u [–]	Γ [–]	T^* [s]	F_y^* [kN]	d_y^* [m]	d_u^* [m]	A_y [g]	μ [–]
$-U_x$	0.0033	0.0050	1.24	0.65	0.12	3891	0.0017	0.0076	0.39	4.53
$-U_y$	0.0062	0.0154	1.62	0.86	0.13	3781	0.0016	0.0179	0.45	10.86
$+U_x$	0.0065	0.0037	0.73	0.86	0.13	3590	0.0016	0.0043	0.36	2.69
$+U_y$	0.0264	0.0046	0.26	1.08	0.26	1966	0.0026	0.0042	0.43	2.07

6.2.2 Fragility Curves and Damage Distribution

Since the formulation behind the use of this hybrid technique has already been exposed in section 5.2, it will be referred only the fundamental parameters used to construct fragility curves, which were based on the performance point definition of the structure. These curves were developed for the values of *analysis 1* since the corresponding values are likely more accurate, in particular the spectral displacement values.

Firstly, structural fragility was assessed by the median value of spectral displacement of the damage state d_s, $\overline{S_{dds}}$ and the standard deviation of the natural logarithm of spectral displacement of damage state d_s, β_{ds}, which were obtained from table 5.9 c of HAZUS MH-MR3 [FEMA 2003] for unreinforced masonry bearing walls URMM (medium height building) class and considering a low-code seismic design level (assigned henceforth as $H_{5.9}$). It was applied another group of given parameters representing special buildings structural fragility for the same building class URMM (assigned from now on as $H_{6.4}$), which is presented in table 6.4 c of the same manual [FEMA 2003]. These values were equally assigned for both directions and they are shown in table 6.2.

Secondly, according to the formulation described in sec 5.2, another methodology was applied, henceforth named $DLSF$, based on particular points of the capacity curve (a function of the yielding and ultimate capacity).

Figures 6.4 and 6.5, on page 70 and 71, respectively, illustrate the confrontation between fragility curves for each direction, respectively. For $H_{5.9}$ (a) and $H_{6.4}$ (b) curves, almost no evidences of damage were found for the performance point spectral displacement value for both directions, whereas for $DLSF$ definition the fragility curve shows larger values of damage. As d_{max} is larger in the U_y direction for the both methods, the corresponding expectable damages result slightly higher when compared to the longitudinal direction U_x (see figure 6.5 on page 71).

The damage distribution was simply estimated from fragility curves, evaluating the level of each damage grade for the considered demand displacement. Figure 6.6 on page 70 illustrates such distributions from where it is possible to observe $H_{5.9}$ damage probabilities in the U_x direction of 95.9%, 3.5% and 0.6%, accordingly for structural damage grades D_{k_0}, D_{k_1} and D_{k_2}, which corresponds to none, slight and moderate structural damage grades, respectively. In the U_y direction and for the same damage grades D_{k_0}, D_{k_1} and D_{k_2} damage distribution probabilities were estimated in 85.1%, 11.2% and 3.6%, respectively. The damage distribution of $H_{6.4}$ resulted even more sharp than the previous one, raising no significant concern. Notwithstanding, $DLSF$ damage distribution is evidently centred around D_{k_2}, valuing the respective probability of damage of 38.0% and 52.3% in the U_x and U_y directions. As figure 6.6, on page 6.6 illustrates there are significant differences in $H_{5.9}$ and $H_{6.4}$ distributions when compared to $DLSF$. In order to compare results between hybrid and indirect techniques it was selected the damage distribution $DLSF$ as the representative distribution of the hybrid technique since it is consistent with the damage observed on walls in the previous subsection 6.2.3.

Table 6.2: Values proposed by HAZUS-MH-MR3 [FEMA 2003], for the URMM (Unreinforced Masonry Medium Height Building) Low-code building class.

	Damage state, S_{d_i}							
	Slight		Moderate		Severe		Extensive to collapse	
	S_{d_1} [m]	β_1 [–]	S_{d_2} [m]	β_2 [–]	S_{d_3} [m]	β_3 [–]	S_{d_4} [m]	β_4 [–]
$H_{5.9}$	0.016	0.91	0.032	0.92	0.080	0.87	0.187	0.91
$H_{6.4}$	0.020	0.81	0.040	0.84	0.100	0.87	0.233	0.82

6.2.3 Damage and Failure of Walls

In this subsection special attention was given to the damage evolution for the structural elements which was displayed wall-by-wall and step-by-step through the user-friendly software capability. This interesting function allows the user to immediately identify the most vulnerable elements, from which it is expectable the structure starts to collapse. Then, this evaluation can be individualised with more detail for the development of rehabilitation solutions for each type of damage. The individual wall damage assessment through pushover analysis was only developed for *analysis 2* in which damage on walls was found more meaningful.

Starting with the U_x direction, as illustrated in figure 6.7 on page 73, the walls from the lower storeys which were constrained to roughly represent storeys laterally against the ground, have shown practically no damage. From figure 6.1 on page 64 it is visible the location of walls within the building aggregate, giving support to the following comments. Spandrel beams were the most affected element with respect to flexural bending damage reaching failure in a few cases, as observed on walls *P5* and *P11*. Shear damage was sporadically observed in some piers on walls *P3*, *P5* and *P14* while tension failure was assigned to rigid nodes on the majority of walls. The same figure illustrates the damage distribution for *analysis 2* on wall *P5*, one of the most damaged walls in the U_x direction. As illustrated, compression failure can be observed in piers corresponding to the storey

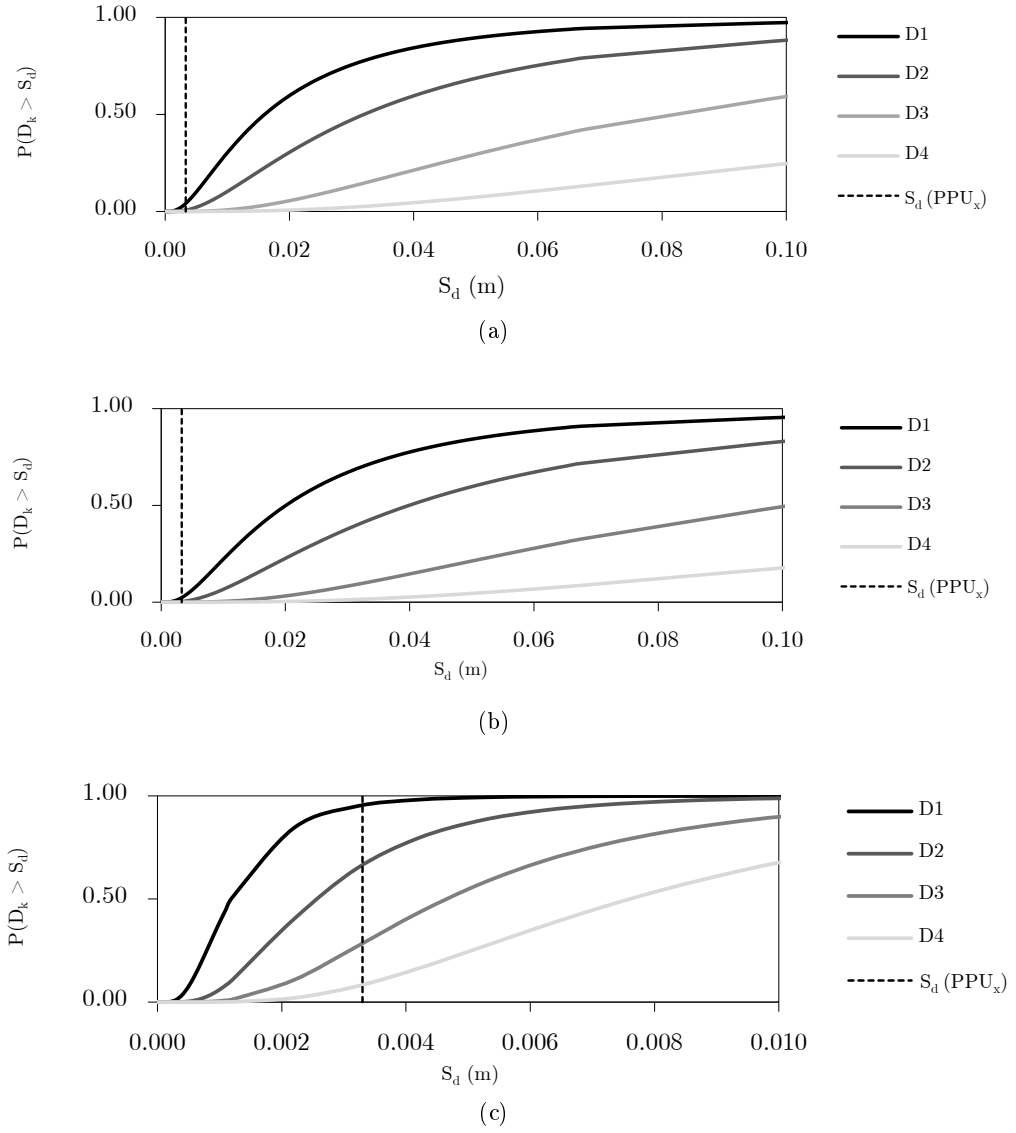

Figure 6.4: Fragility curves corresponding to the U_x direction of *analysis 1*. (a) $H_{5.9}$. (b) $H_{6.4}$. (c) $DLSF$ fragility curves defined through the nominal mean values described in section 5.2 [Grünthal 1998].

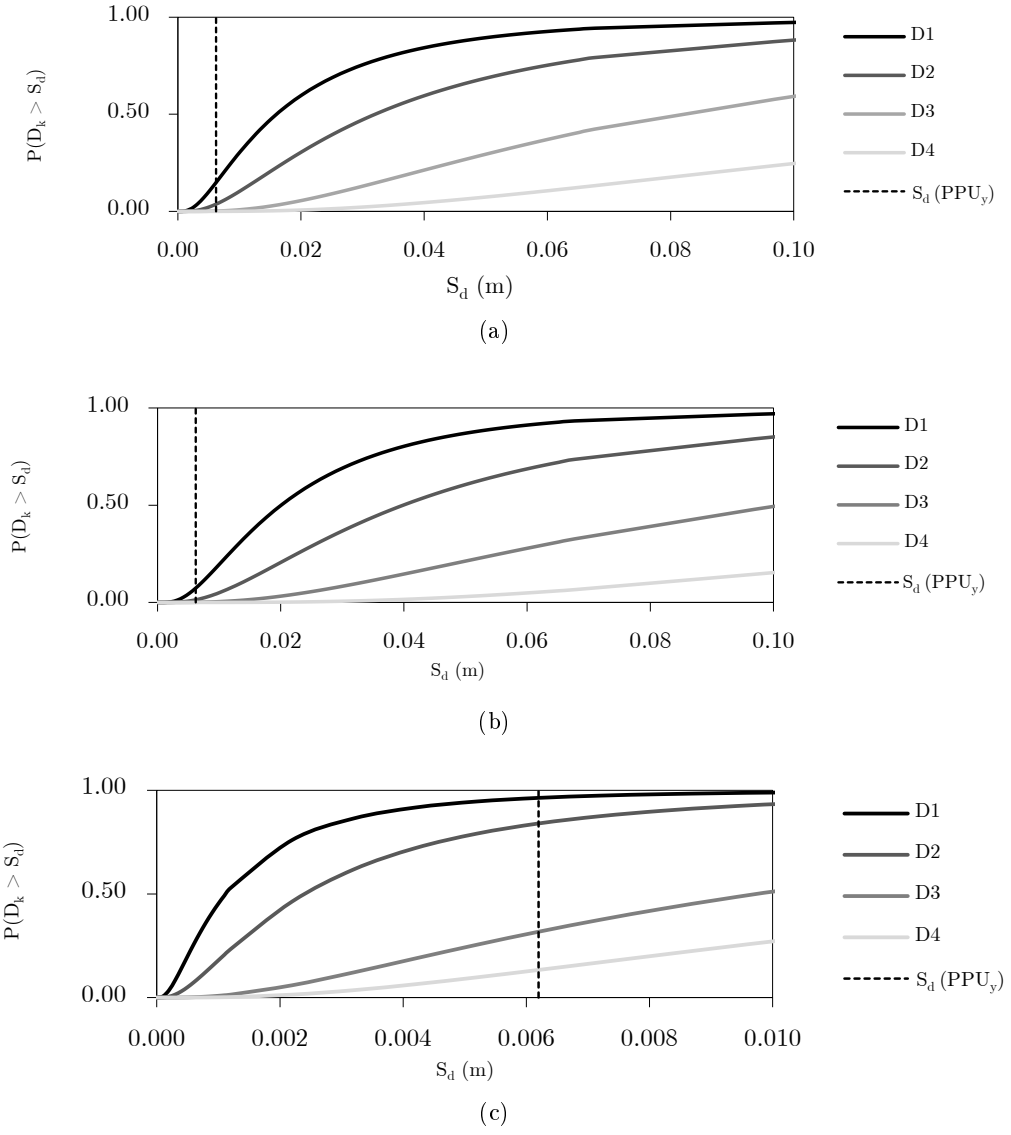

Figure 6.5: Fragility curves corresponding to the U_y direction of *analysis 1*. (a) $H_{5.9}$. (b) $H_{6.4}$. (c) $DLSF$ fragility curves defined through the nominal mean values described in section 5.2 [Grünthal 1998].

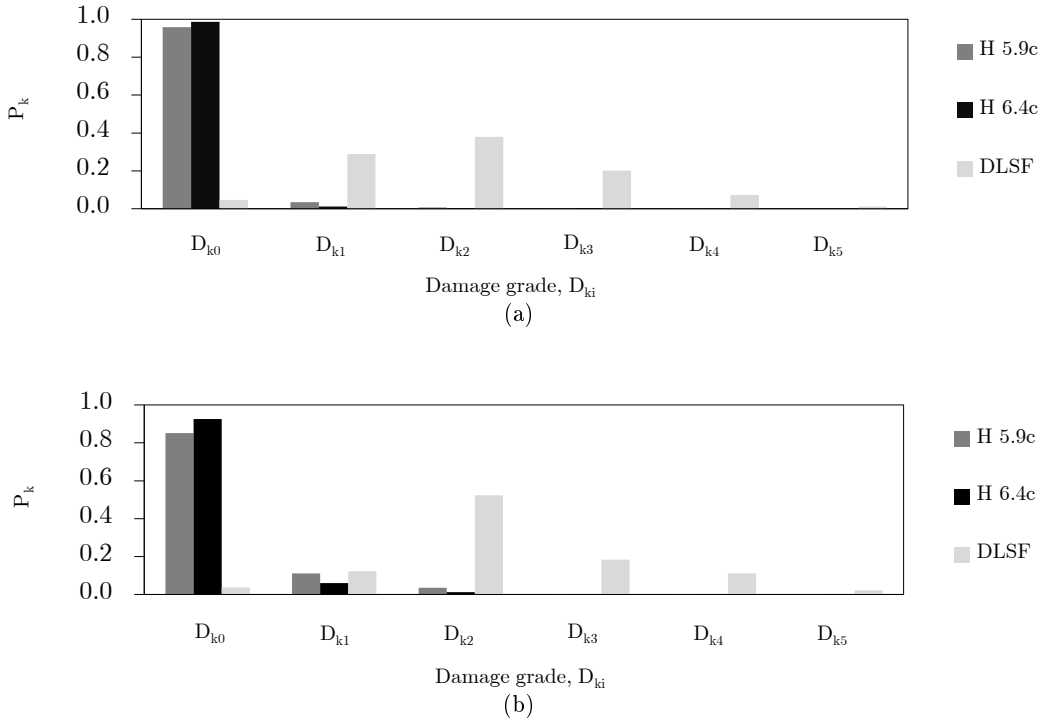

Figure 6.6: Damage distribution comparison between $H_{5.9}$, $H_{6.4}$ and $DLSF$ (defined through the nominal mean values described in section 5.2). (a) U_x and (b) U_y directions.

level 1. With respect to *analysis 2* damage distribution it is interesting to observe that interior walls aligned with the transversal direction U_y show practically no damage in piers elements. No more significant damages were assigned in this direction and no evidences of any type of failure mechanisms were found.

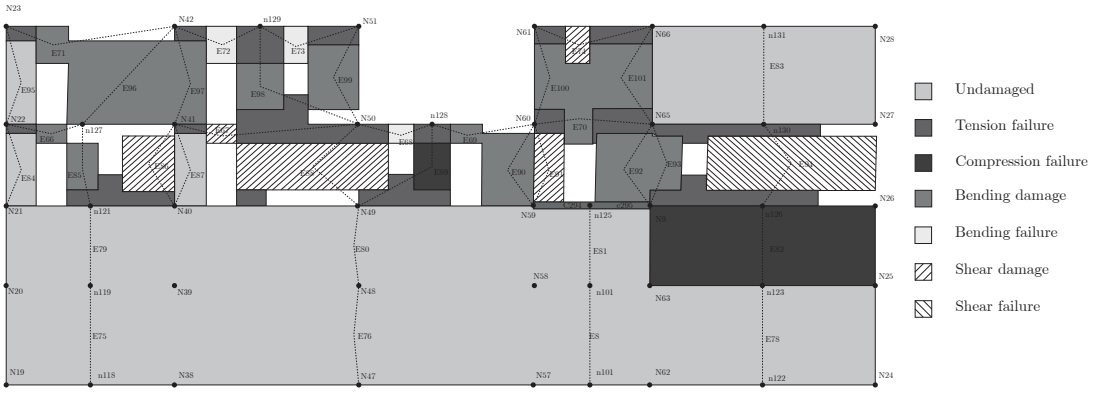

Figure 6.7: Damage distribution on wall *P5* for the U_x direction of *analysis 2*.

With respect to the U_y direction walls from *P1* to *P9* have shown meaningful signs of the presence of the well-known soft-storey mechanism at the storey level 3, where the structure is no more laterally constrained. Piers along this storey reached the shear failure, contributing to the development of this in-plane failure mechanism. On wall *P2* and *P3* several piers have reached the flexural bending failure at the mentioned vulnerable storey level 3. Tension failure is observed in rigid nodes approximately with the same frequency as in the previous direction, as well as compression failure, which occurs at the storey level 1 on walls *P5* and *P11*. Figure 6.8 on page 73 shows the damage distribution on the same wall *P5* this time for the U_y direction.

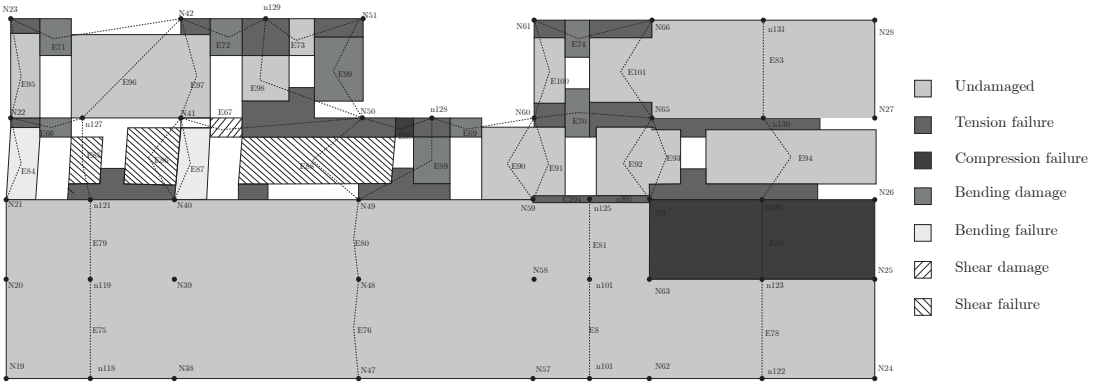

Figure 6.8: Damage distribution on wall *P5* for the U_y direction of *analysis 2*.

6.3 Vulnerability Index for Individual Buildings

In this section two different indirect techniques were applied for the vulnerability assessment of the building aggregate through estimating vulnerability index values I_V for each individual structural unit, whose formulations were described in subsection 5.3.1. Then a mean vulnerability index I_{V_m} was estimated representing the building aggregate vulnerability index. Firstly, it was applied Vicente's proposal for the evaluation of the vulnerability index of individual buildings [Vicente 2008]. Secondly a similar proposal developed by Formisano *et al.* was used with exactly with the same purpose [Formisano *et al.* 2011b].

The parameters belonging to each formulation were evaluated accounting for the information available in *Scheda di Aggregato* report summarised in Chapter 3. In order to better understand the most vulnerable units according to these methods, figure 6.9 illustrates and identifies the location of each structural unit within the building aggregate. It was considered that the individual evaluation of these structural unit parameters were estimated with reasonable accuracy. The results obtained are shown in table 6.3, where $I_{V_{vic}}$ and $I_{V_{for}}$ represent henceforth the vulnerability index of Vicente and Formisano *et al.* distinct formulations, respectively. Figure 6.10 illustrates the differences between the obtained vulnerability index values. In both formulation structural unit *US F* and *US B* result as the most and less vulnerable units of the building aggregate, accordingly. Row end positioned buildings *US A* and *US F* show higher vulnerability index values. These vulnerability index values differ 14.9%, 36.7% and 13.7% in structural units *US A*, *US B* and *US C*, respectively, being these values higher in Vicente's methodology. Although both methods were based on GNDT methodology they show several differences regarding their formulation [GNDT-SSN 1994]. As shown in tables 5.2 and 5.3, in section 5.3 Vicente's methodology accounts fourteen parameters for individual building assessment while Formisano *et al.* methodology gathers ten parameters for individual buildings assessment plus five new parameters related to the aggregated conditions among adjacent buildings. Likewise their formulation definition for these parameters were also developed for distinct class values C_{vi} and weights p_i.

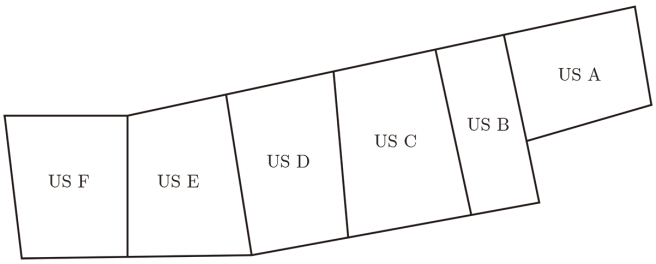

Figure 6.9: Building aggregate structural units individualisation.

The mean vulnerability index values $I_{V_{vic,m}}$ and $I_{V_{for,m}}$ were evaluated as 38.7 and 34.6, respectively. Over these values distinct mean damage grade μ_D were estimated for several seismic intensities according to the EMS–98 macroseismic scale [Grünthal 1998]. The ductility coefficient Q of the equation 5.8 was considered equal to 2.3, as suggested for this type of masonry [Vicente 2008]. Figure 6.11 shows the fragility curves comparison between the two vulnerability index values, where no relevant differences

Table 6.3: Structural unit vulnerability index values for both methodologies.

	US F	*US E*	*US D*	*US C*	*US B*	*US A*
$I_{V_{vic}}$	60.4	39.0	39.0	33.3	23.8	36.5
$I_{V_{for}}$	57.3	38.8	36.9	28.7	15.1	31.1

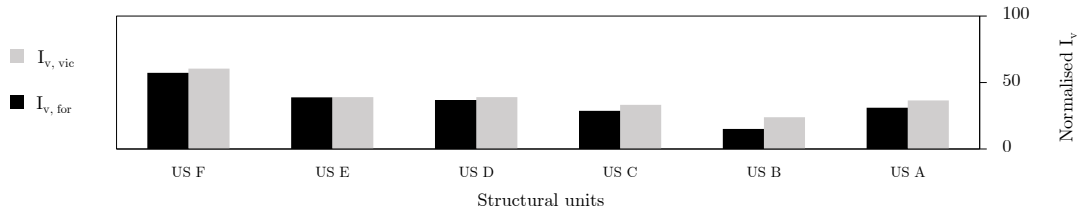

Figure 6.10: Comparison between Vicente and Formisano *et al.* methodologies for each structural unit.

were noted revealing slight dependence between seismic intensity range of VII–IX. The resulting vulnerability curves obtained for both mean fragility index values are shown in figure 6.12. Moreover, figure 6.13 compares damage distributions caused by different selected earthquake intensities in terms of the mean damage grade, μ_D. In order to obtain such distribution the parameter t, which is responsible for the dispersion of beta probability density function developed by Bernardini *et al.*, was assigned equal to 12.0 [Vicente 2008] [Bernardini *et al.* 2007b].

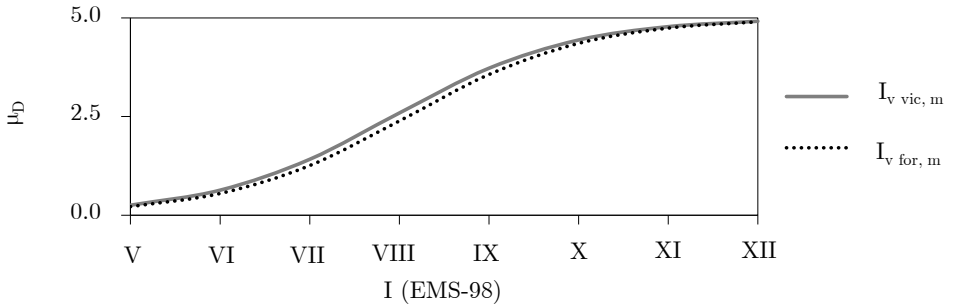

Figure 6.11: Fragility curves representing the mean damage grade μ_D for different seismic EMS–98 intensities, estimated for mean vulnerability index values (a) $I_{V_{vic,m}}$ and (b) $I_{V_{for,m}}$.

6.4 Vulnerability Index for Building Aggregates

The following methodology was developed by Vicente *et al.* for the seismic assessment of building aggregates [Ferreira *et al.* 2012] and it is based on the previous method developed by Vicente for individual buildings vulnerability assessment [Vicente 2008].

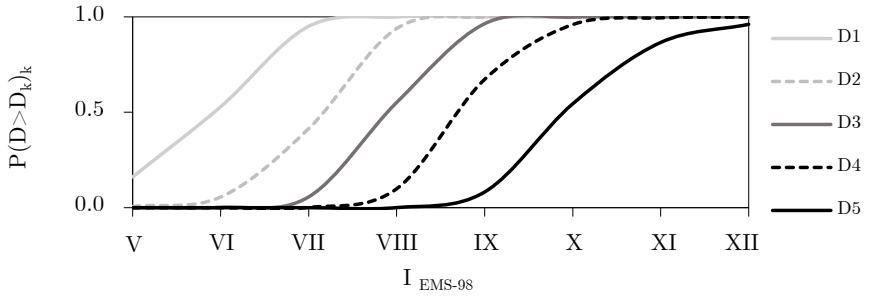

(a)

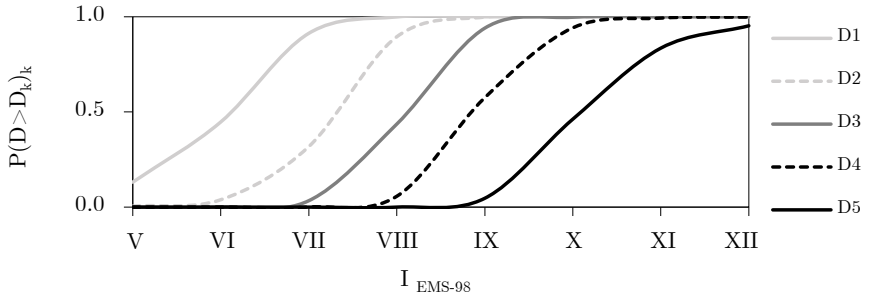

(b)

Figure 6.12: Fragility curves representing the mean damage grade μ_D corresponding to different EMS–98 intensities. (a) Fragility curves corresponding to the mean vulnerability index $I_{V_{vic,m}}$. (b) Fragility curves corresponding to the mean vulnerability index $I_{V_{for,m}}$

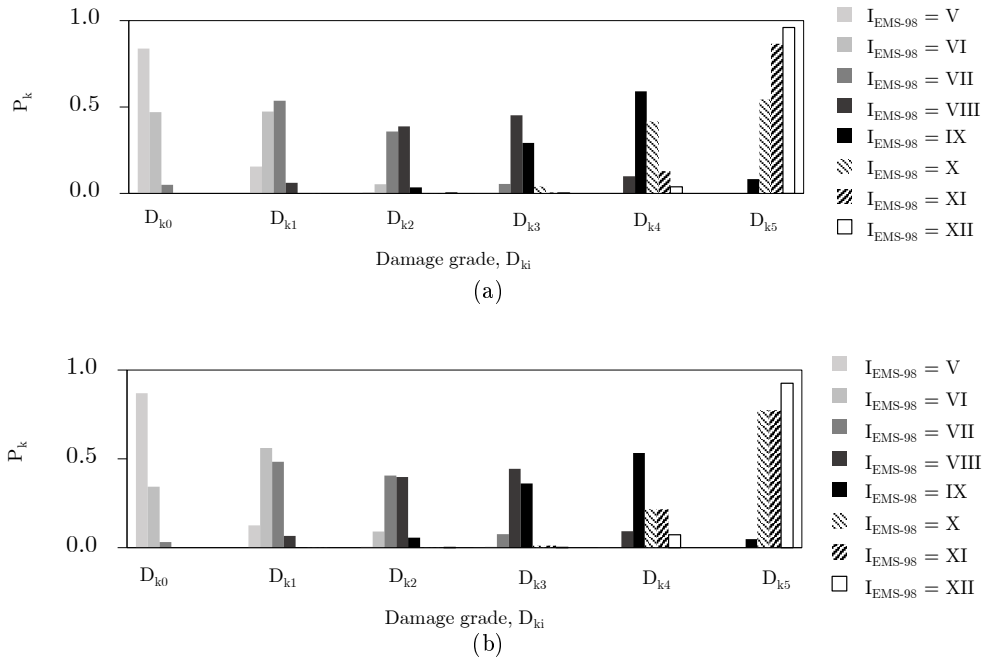

Figure 6.13: Damage scenario (EMS–98 macroseismic scale) for the mean damage grade μ_D values for (a) Vicente and (b) Formisano *et al.* formulations.

Further detailed information regarding this procedure can be consulted in section 5.3.2 of this dissertation. The vulnerability index I_{V_a} estimated for the building aggregate under analysis was 38.3. On one hand this value is too close to the mean vulnerability index $I_{V_{vic,m}}$, while on the other hand the aggregate vulnerability index value I_{V_a} differs approximately 10% when compared to Formisano *et al.* mean vulnerability index value $I_{V_{for,m}}$. The approach to the vulnerability functions estimation and the respective mean damage grade was exactly the same as in the previous section 6.3. In this way, the following figure 6.14 illustrates the vulnerability curve representing the mean damage grade values μ_D for different seismic intensities obtained through the aggregate vulnerability index I_{V_a}.

6.5 Comparison of Results

In this section the previous methodologies will be compared to each other. Firstly, it is explained the correlation law used to associate EMS–98 scale to PGA values in order to compare the damage distribution histograms obtained in subsection 6.2.2 with the ones obtained using indirect techniques, discussed in previous sections 6.3 and 6.4. Afterwards they will be compared individually all the methodologies applied, with respect to the damage probability estimation for the D_{k_i} damage grades for two particular macroseismic intensities.

The mentioned correlation between EMS–98 scale and the PGA value is defined by the following equation 6.1, a function developed by Lagomarsino and Giovinazzi which allows

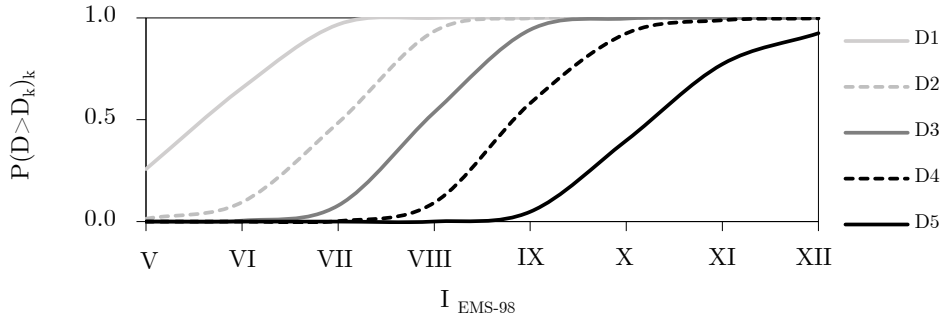

Figure 6.14: Fragility curves representing the mean damage grade μ_D for different EMS-98 intensities, estimated for the aggregate vulnerability index value I_{V_a}.

to compare the damage distribution of both hybrid and indirect techniques [Lagomarsino and Giovinazzi 2006].

$$a_g = c_1 c_2^{(I-5)} \tag{6.1}$$

where a_g is the peak ground acceleration in g, I is the EMS–98 macroseismic intensity value, c_1 is the coefficient who defines the PGA value for a default macroseismic intensity V and c_2 defines the slope of the correlation curve. As shown in table 6.4 three different correlation laws developed by Guarenti–Petrini, Margottini and Murphy–O'Brien, were used to estimate the corresponding EMS–98 intensity I for a peak ground acceleration value a_g equal to 0.255 g [Guarenti and Petrini 1989] [Margottini *et al.* 1992] [Murphy and O'Brien 1977]. Therefore, for this PGA value a macroseismic intensity VIII was determined, according to Guarenti–Petrini correlation law. On the contrary, using the correlations proposed by Margottini and Murphy–O'Brien the same PGA has led to an equivalent EMS–98 macroseismic intensity of IX. In this way, considering and equivalent EMS–98 macroseismic intensity based on the same PGA value used to perform the pushover analyses it is possible to compare the damage distribution obtained through hybrid techniques with the indirect techniques results. In the following paragraphs will be discussed the comparisons between those techniques.

Table 6.4: Values of c_1 and c_2 for $I_{EMS-98} - PGA$ correlation laws according to different authors.

Correlation law	c_1	c_2
Guarenti–Petrini	0.03	2.05
Margottini	0.04	1.65
Murphy–O'Brien	0.03	1.75

Figure 6.15 illustrates the following damage distribution for EMS–98 macroseismic intensities VIII and IX of all the applied methodologies together. Facing $I_{V_{vic,m}}$ and $I_{V_{for,m}}$ damage distributions it was observed a maximum deviation in D_{k_3} equal to 7.3% and 7.4%, for $I_{EMS-98} = VIII$ and $I_{EMS-98} = IX$, respectively. When comparing $I_{V_{vic,m}}$ with I_{V_a} these difference was substantially reduced to 1.1% for $I_{EMS-98} = VIII$. From comparing $I_{V_{vic,m}}$ to $DLSF$ distributions, differences resulted more noticeable since

they have reached 25.1% and 51.8% for the U_x direction and 26.8% and 48.8% for the transversal direction U_y. When compared to $I_{V_{vic,m}}$ general results, smaller deviations were obtained for most of the comparisons with $I_{V_{for,m}}$. For $I_{EMS-98} = VIII$ the maximum deviation value of 6.4% was found comparing it to I_{V_a}. The maximum difference for $I_{EMS-98} = IX$ was markable, since it goes against the trend observed, in which higher deviation values were expected for this intensity, being in this case 0.4%. The comparison between $I_{V_{for,m}}$ and the longitudinal direction of $DLSF$ reached the largest difference of 18.5% and 45.6% for $I_{EMS-98} = VIII$, whereas for $I_{EMS-98} = IX$ the maximum difference was 19.5% and 46.4%, respectively. Finally comparing I_{V_a} for both directions of $DLSF$ distribution, is was registered a maximum deviation of 24.2% and 46.0% in the U_x, while in the U_y direction these differences were 25.9% and 46.6%, respectively. Figure 6.16 illustrates the corresponding damage grade D_{k_i} for each maximum deviation percentage for both $I_{EMS-98} = VIII$ and $I_{EMS-98} = IX$ intensities. From comparing the vulnerability index based on different methodologies for an earthquake with intensity $I_{EMS-98} = VIII$, better approximations were found between the I_{V_a} and $I_{V_{vic,m}}$, where the most significant difference among the corresponding damage distributions shown a maximum value of 1.1%, respectively for damage grade D_{k_1}. The same comparison but for a $I_{EMS-98} = IX$ earthquake have evidenced the $I_{V_{for,m}}$ as the best approximation to I_{V_a} with maximum discrepancy of 0.4% for damage grade D_{k_4}. Finally, comparing these last methodologies to the ones derived from the numerical analysis it is possible to observe larger disparity in percentage terms for both macroseismic intensities, being this discrepancy even higher for $I_{EMS-98} = IX$.

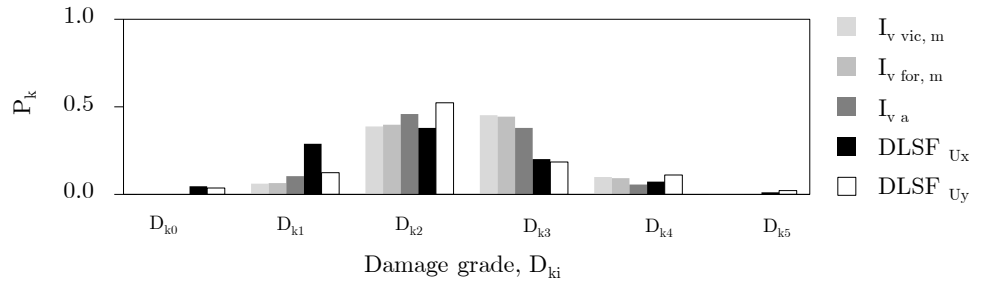

(a)

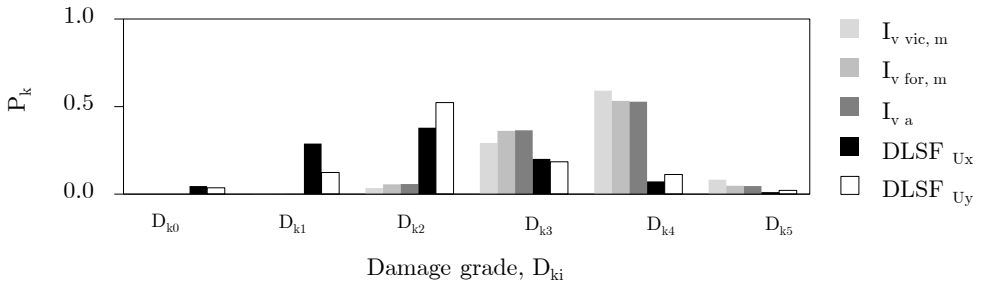

(b)

Figure 6.15: Damage distribution comparison between the three analysed vulnerability index formulations for different macroseismic intensities. (a) $I_{EMS-98} = VIII$. (c) $I_{EMS-98} = IX$.

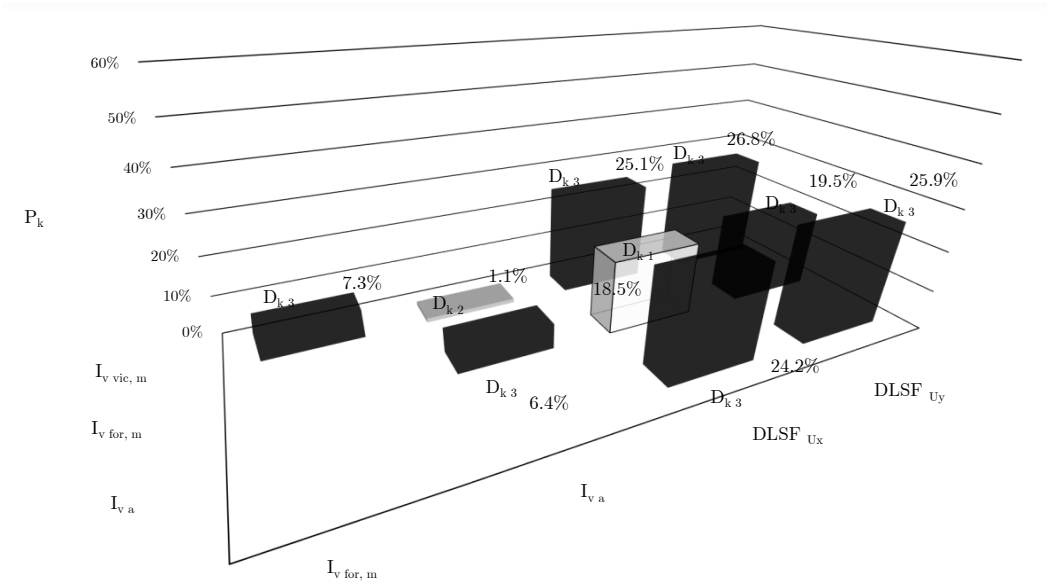

(a)

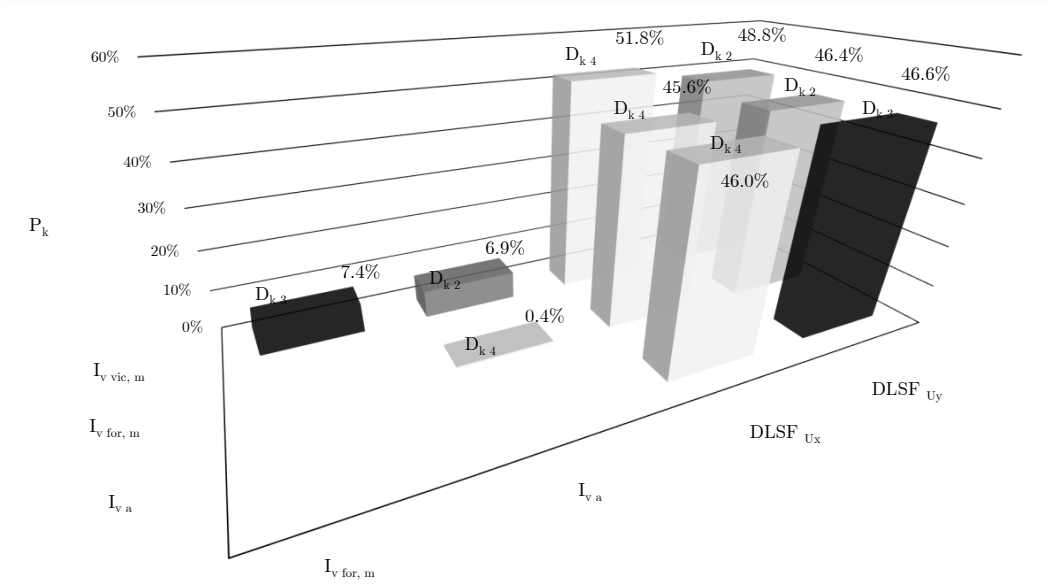

(b)

Figure 6.16: Damage grade D_{k_i} corresponding to the maximum deviation value among damage distribution percentage of all methodologies. (a) $I_{EMS-98} = VIII$. (b) $I_{EMS-98} = IX$.

Chapter 7

Conclusions and Future Work

7.1 General Comments

The work developed in this dissertation was part from this initial learning process in seismic engineering, particularly in the seismic vulnerability assessment of old masonry building aggregates. The natural lack of experience in these matter may have not led to the best contribute for science, but in general, the objectives proposed were attained. Among other tasks, it was developed the knowledge over different methodologies related to the seismic vulnerability assessment of existing buildings. In particular, non-linear static analysis was performed to assess the seismic vulnerability of the building aggregate through different fragility curve parameter definitions. Moreover, the seismic vulnerability was assessed resourcing to the vulnerability index methodology, where the influence of adjacent buildings was evaluated.

Building aggregates result as a middle term scale class of buildings, which optimal assessment should embrace numerical analysis for a more detailed analysis, depending on the objective of the project in hands. The accuracy in the outcomes obtained through non-linear static analysis were found clearly influenced by the input analysis parameters, such as the mechanical and geometrical properties of the structure. Therefore, the structural survey accuracy is reflected in the analyses results. With respect to building aggregate case study, this survey, provided by the University of Pisa, was found to be insufficient and inconclusive. Moreover, the lack of photo registration highlighting the damage observed in the structure did not allow detailed interpretation of such data.

7.2 Main Conlusions

Working with 3muri® software was not an easy challenge as expected, mostly due to the particularities of building aggregate case study and to the lack of structural information regarding several properties, who had been assigned through standard assumptions for these type of structures, which brought several convergence and numerical errors. The fact of not being widely used in Portugal, turned the author mission even more difficult. It was found the mechanical properties of structural materials as the major source responsible for those errors, due to their heterogeneity. This program is capable to deal with masonry or mixed structures, but it is not prepared to assess mixed masonry buildings with RC walls. Once the case study had RC elements the author, advised by few opinions from experts with this particular software, assigned a new masonry material

with mechanical properties corresponding to reinforced concrete. Thus, the building aggregate, which was already very stiff (due to the large quantity and thickness of walls) became even more stiffer. While in-plan irregularities were successfully overcome, causing no numerical issues, in-height irregularities were considered more problematic, since they affect the nodal displacements, which can somehow compromise the safety verification and the analysis convergence. It is thought that this initial aspect influences directly the pushover analysis and the respective outputs. Besides these inherent difficulties this software remains extremely useful for global safety assessment of masonry structures relatively regular. Nevertheless, its capabilities were found very useful, in particular with respect to the damage assessment facilities. The results from the pushover analysis indicate the safe condition with respect to the ULS limit state, since the maximum spectral displacement obtained for the longitudinal and transversal direction were respectively 0.33 cm and 0.62 cm against the 0.50 cm and 1.54 cm ultimate displacements. The analysis performed indicates the transversal direction as the most vulnerable, which is coherent with the real damage verified in the *Scheda di Aggregato* report, in which transversal walls were significantly more damaged. The base shear force values have confirmed the expected resistance of the structure due to its large stiffness and overall geometry. The lower node displacement values of the pushover analysis were a consequence of the effort of representing the behaviour of the slope between the two principal façades through modifying the lateral supporting condition of the structure. This assumption is clearly found too conservative and is thought to be related with some inconsistencies regarding pushover and capacity curves.

The damage and failure of walls estimated through the pushover analysis identifies, for the U_x direction spandrel beams as the most damaged element due to flexural bending failures. Regarding the U_y longitudinal direction it was observed a symptom of soft-storey mechanism at the third floor level, as a direct consequence of the assumption mentioned above, related to the lateral supporting condition of the north façade, that is thought to be somehow exaggerated. It is known that walls along this direction were significantly affected by diagonal shear cracks, which may transcribe the beginning of the referred mechanism. In general, it is sensible to affirm that the damage estimated by the pushover curves are somehow assimilated to the real damage distribution in the aggregate, both in terms of extension and in type of failures.

With respect to all fragility curves, the methodology based on the capacity curve led to better results, likely to be approximated to the real observed damage. Nonetheless, this methodology was found more conservative when compared to the *Scheda di Aggregato* report data, in which the damage grade D_{k_3} ruled the damage distribution.

Indirect techniques were carried out to compare their accuracy when compared with hybrid techniques. With respect to the individual structural assessment, the methodology proposed by Vicente shown slight differences by excess in structural units vulnerability index, when compared to Formisano *et al.* methodology. For structural units USF, USE and USD were attributed the highest vulnerability index values, of 60.4, 39.0 and 39.0 for Vicente methodology, while for Formisano *et al.* methodology these values were 57.3, 38.8 and 36.9. It was found important deviations between these two methodologies for structural units USA, USB and USC, which identifies the parameters relative to masonry material heterogeneity as the most different among both methodologies. On the contrary, structural units USD, USE and USF shown great resemblance between them, with deviations below 5.5%. Moreover, to row end structural units USA and USF are

associated a higher vulnerability index values, in agreement with the later studies conclusions regarding building aggregates vulnerability assessment. Mean vulnerability index values were estimated for the previous methodologies in order to construct a prediction of the building aggregate vulnerability suitable to be compared with the building aggregate vulnerability index formulation, proposed by Vicente *et al.*. This vulnerability index evaluated for the aggregate was estimated as 38.3, against the values 34.6 (for Formisano *et al.* mean vulnerability index) and 38.7 (for Vicente mean vulnerability index). Therefore, on one hand, aggregate vulnerability index methodology approximates very accurately the mean vulnerability index values of Vicente's methodology. On the other hand the vulnerability index of Vicente and Formisano *et al.* were found to be in conformity for comparatively regular buildings. The conversion of the mechanistic approach using the EMS–98 macroseismic scale was found to be a reasonable way of establish comparisons with indirect approaches. Thus, it was possible to conclude that for a seismic intensity $I_{EMS-98} = VIII$ indirect techniques were found more representative of the real damage distribution in the building aggregate, from which aggregate vulnerability index methodology has shown as the less conservative of the three vulnerability index methodologies. With respect to the $I_{EMS-98} = IX$ indirect techniques revealed to be too conservative, while mechanistic techniques on the contrary failed the approximation by default. These comparisons among hybrid and indirect techniques were found to be somehow inaccurate for extreme macroseismic intensities very similar for medium macroseismic intensities. With this dissertation it was evident data accuracy subsequent implications on numerical analysis outputs, which can lead to unreliable results and interpretations. This way, these computational analysis should be compared to quick vulnerability assessment methods in order to detect possible problems of numerical model environment. To avoid this, scientists should be aware and conscious if the knowledge level and survey related to a generic study gathers all data necessary to obtain feasible results. When this knowledge requirements are considered insufficient, it is preferable to conduct the analysis through empirical methodologies, which are proven to give satisfactory predictions about damage either assessing individual buildings or building aggregates seismic vulnerability.

7.3 Future Work

Further developments on the seismic vulnerability assessment through numerical and index method analysis may be taken to extent comparisons and generally improve the results obtained. With respect to this particular building aggregate case study the following future tasks and ideas may be raised:

- It is mandatory a detailed review of the developed survey, regarding the soil type, the mechanical properties of the existing structural materials, the geometrical properties of the aggregate (in particular the wall's thickness) and the level of damage observed in each structural unit in order to re-evaluate the accuracy of the results obtained through numerical analysis;

- A survey under the referred terms would motivate further analyses to be considered to calibrate the actual numerical model. As alternative, different soil category types, return periods and peak ground accelerations should be analysed to assess the respective responses;

- Numerical analyses are suitable to be performed both for the building aggregate itself and for the each structural unit, independently;
- Further comparisons between the damage distributions estimated through the previous numerical analysis and the ones provided by the vulnerability index methodologies should be developed to estimate properly the accuracy of such methodologies;
- Extend these referred procedures to distinct building aggregates, rather homogeneous, to understand the influence of structural diversity. It may be useful to evaluate the impact of current mechanical properties assigned for concrete walls over the non-linear static analysis and to track convergence problems on the modelling;
- Expand numerical analysis through 3muri® to similar stone masonry old building aggregates in *San Pio delle Camere* to compare the reliability of those models and to understand how diverse the damage distribution of different buildings within the same historical centre can result;
- The use of different vulnerability index formulations to assess historical centres at a large scale (with larger samples), with the prediction of damage scenarios, would increase the confidence and accuracy level regarding the vulnerability index methodology proposed to the assessment of building aggregates;
- Explore the new available add-in feature in 3muri®, which is expected to overcome the roof system assignment handicap, giving a better approximation of the influence of the roof system over the resistant façade wall system.

Appendices

Appendix A

Scheda di Aggregato Report

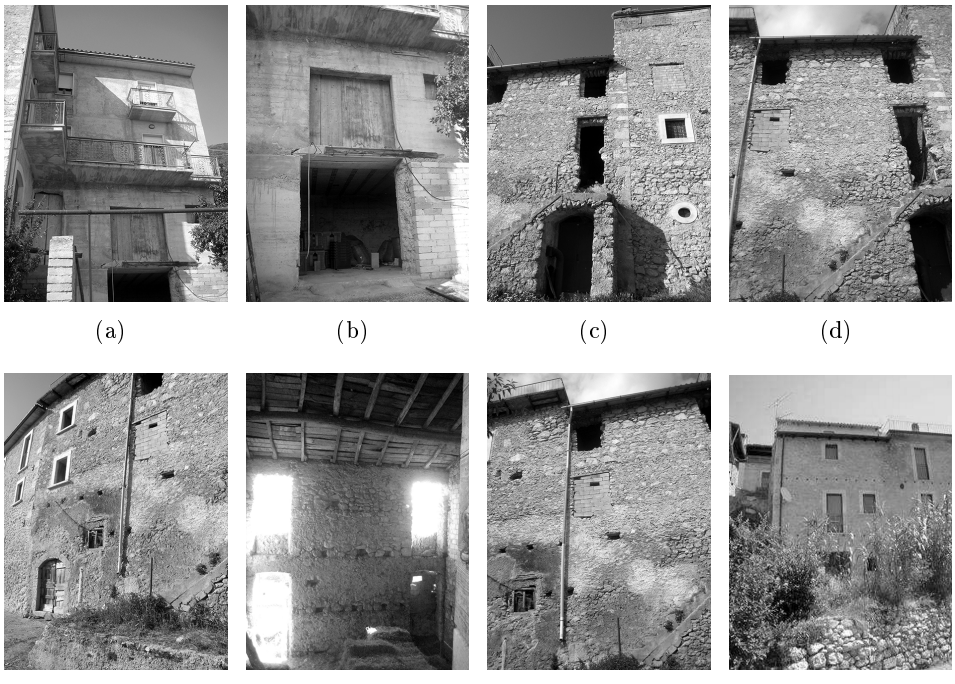

(a) (b) (c) (d)

(e) (f) (g) (h)

Figure A.1: Building aggregate individual structural units, given by *Scheda di Aggregato* [Scheda di Aggregato 2010]. (a) and (b) Structural unit *US A*. (c) Structural units *US C* and *US B*. (d) and (e) Structural unit *US A*. (f) Structural units *US D* and *US C*. (g) Structural units *US E*, *US D* and *US C*. (h) Structural unit *US F*.

Table A.1: General information regarding this building aggregate, adapted from *Scheda di Aggregato* [Scheda di Aggregato 2010].

Structural Units	*US A*	*US B*	*US C*	*US D*	*US E*	*US F*
Inter-story height	3.2	3.2	3.2–2.6	3.2–2.6	3.2–2.6	3.2–2.6
Number of floors	4	4	3	3–4	4	4
Number of floors against ground	2	2	2	2	2	2
Regularity in-height	yes	yes	yes	no	no	no
Presence of *Ipogee* cavities	no	no	yes	yes	yes	yes
Total height	12.8	12.8	8.4	11.0	11.0	11.0
Type of use	A	A	F	A	A	A
Percentage of use (%)	>65%	>65%	aban.	>65%	>65%	>65%
Survey quality	E	E	E	E	E	E
Serviceability class	E	E	E	E	F	F
Amplification interventions	no	no	no	no	no	no
Increased storey	yes	yes	yes	no	no	no
Retrofitting	no	yes	no	yes	yes	yes
Usage maintenance	no	no	no	no	no	no
Vertical structure typology	G, F, I	C, G, F	C	C	C	C
Horizontal structure typology	L, E	F, D, L	F	C, F	C, F	F, C
Roof typology	D	D	C	M	I	C, L
Stairs typology	I	H	–	A	I	–
Anti-seismic conservation status	1	1	4	2	1	1
State of occupation	1	1	3	1	3	3
Vulnerability class	C	B	aban.	A	A	B
Damage classification	V20	V10, H12, V6	–	V17, V4, H12, V10, H6, H3	V10	V17, V10, H12, H3

Active mechanism	M6	M3	M3	M9, M14, M3, M16	M3	M9*, M3, M16
Intensity	D2	D2	D4	D3	D3	D3

Table A.2: Damage classification observed in the building aggregate, adapted from *Scheda di Aggregato* [Scheda di Aggregato 2010].

Damage Type	Description
H3	Vault damaged in its key
H6	Detachment of the vault from the wall
H12	Detachment between floor and wall
V4	Diagonal cracks pattern on top corners of walls
V6	Diagonal crack pattern in the parapets above and through lintels of doors and windows
V10	Diagonal crack pattern in the transversal parapets
V17	Diagonal crack between the discontinuities of two adjacent buildings due to in-height differences
V20	In-plan deformation on wall in the transversal direction
V20	Non generalised detachment due to several irregularities (materials discontinuity, reduction of the resistant transversal section, presence of cavities, etc.)

Table A.3: Active mechanisms observed in the building aggregate, adapted from *Scheda di Aggregato* [Scheda di Aggregato 2010].

Mechanism Type	Description
M3	Global overturning of the wall
M6	Flexural failure of the wall
M9	Adjacent structures irregularities
M13	Overturning of gable walls
M14	Overturning of the top corners of walls
M16	Vault and arch rotations

(a)

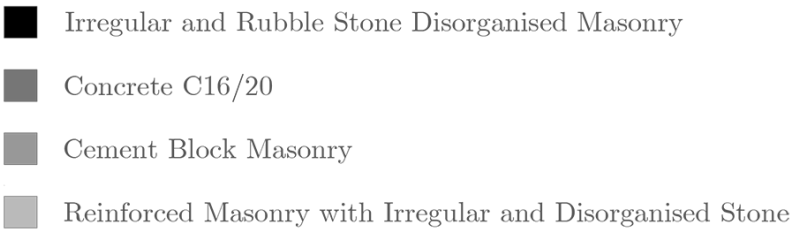

(b)

Figure A.2: Building aggregate structural materials distribution according to the *Scheda di Aggregato* [Scheda di Aggregato 2010].

Appendix B

Capacity Spectrum Method Formulation

B.1 General

This non-linear static analysis method compares graphically the global force-displacement capacity curve with the earthquake response spectrum. Both bilinear capacity curve and response spectrum have to be converted into spectral acceleration S_a and spectral displacement S_d. to reduce the MDoF system to an equivalent SDoF system. By using a trial and error procedure one can estimate the performance point, which describe the spectral displacement of the building due to the given earthquake. The following sections B.3 and B.4 were partially transcribed from actual European (EC8) and Italian (NTC08) codes [CEN 2004] [DM 2008].

B.2 Bilinear Capacity Curve

Deformation capacities are evaluated through the structure capacity curve, which plots the base shear force against the node control displacement assigned for the structure. The following procedure, N2 Method was proposed by Fajfar *et al.* and it is adopted in the mentioned seismic codes within this purpose. For the safety assessment, this method suggests a representation of a bilinear capacity curve, with respect of an equivalent SDoF system. This curve is defined for 70% of the maximum base shear force value of the MDoF system, in such a way that the areas below both system's curves are equal. This method allow the determination of the reference period T^* for the performance point, as explained below.

B.3 Determination of the Performance Point for Non-linear Static Analysis

The performance point of a structure, usually known as demand displacement, is determined from the elastic response spectrum. The relation between normalised lateral forces $\overline{F_i}$ and normalised displacements Φ_i is defined by equation

$$\overline{F_i} = m_i \Phi_i \tag{B.1}$$

where m_i is the mass in the i–th storey. Displacements are normalised in such a way that $\Phi_n = 1$, where n is the control node. Consequently, $\overline{F_n} = m_n$.

B.3.1 The Equivalent SDoF System

The mass of an equivalent SDoF system m^* is determined as:

$$m^* = \sum m_i \Phi_i = \sum \overline{F_i} \tag{B.2}$$

The mass participation factor Γ is given by the following equation:

$$\Gamma = \frac{m^*}{\sum m_i \Phi_i^2} = \frac{\sum \overline{F_i}}{\sum (\frac{\overline{F_i^2}}{m_i})} \tag{B.3}$$

The force F_b^* and displacement d_n^* of the equivalent SDoF system are computed as:

$$F_b^* = \frac{F_b}{\Gamma} \tag{B.4}$$

$$d_n^* = \frac{d_n}{\Gamma} \tag{B.5}$$

where F_b and d_n are, respectively, the base shear force and the control node displacement of the MDoF system.

B.3.2 The Idealised Elasto-perfectly Plastic Force-Displacement Relationship

The yield force F_y^*, which represents also the ultimate strength of the idealised system, is equal to the base shear force at the formulation of the plastic mechanism. The initial stiffness of the idealised system is determined in such a way that the area under the actual and the idealised force-displacement curves are equal. Based on this assumption, the yield displacement of the idealised SDoF system d_y^* is given by:

$$d_y^* = 2(d_u^* - \frac{E_m^*}{F_y^*}) \tag{B.6}$$

where E_m^* is the actual deformation energy up to the function of the plastic mechanism.

B.3.3 The Period of the Idealised Equivalent SDoF System

The period T^* of the idealised equivalent SDoF system is determined by:

$$T^* = 2\pi \sqrt{\frac{m*}{k*}} \tag{B.7}$$

where the secant stiffness k^* is given by the following equation:

$$k^* = \frac{F_y^*}{d_y^*} \tag{B.8}$$

B.3.4 Demand Displacement of the Equivalent SDOF System

The performance point of the structure with period T^* and unlimited elastic behaviour is given by:

$$d^*_{e,max} = S_e(T)^* \left[\frac{T^*}{2\pi}\right] \tag{B.9}$$

where $S_e(T^*)$ is the elastic acceleration response spectrum at the period T^*. For the determination of the performance point d^*_{max} for structures in the short-period range and for structures in the medium and long-period ranges different expressions should be used as indicated below. The limit period between the short and medium period range is T_c. For $T^* < T_c$ (short period range) the performance point d^*_{max} is determined through equation B.10, whereas for $T^* \geq T_c$ (medium and long period range), d^*_{max} is given by equation B.12

$$d^*_{max} = \begin{cases} d^*_{e,max} = S_{De}(T^*) & \text{if} \quad \frac{F^*_y}{m^*} \geq S_{De}(T^*), \\ \frac{d^*_{e,max}}{q^*}[1 + (q^* - 1)\frac{T_c}{T^*}] \geq d^*_{e,max} & \text{if} \quad \frac{F^*_y}{m^*} < S_{De}(T^*) \end{cases} \tag{B.10}$$

where q^* is the ratio between the acceleration in the structure with unlimited elastic behaviour $S_{De}(T^*)$ and in the structure with limited strength $\frac{F^*_y}{m^*}$.

$$q^* = \frac{S_e(T^*)m^*}{F^*_y} \tag{B.11}$$

$$d^*_{max} = d^*_{e,max} \tag{B.12}$$

where it is imposed $d^*_{max} < 3d^*_{e,max}$.

B.3.5 Demand Displacement of the MDOF System

The performance point corresponding to the control node of the MDoF system is given by:

$$d_{max} = \Gamma d^*_{max} \tag{B.13}$$

B.4 Energy Dissipation Effect

The ductility demand is an indirect factor in the seismic vulnerability evaluation and subsequently in the damage level. Thus, the current procedure allows to immediate understand the structural safety level and the possible effects arising from reinforcement strategies, acting over the capacity and ductility of the structure [Vicente 2008].

In order to account energy dissipation effects, which are particularly relevant in the non-linear structural analysis field, the demand requested by the external force is reduced [STADATA 2011] through an inelastic spectrum developed by Fajfar [Fajfar 2000], the so called N2 Method. Starting from the elastic response spectrum of a SDoF equivalent system in the ADRS format (S_{ae} versus S_{de}), the inelastic spectrum is defined in the same format (S_a versus S_d) for a constant ductility value, applying a reduction factor in

terms of strength due to ductility R_μ according to the following expressions developed by Vidic *et al.* [Vidic *et al.* 1994].

$$S_a = \frac{S_{ae}}{R_\mu} \quad S_d = \frac{\mu}{R_\mu} S_{de} = \mu \frac{T^2}{4\pi^2} S_a \tag{B.14}$$

where, μ is the ductility factor, defined as the ratio between the ultimate and yielding displacements and R_μ equal to the ratio between accelerations of the elastic and inelastic system.

$$R_\mu = \frac{S_{ae}(T^*)}{S_{ay}} \tag{B.15}$$

This reduction factor is a function of available stiffness and ductility in which structures are divided into rigid or flexible, by means of its fundamental period T^* and the following equation.

$$\begin{cases} R_\mu = (\mu - 1)\frac{T^*}{T_c} + 1 & \text{for} \quad T^* < T_c \\ \\ R_\mu = \mu & \text{for} \quad T^* \geq T_c \end{cases} \tag{B.16}$$

where T_c is the response spectrum transition period between the constant acceleration and constant velocity branches. This way the demand displacement, as proposed by Fajfar, is a function of T^* and μ, obtained by the following equations [Fajfar 2000].

$$S_d = \begin{cases} \mu D_y^* = \frac{S_{ae}}{R_\mu}\left[1 + (R_\mu - 1)\frac{T_c}{T^*}\right] & \text{for} \quad T^* < T_c \\ \\ S_{de}(T^*) & \text{for} \quad T^* \geq T_c \end{cases} \tag{B.17}$$

Appendix C

Masonry Macro-element and Three Dimensional Nodes

C.1 Masonry Macro-element Formulation

According to the definition presented in the 3muri® user manual [STADATA 2011] and the following figure C.1, a panel of width b and thickness s is considered divided in two main parts with different mechanical behaviour. Axial deformability is concentrated in both end elements ① and ③ of infinitesimal thickness and infinitely rigid to shear action. In the main body ②, with height h, only tangential deformability is allowed, being this component axially and flexural not deformable. The complete cinematic model for the macro-element is defined with three degrees of freedom of nodes i and j and those belonging to the interface nodes [STADATA 2011].

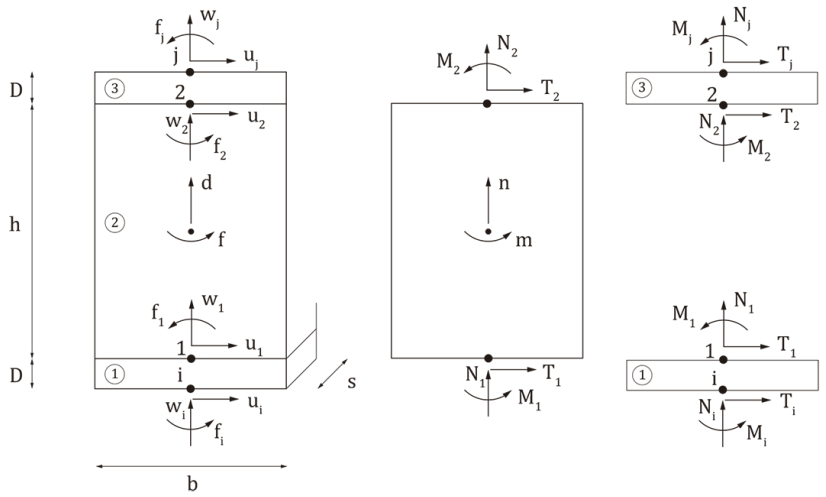

Figure C.1: Kinematic model of the macro-element, adapted from [STADATA 2011].

A non-linear beam element model, implemented in the software for modelling masonry piers and spandrels, has the following features:

- Initial stiffness given by elastic (cracked) stiffness;

- Bilinear behaviour with maximum values of shear and bending moment as calculated in ultimate limit states;
- Redistribution of the internal forces according to the element equilibrium;
- detection of damage limit states considering global and local damage and local damage parameters;
- Stiffness degradation in plastic range;
- Ductility control by definition of maximum drift (δ_u) based on the failure mechanism, according to the Italian code and EC8:

$$\delta_m^{DL} = \frac{\delta_m}{h_m} = \begin{cases} 0.4\%, \text{for Shear;} \\ 0.6\%, \text{for Compression-bending.} \end{cases} \tag{C.1}$$

- Element expiration at ultimate drift without interruption of global analysis.

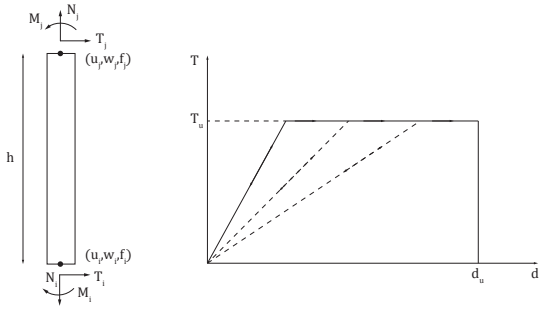

Figure C.2: Non-linear beam degrading behaviour, adapted from [STADATA 2011]

The elastic behaviour of this element is given by equation C.2,

$$\begin{Bmatrix} T_i \\ N_i \\ M_i \\ T_j \\ N_j \\ M_j \end{Bmatrix} = \begin{bmatrix} \frac{12EI}{h^3(1+\psi)} & 0 & -\frac{6EI}{h^2(1+\psi)} & -\frac{12EI}{h^3(1+\psi)} & 0 & -\frac{6EI}{h^2(1+\psi)} \\ 0 & \frac{EA}{h} & 0 & 0 & -\frac{EA}{h} & 0 \\ -\frac{6EI}{h^2(1+\psi)} & 0 & \frac{EI(4+\psi)}{h(1+\psi)} & \frac{6EI}{h^2(1+\psi)} & 0 & \frac{EI(2-\psi)}{h(1+\psi)} \\ -\frac{12EI}{h^3(1+\psi)} & 0 & \frac{6EI}{h^2(1+\psi)} & \frac{12EI}{h^3(1+\psi)} & 0 & \frac{6EI}{h^2(1+\psi)} \\ 0 & -\frac{EA}{h} & 0 & 0 & \frac{EA}{h} & 0 \\ -\frac{6EI}{h^2(1+\psi)} & 0 & \frac{EI(2-\psi)}{h(1+\psi)} & \frac{6EI}{h^2(1+\psi)} & 0 & \frac{EI(4+\psi)}{h(1+\psi)} \end{bmatrix} \begin{Bmatrix} u_i \\ w_i \\ \phi_i \\ u_j \\ w_j \\ \phi_j \end{Bmatrix} \tag{C.2}$$

where,

$$\psi = 24\,(1+\nu)\,\chi\frac{{r_i}^2}{h} = 24\left(1+\frac{E-2G}{2G}\right)1.2f\frac{b^2}{12h^2} = 1.2\frac{E}{G}\frac{b^2}{h^2} \tag{C.3}$$

The non-linear behaviour is activated when one of the nodal generalized forces reaches its maximum value estimated according to minimum of the following strength criteria: flexural-rocking; shear-sliding or diagonal shear cracking [STADATA 2011].

C.1.1 Bending: Rocking Behaviour

The ultimate bending moment (rocking behaviour) is defined by the following equation C.4:

$$M_u = \frac{l^2 t \sigma_0}{2}\left(1 - \frac{\sigma_0}{0.85 f_m}\right) = \frac{Nl}{2}\left(1 - \frac{N}{N_u}\right) \tag{C.4}$$

where l is the width of the panel, t the thickness, N the axial compressive action (assumed positive in compression), σ_0 the mean compressive strain in a generic section equal to $\sigma_0 = \frac{N}{It}$ and f_m is the mean compression strength of the masonry.

This approach performs a non-linear re-distribution of stresses (rectangular stress block with factor equal to 0.85). In existing buildings the mean strength f_m is divided by the confidence factor CF according to the structural knowledge level [OPCM 2003]. As defined in equation C.5, the global equilibrium must be satisfied, which implies a shear value re-calculation, if the actual moment is reduced to the ultimate bending moment value.

$$V_i = -V_j = \frac{M_i + M_j}{h} \tag{C.5}$$

C.1.2 Shear: Mohr-Coulomb Criterion

The ultimate shear, according to Mohr-Coulomb criterion, is defined by equation C.6, as:

$$V_u = l' t f_\nu = l' t \left(f_{\nu_0} + \mu \sigma_n\right) = l' t f_{\nu_0} + \mu N \tag{C.6}$$

where l' is the length of the compressed section of the panel, t the thickness, f_ν the shear strength of the masonry, f_{ν_0} the shear strength of the masonry without compression, η the friction coefficient (usually 0.4) and σ_n the normal mean compressive stress, referred to the effective area. For pushover analysis procedures the Italian code suggests the shear strength f_ν divided by the confidence factor CF. The effective compressed length l' is used when the eccentricity $e = \frac{|M|}{N}$ exceeds the limit value of $l/6$ in one of the ends (if $e < l/6$ all the points of the section are compressed). In general length l' can be expressed as the following equation C.7 [STADATA 2011].

$$l' = 3\left(\frac{l}{2} - e\right) = 3\left(\frac{l}{2} - \frac{|M|}{N}\right) \tag{C.7}$$

If the current shear value V exceeds the ultimate value V_u it must be reduced but changing the shear value, which means reducing the current bending moment values of M_i and M_j, to ensure the equilibrium. A reduction of the moment causes a reduction of the eccentricity e and consequently increases the l' value: a limit value of l' has to be expressed to be consistent to ultimate shear and moment values. According to equation C.8, the generic bending moment M can be expressed as $\alpha V h$, in which the coefficient α can assume different values (0.5 and 1.0 for double bending constraints and cantilevers, respectively):

$$l' = 3\left(\frac{l}{2} - \frac{\alpha V h}{N}\right) \tag{C.8}$$

Under the hypothesis that any possible reduction of the moments, caused by a shear reduction, doesn't change the static system, the ratio of the moments M_i and M_j must be unchanged, so α can be constant and expressed by equation C.9,

$$\alpha = \frac{M_{max}}{M_{max} + M_{min}} \tag{C.9}$$

where M_{max} is the maximum absolute value between M_i and M_j; note that α cannot be negative.

The shear strength, according to Italian code is defined by the following equations C.10, C.11, C.12 and C.13.

$$V_R = (f_{\nu_0} + 0.4\sigma_0)\, l't = f_{\nu_0} l't + 0.4N \tag{C.10}$$

Under the the limit condition $V = V_R$,

$$V_R = 3\left(\frac{l}{2} - \frac{\alpha V_R h}{N}\right) f_{\nu_0} t + 0.4N = 1.5 f_{\nu_0} lt + 0.4N - 3\alpha f_{\nu_0} ht \frac{V_R}{N} \tag{C.11}$$

and then,

$$V_R = \frac{1}{2} N \frac{3 f_{\nu_0} lt + 0.8N}{3\alpha f_{\nu_0} ht + N} \tag{C.12}$$

l' can be expressed as:

$$l'_R = \frac{3}{2}\left(l - \frac{3\alpha f_{\nu_0} lt + 0.8\alpha N}{3\alpha f_{\nu_0} ht + N} h\right) \tag{C.13}$$

This is the value of the actual compressed section of the panel under the limit condition of shear failure. Furthermore must be $\frac{N}{0.85 f_m t} < V_R \leq l$, where the extremes of the interval are the conditions of the whole section compressed and the limit state for bending (the stress block is completed in the compressed section part). If the previous inequality is not satisfied the value of l' will be assumed as the correspondent extreme of the interval. In addition to the Mohr-Coulomb resistance, the value of the shear tension f_ν must not exceed the limit value of $f_{\nu,lim}$:

$$f_\nu = \frac{T}{l't} \leq f_{\nu,lim} \tag{C.14}$$

If it exceeds the failure the shear value can be fixed as $V_{lim} = f_{\nu,lim} l't$. The effective compressed length l' has to be consistent with the value of V_{lim} and so may be different from l'_R: if the failure occurs for an exceeding value of the limit shear tension, the element shear has to be reduced and this causes the reduction of the moments to grant the global equilibrium of the panel according to α. The limit compressed length l'_{lim}, consistent with this failure mode, can be evaluated imposing $V = V_{lim}$:

$$V_{lim} = \frac{3}{2} N \left(\frac{f_{\nu,lim} lt}{3\alpha f_{\nu,lim} ht + N}\right) \tag{C.15}$$

and so,

$$l'_{lim} = \frac{3}{2}\left(l - \frac{3\alpha f_{\nu,lim} lt}{3\alpha f_{\nu,lim} ht + N} h\right) \tag{C.16}$$

with l'_{lim} in between $\frac{N}{0.85 f_m t} < l'_{lim} \leq l$. Finally the limit shear V_u is the minimum between V_{lim} and V_R.

$$V \leq V_u = min\left(V_R; V_{lim}\right) \tag{C.17}$$

In case of the current shear overcomes the limit shear V_{lim} it is reduced to V_u and also the moments have to be reduced accordingly to ensure the same elastic scheme. Figure C.3 shows the behaviour laws behind the resistant criteria typically used for shear and bending-rocking failures in masonry panels.

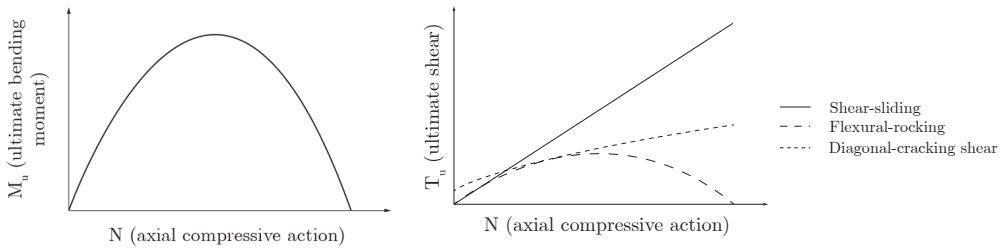

Figure C.3: Comparison between resistant criteria for masonry [STADATA 2011].

$$M_{max} = T_u \alpha h M_{min} = T_u \left(1 - \alpha\right) h T \equiv T_u \tag{C.18}$$

C.1.3 Shear: Turnšek and Cacovic Criterion

Exclusively for existing buildings, the Italian code enables the shear failure computation according to Turnšek and Cacovic criterion. The ultimate shear is defined by equation C.19,

$$V_u = lt\frac{1.5\tau_0}{b}\sqrt{1 + \frac{\sigma_0}{1.5\tau_0}} = lt\frac{f_t}{b}\sqrt{1 + \frac{\sigma_0}{f_t}} = lt\frac{1.5\tau_0}{b}\sqrt{1 + \frac{N}{1.5\tau_0 lt}} \tag{C.19}$$

where f_t and τ_0 are the design value of tension strength in diagonal cracking of masonry and its shear value, respectively. The coefficient b is defined according to the ratio of the height h and the length l of the wall.

C.1.4 Masonry Spandrel Beams

The previous strength criteria can be only used with effective axial compression, usually ensured in piers but not for spandrel beams, in which the shear strength can be assumed by equation C.20,

$$V_{u,spandrel} = htf_{\nu_0} \tag{C.20}$$

where, h is the height of the section of the panel and t the thickness. Thus, the maximum bending moment is given by the following equation C.21,

$$M_{u,spandrel} = \frac{hH_p}{2}\left(1 - \frac{H_p}{0.85 f_h h t}\right) \tag{C.21}$$

where H_p is the minimum value between the tensile strength of the stretched interposed element inside the spandrel beam (for example a tie-rod) and $0.4 f_h.h.t$, where f_h is the compression strength of the masonry in the horizontal direction in the plane of the wall [STADATA 2011].

C.2 Three Dimensional Nodes

The relationships between the five degrees of freedom of the three-dimensional nodes (u_x, u_y, u_z, θ_x and θ_y) and the three degrees of freedom of the two-dimensional nodes (wall modelling plan) are shown in the following equation C.22.

$$\begin{cases} u = u_x cos\theta + u_y sin\theta \\ w = u_z \\ \varphi = \varphi_x sin\theta - \varphi_y cos\theta \end{cases} \tag{C.22}$$

u, w and φ represent the displacement components according to the degrees of freedom found in the fictitious nodes that belongs to the generic wall facing the plan according the angle φ (figure C.4 (a)). The forces transmitted by the macro-elements belonging to individual walls are carried out to the overall reference axis as shown in the following figure C.4 (b). Nodes belonging to a single wall remain two-dimensional nodes with the corresponding three degrees of freedom, instead of five.

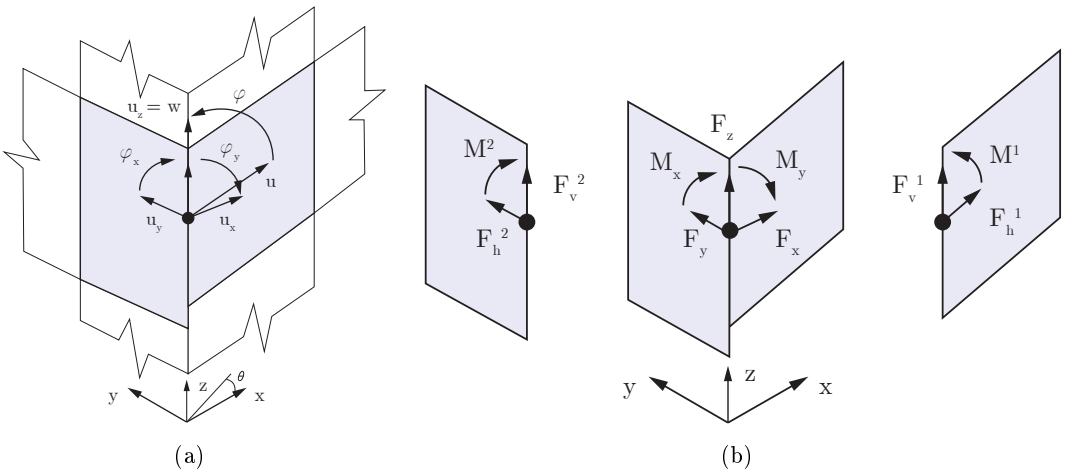

Figure C.4: (a) Displacement components of a single wall. (b) Two-dimensional node to three-dimensional node transformation process, both adapted from [STADATA 2011].

$$\begin{cases} F_x = F_h^1 cos\theta_1 + F_h^2 cos\theta_2 \\ F_y = F_h^1 sin\theta_1 + F_h^2 sin\theta_2 \\ F_z = F_v^1 + F_v^2 \\ M_x = M^1 sin\theta_1 + M^2 sin\theta_2 \\ M_y = -M^1 cos\theta_1 - M^2 cos\theta_2 \end{cases} \tag{C.23}$$

Appendix D

Binomial and Beta Probability Functions Formulation

In this dissertation both binomial and beta probability functions were used to construct damage distribution histograms. These probabilistic functions developed by Lagomarsino and Giovinazzi surpass by themselves the damage state deviation complex estimation process [Lagomarsino and Giovinazzi 2006]. The damage level D_k is defined according to the specifications of the EMS-98 scale [Grünthal 1998], wherein five levels of damage, beyond the null (zero) damage, are assumed. The probability associated to the distribution function of each damage grade , with $k = 0, 1, 2, 3, 4$ and 5, is calculated by the binomial probability mass function, according to equation D.1.

$$PMF : p_k = \frac{5!}{k!(5-k)!}\left(\frac{\mu_D}{5}\right)\left(1-\frac{\mu_D}{5}\right)^{5-k}; n \geq \tag{D.1}$$

where, p_k is the occurrence probability of a determined damage grade, D_k. The damage distribution adopted in this particular study was constructed through a beta probability density function using the following equation D.2 accordingly to its original formulation proposed by Bernardini *et al.* [Bernardini *et al.* 2007b] [Bernardini *et al.* 2007a].

$$PDF : p_\beta(x) = \frac{\Gamma(t)}{\Gamma(r)\Gamma(t-r)}\frac{(x-a)^{r-1}(b-x)^{t-r-1}}{(b-a)^{r-1}}; a \leq x \leq b \tag{D.2}$$

where r and t are the parameters which control the function dispersion, a and b are the distribution limits and Γ is the well-known *Gamma* function, the extension of the factorial function with its argument shifted down by 1. Assuming $a = 0$ and $b = 5$ we have the following simplified expression D.3.

$$p_\beta(x) = \Gamma(t, r)\frac{x^{r-1}(5-x)^{t-r-1}}{5^{t-1}} \tag{D.3}$$

where, for a continuous variable x, the variance σ_x^2 and the mean value μ_x are related with r and t by the following equations D.4 and D.5.

$$r = t\frac{\mu_x}{5} \tag{D.4}$$

$$t = \frac{\mu_x(5-\mu_x)}{\sigma_x^2} - 1 \tag{D.5}$$

A discrete distribution is obtained defining the associated probability of each damage grade D_k, by the following expression D.6, which is this way characterised for its mean damage grade μ_D and for the variance σ_D^2. Assuming a similar relation between the parameters of the beta discrete and continuous distributions, the variance of the damage discrete distribution is given by equation D.7.

$$\begin{aligned} P(D_0) = p(0) &= \textstyle\int_0^{0.5} k(t,r)x^{r-1}(5-x)^{t-r-1}\,\mathrm{d}x \\ P(D_k) = p(k) &= \textstyle\int_{k-0.5}^{k+0.5} k(t,r)x^{r-1}(5-x)^{t-r-1}\,\mathrm{d}x \quad k = 1,2,3 \textit{ or } 4 \\ P(D_5) = p(5) &= \textstyle\int_{4.5}^{5} k(t,r)x^{r-1}(5-x)^{t-r-1}\,\mathrm{d}x \end{aligned} \tag{D.6}$$

$$\sigma_D^2 = \frac{\mu_D(b+a-\mu_D)-ba}{t+1} \tag{D.7}$$

Variance σ_D^2 is then a function of the mean damage grade μ_D and parameters a, b and t, being the value of the last parameter t in correspondence with the intrinsic variance value of the constant distributions in damage probability matrices of the EMS-98 macroseismic scale [Grünthal 1998].

Bibliography

[Ademović 2011] N. Ademović. *Structural and Seismic Behaviour of Typical Masonry Buildings from Bosnia and Herzegovina*. Master's Thesis in Structural Analysis of Monuments and Historical Constructions, University of Minho, Braga, Portugal, 2011.

[Ademović and Oliveira 2012] N. Ademović and D. V. Oliveira. Seismic Assessment of a Typical Masonry Residential Building in Bosnia and Herzegovina. In *Proceedings of the* 15^{th} *WCEE - World Conference of Earthquake Engineering*, pp. 1–10, Lisbon, Portugal, 2012.

[Alexandris *et al.* 2004] A. Alexandris, E. Protopapa and I. Psycharis. Collapse Mechanisms of Masonry Buildings derived by the Distinct Element Method. In *Proceedings of the* 13^{th} *WCEE - World Conference of Earthquake Engineering*, number 548, pp. 1–14, Vancouver, Canada, 2004.

[Almeida 2009] J. F. Almeida. *Estudo de Soluções Estruturais para Reabilitação de Edifícios em Alvenaria de Pedra*. Master's thesis in structural engineering, University of Oporto, Oporto, Portugal, 2009.

[Amadio *et al.* 2011] C. Amadio, G. Rinaldin, A. Puppin and M. Camillo. Analisi Semplificata della Vulnerabilità Sismica di un Aggregato Edilizio in Muratura: il Complesso Denominato "Vaticano" (Trieste). In *Proceedings of the* 14^{th} *National Congress in Seismic Engineering*, pp. 1–10, Bari, Italy, 2011. ANIDIS - National Association of Earthquake Engineering.

[Ameri *et al.* 2012] G. Ameri, F. Gallovic and F. Pacor. Complexity of the Mw 6.3 2009 L'Aquila (central Italy) Earthquake: Broadband Strong Motion Modelling. *Journal of Geophysical Research*, 117:1–18, 2012.

[Attanasio *et al.* 2011] V. Attanasio, V. Baccino, F. Lemmi and E. Bonannini. Inquadramento Storico Urbanistico. In *Studi e Indagini sul Rischio Sismico del Centro Storico di San Pio delle Camere (AQ)*, chapter 2, pp. 15–32. University of Pisa, Pisa, Italy, ets edition, 2011.

[Augusti *et al.* 2001] G. Augusti, M. Ciampoli and P. Giovenale. Seismic Vulnerability of Monumental Buildings. *Elsevier Science Ltd - Structural Safety*, 23(3):253–274, 2001.

[Barbat 2003] A. H. Barbat. Indicators for Disaster Risk Management: Detailed Application of the Holistic Approach for Seismic Risk Evaluation in an Urban Center

Using Relative Indices. Technical report, Universidad Nacional de Colombia, Manizales, Colombia, 2003.

[Barbat *et al.* 2008] A. H. Barbat, S. Lagomarsino and L. Pujades. Vulnerability Assessment of Dwelling Buildings, chapter 6, pp. 115–134. Assessing and Managing Earthquake Risk. *Springer*, Dordrecht, Netherlands, 2008.

[Bazzurro *et al.* 2009] P. Bazzurro, G. Franco and J. Alarcon. Observations from the Magnitude 6.3 l'Aquila Earthquake. In , Vol. AIR Currents, pp. 1–7. AIR Worldwide Corporation, Boston, USA, 2009.

[Benedetti and Petrini 1984] D. Benedetti and V. Petrini. On the Seismic Vulnerability of Masonry Buildings: Proposal of an Evaluation Procedure. *L'industria Italiana delle Costruzioni*, 18(149):66–78, 1984.

[Bernardini *et al.* 1988] A. Bernardini, R. Gori and C. Modena. Valutazioni di Resistenza di Nuclei di Edifici in Muratura per Analisi di Vulnerabilità Sismica. Technical Report 2/88, University of Padua, Padua, Italy, 1988.

[Bernardini *et al.* 1990] A. Bernardini, R. Gori and C. Modena. Application of Coupled Analytical Models and Experiential Knowledge to Seismic Vulnerability Analyses of Masonry Buildings. Earthquake Damage Evaluation and Vulnerability Analysis of Building Structures, Oxon, UK, omega scientific edition, 1990.

[Bernardini *et al.* 2007a] A. Bernardini, S. Giovinazzi, S. Lagomarsino and S. Parodi. Matrici di Probabilità di Danno nella Scala EMS-98. In *Proceedings of the* 12^{th} *National Congress in Seismic Engineering*, pp. 1–11, Pisa, Italy, 2007. ANIDIS - Italian National Association of Earthquake Engineering.

[Bernardini *et al.* 2007b] A. Bernardini, S. Giovinazzi, S. Lagomarsino and S. Parodi. Vulnerabilità e Previsione di Danno a Scala Territoriale Secondo una Metodologia Macrosismica coerente con la Scala EMS-98. In *Proceedings of the* 12^{th} *National Congress in Seismic Engineering*, Vol. 1, Pisa, Italy, 2007. ANIDIS - Italian National Association of Earthquake Engineering.

[Binda *et al.* 2010] L. Binda, G. Baronio, D. Penazzi, M. Palma and C. Tiraboschi. Caratterizzazione di Murature in Pietra in Zona Sismica: Data-base sulle Sezioni Murarie e Indagini sui Materiali. 2010.

[Biro, T. 2009] Biro, T. GeoSIG: GSR-18 Computer Program that Provides Earthquake, Seismic, Structural, Dynamic and Static Monitoring and Measuring Solutions. GeoSig Ltd, Othmarsingen, Switzerland, 2009.

[Borgesa and Castagnone 2011] L. Borgesa and A. Castagnone. Verifiche Sismiche Edifici in Muratura. Technical report, University of Genoa, Genoa, Italy, 2011.

[Borri and Cangi 2004] A. Borri and G. Cangi. Vulnerabilità ed Interventi di Prevenzione Sismica nei Centri Storici Umbri dell'alta Val Tiberina. In *Proceedings of the* 11^{th} *National Congress in Seismic Engineering*, pp. 1–12, Genoa, Italy, 2004. ANIDIS - National Association of Earthquake Engineering.

[Borri *et al.* 2006] A. Borri, G. Cangi and de A. Maria. Studio sulla Vulnerabilità Sismica del Patrimonio Edilizio. Il Centro Storico di Gubbio (PG). 2006.

[Bothara and Brzev 2011] J. Bothara and S. Brzev. Improving the Seismic Performance of Stone Masonry Buildings. Number WHE-2011-01. EERI, Earthquake Engineering Research Institute, Oakland, California, USA, first edition, 2011.

[Calderini 2004] C. Calderini. *Un Modello Costitutivo per la Muratura: Formulazione ed implementazione per l'analisi di strutture complesse*. Phd thesis in structural engineering, University of Genoa, Genoa, Italy, 2004.

[Caliò *et al.* 2012] I. Caliò, M. Marletta and B. Pantò. A New Discrete Element Model for the Evaluation of the Seismic Behaviour of Unreinforced Masonry Buildings. *Elsevier Science Ltd - Engineering Structures*, 40:327–338, 2012.

[Calvi 2007] G. M. Calvi. Guidelines for Seismic Vulnerability Reduction in the Urban Environment, chapter 4, pp. 1–333. Lessloss: Risk Mitigation for Earthquakes and Landslides. IUSS Press, Pavia, Italy, 2007.

[Calvi *et al.* 2006] G. M. Calvi, R. Pinho, G. Magenes, J. Bommer and H. Crowley. Development of Seismic Vulnerability Assessment Methodologies Over the Past 30 Years. *ISET Journal of Earthquake Technology*, 43(472):75–104, 2006.

[Cambri *et al.* 2011] R. Cambri, R. Piccione, R. Vercelli and G. Mariani. Tipologie della Cavità Ipogee. In *Studi e Indagini sul Rischio Sismico del Centro Storico di San Pio delle Camere (AQ)*, chapter 4, pp. 57–73. University of Pisa, Pisa, Italy, ets edition, 2011.

[Candeias 2008] P. Candeias. *Seismic Vulnerability Assessment of Masonry Buildings*. Phd thesis in structural engineering, University of Minho, Braga, Portugal, 2008.

[Candela *et al.* 2011] M. Candela, S. Cattari, S. Lagomarsino, M. Rossi, R. Fonti and E. Pagliuca. Prove in situ per la Valutazione della Risposta nel Piano di un Pannello Murario in un Edificio a L'Aquila. In *Proceedings of the* 11^{th} *National Congress in Seismic Engineering*, pp. 1–20, Bari, Italy, 2011. ANIDIS - Italian National Association of Earthquake Engineering.

[Caniggia and Maffei 1979] G. Caniggia and G. L. Maffei. Composizione Architettonica e Tipoligia Edilizia: letture dell'edilizia di base. Venice, Italy, 1979.

[Carocci 2001] C. F. Carocci. Historical Constructions: Guidelines for the Safety and Preservation of Historical Centres in Seismic Areas. 2001.

[Carocci *et al.* 2010] C. Carocci, C. Tocci, S. Cattari and S. Lagomarsino. Linee Guida per il Rilievo, L'analisi ed il Progetto di Interventi di Riparazione e Consolidamento Sismico di Edifici in Muratura in Aggregato. Technical report, Naples, Italy, 2010.

[Carvalho 2007] E. Carvalho. Probabilistic Methods for Seismic Assessment of Existing Structures, chapter 6, pp. 1–174. Lessloss: Risk Mitigation for Earthquakes and Landslides. IUSS Press, Pavia, Italy, 2007.

[Cattari *et al.* 2004] S. Cattari, E. Curti, S. Giovinazzi, S. Lagomarsino, S. Parodi and A. Penna. A Mechanical Model for the Vulnerability Assessment and the Damage Scenario of Masonry Buildings at Urban Scale. In *Proceedings of the* 11^{th} *National Congress in Seismic Engineering*, Genoa, Italy, 2004. ANIDIS - National Association of Earthquake Engineering.

[Cella *et al.* 1994] F. Cella, S. Grimaz, F. Meroni, V. Petrini, R. Tomasoni and G. Zonno. A Case Study for Vulnerability Assessment using GIS Connected to Export System. In *Proceedings of the* 9^{th} *Arc/info European user Conference*, pp. 421–448, Paris, France, 1994.

[CEN 2004] CEN. Eurocode 8: Design of Structures for Earthquake Resistance Part 1: General Rules, Seismic Actions and Rules for Buildings. Eurocode 8, Brussels, Belgium, 2004.

[Chever 2012] L. Chever. Use of Seismic Assessment Methods for Planning Vulnerability Reduction of Existing building Stock. In *Proceedings of the* 15^{th} *WCEE - World Conference of Earthquake Engineering*, pp. 1–10, Lisbon, Portugal, 2012.

[Chopra and Goel 1999] A. K. Chopra and R. Goel. Capacity-Demand-Diagram Methods for Estimating Seismic Deformation of Inelastic Structures: SDoF Systems. Technical report, University of California, Berkeley, CA, USA, 1999. Report PEER-1999/02.

[Corradi *et al.* 2003] M. Corradi, A. Borri and A. Vignoli. Experimental Study on the Determination of Strength of Masonry Walls. *Elsevier Science Ltd - Construction and Building Materials*, 17(5):325–337, 2003.

[Corsanego and Petrini 1990] A. Corsanego and V. Petrini. Seismic Vulnerability of Buildings. In *Proceedings of the SEISMED 3*, Trieste, Italy, 1990. SEISMED - Cooperative Project for Seismic Risk Reduction in the Mediterranean Regions.

[Costa 2008] S. Costa. *Avaliação Sísmica do Parque Edificado da Avenida Dr. Lourenço Peixinho - Aveiro*. Master's Thesis in Structural Engineering, University of Oporto, Oporto, Portugal, 2008.

[Crowley *et al.* 2008] H. Crowley, B. Borzi, R. Pinho, M. Colombi and M Onida. Comparison of Two Mechanics-Based Methods for Simplified Structural Analysis in Vulnerability Assessment. *Advances in Civil Engineering, Hindawi Publishing Corporation*, pp. 1–19, 2008.

[D'Ambra 2011] C. D'Ambra. *Vulnerabilità e Miglioramento Sismico di Edifici in Aggregato: il Caso Studio di Piazza delle Prefettura a L'Aquila*. PhD Thesis in Structural and Materials Engineering, University of Naples Federico II, Naples, Italy, 2011.

[D'Ayala and Speranza 2002] D. D'Ayala and E. Speranza. An Integrated Procedure for the Assessment of Seismic Vulnerability of Historic Buildings. In *Proceedings of the* 12^{th} *ECEE - European Conference on Earthquake Engineering*, number 561, pp. 1–10, London, UK, 2002. Elsevier Science Ltd.

[D'Ayala and Speranza 2003] D. D'Ayala and E. Speranza. Definition of Collapse Mechanisms and Seismic Vulnerability of Historic Masonry Buildings. *Earthquake Spectra*, 19(3):479–509, 2003.

[D'Ayala and Speranza 2004] D. D'Ayala and E. Speranza. Un criterio per la formulazione e la calibrazione di curve di fragilità e scenari di danno: il caso di Nocera Umbra (PG). In *Proceedings of the* 11^{th} *National Congress in Seismic Engineering*, pp. 1–12, Genoa, Italy, 2004. ANIDIS - National Association of Earthquake Engineering.

[DM 1996] DM. Decreto Ministeriale 16/01/1996. Norme Tecniche per le Costruzioni in Zone Sismiche, 1996.

[DM 2005] DM. Decreto Ministeriale 14/09/2005. Norme Tecniche per le Costruzioni in Zone Sismiche, 2005.

[DM 2008] DM. Decreto Ministeriale 14/01/2008. Norme Tecniche per le Costruzioni in Zone Sismiche, 2008.

[Dolce *et al.* 2003] M. Dolce, A. Masi, M. Marino and M. Vona. Earthquake Damage Scenarios of the Building Stock of Potenza (Southern Italy) Including Site Effects. *Bulletin of Earthquake Engineering*, 1:115–140, 2003.

[Dolce *et al.* 2006] M. Dolce, A. Kappos, A. Masi, G. Penelis and M. Vona. Vulnerability Assessment and Earthquake Damage Scenarios of the Building Stock of Potenza (Southern Italy) using Italian and Greek Methodologie. *Elsevier Science Ltd - Engineering Structures*, 28(3):357–371, 2006.

[Erdik 2007] M. Erdik. Earthquake Disaster Scenario Prediction and Loss Modelling for Urban Areas, chapter 7, pp. 1–165. Lessloss: Risk Mitigation for Earthquakes and Landslides. IUSS Press, Pavia, Italy, 2007.

[Fajfar 1999] P. Fajfar. Capacity Spectrum Method Based on Inelastic Demand Spectra. *Earthquake Engineering and Structural Dynamics*, 28:979–993, 1999.

[Fajfar 2000] P. Fajfar. A Nonlinear Analysis Method for Performance Based Seismic Design. *Earthquake Spectra*, 16(3):573–592, 2000.

[Favilli *et al.* 2011] D. Favilli, V. Mamone and R. Condello. La Microzonazione Sismica del Territorio. In *Studi e Indagini sul Rischio Sismico del Centro Storico di San Pio delle Camere (AQ)*, chapter 6, pp. 99–138. University of Pisa, Pisa, Italy, ets edition, 2011.

[FEMA 2003] FEMA. FEMA Mitigation Division. HAZUS-MH MR3: Multi-Hazard Loss Estimation Methodology: Technical Manual. Federal Emergency Management Agency, Washington DC, USA, 2003.

[Ferreira *et al.* 2010] T. Ferreira, R. Vicente, H. Varum, A. Costa and J. A. R. Mendes da Silva. Metodologia de Avaliação da Vulnerabilidade Sísmica das Paredes de Fachada de Edifícios Tradicionais de Alvenaria. In *Proceedings of the* 8^{th} *National Congress of Sismology and Seismic Engineering*, pp. 1–11, Aveiro, Portugal, 2010. University of Aveiro.

[Ferreira *et al.* 2012] T. Ferreira, R. Vicente and H. Varum. Vulnerability Assessment of Building Aggregates: a Macroseimic Approach. In *Proceedings of the* 15^{th} *WCEE - World Conference of Earthquake Engineering*, pp. 1–9, Lisbon, Portugal, 2012.

[Florio 2010] G. Florio. *Vulnerability of Historical Masonry Buildings under Exceptional Actions*. Phd thesis in construction engineering, University of Naples Federico II, Naples, Italy, 2010.

[Formisano *et al.* 2010] A. Formisano, F. M. Mazzolani, G. Florio and R. Landolfo. A Quick Methodology for Seismic Vulnerability Assessment of Historical Masonry Aggregates. In *Urban Habitat Constructions under Catastrophic Events*, Naples, Italy, 2010. COST Action C26.

[Formisano *et al.* 2011a] A. Formisano, G. Florio, R. Landolfo and F. M. Mazzolani. Numerical Calibration of a Simplified Procedure for the Seismic Behaviour Assessment of Masonry Building Aggregates. In *Proceedings of the* 13^{th} *International Conference on Civil, Structural and Environmental Engineering Computing*, number 172, pp. 1–28, Stirlingshire, Scotland, 2011. Civil-Comp Press.

[Formisano *et al.* 2011b] A. Formisano, G. Florio, R. Landolfo and F. M. Mazzolani. Un Metodo per la Valutazione su Larga Scala della Vulnerabilità Sismica degli Aggregati Storici. University of Naples Federico II, 2011.

[Freeman 1998] S. A. Freeman. Development and Use of Capacity Spectrum Method. In *Proceedings of the* 6^{th} *US NCEE - National Conference on Earthquake Engineering/EERI*, number 269, pp. 1–12, Seattle, Washington, USA, 1998.

[Fusco *et al.* 2008] E. Fusco, A. Penna, A. Prota, A. Galasco and G. Manfredi. Seismic Assessment of Historical Natural Stone Masonry Buildings Through Non-Linear Analysis. In *Proceedings of the* 14^{th} *WCEE - World Conference of Earthquake Engineering*, pp. 1–8, Beijing, China, 2008.

[Galasco *et al.* 2004] A. Galasco, S. Lagomarsino, A. Penna and S. Resemini. Non-linear Seismic Analysis of Masonry Structures. In *Proceedings of the* 13^{th} *WCEE - World Conference of Earthquake Engineering*, number 843, pp. 1–15, Vancouver, Canada, 2004.

[Galasco *et al.* 2006] A. Galasco, S. Lagomarsino and A. Penna. On the Use of Pushover Analysis for Existing Masonry Buildings. In *Proceedings of the* 1^{st} *ECEES - European Conference on Earthquake Engineering and Seismology*, number 1080, pp. 1–10, Geneva, Switzerland, 2006.

[Gallonelli 2007] M. Gallonelli. *Dynamic Response of Masonry Buildings with Rigid or Flexible Floors*. Master thesis in earthquake engineering, Rose School, University of Pavia, Pavia, Italy, 2007.

[Gambarrota and Lagomarsino 1997] L. Gambarrota and S. Lagomarsino. Damage Models for the Seismic Response of Brick Masonry Shear Walls. Part II: The Continuum Model and Its Applications. *Earthquake Engineering and Structural Dynamics*, 26:441–462, 1997.

[Giovinazzi 2005] S. Giovinazzi. *The Vulnerability Assessment and Damage Scenario in Seismic Risk Analysis*. Phd thesis, University of Florence, Florence, Italy, 2005.

[Giovinazzi and Lagomarsino 2004] S. Giovinazzi and S. Lagomarsino. A Macroseismic Method for Vulnerability Assessment of Buildings. In *Proceedings of the* 13^{th} *WCEE - World Conference on Earthquake Engineering*, number 896, pp. 1–16, Vancouver, Canada, 2004.

[Giovinazzi *et al.* 2004] S. Giovinazzi, A. Balbi and S. Lagomarsino. Un Modello di Vulnerabilità per gli Edifici nei Centri Storici. In *Proceedings of the* 11^{th} *National Congress in Seismic Engineering*, pp. 1–16, Genoa, Italy, 2004. ANIDIS - National Association of Earthquake Engineering.

[Giovinazzi *et al.* 2006] S. Giovinazzi, S. Lagomarsino and S. Pampanin. Vulnerability Methods and Damage Scenario for Seismic Risk Analysis as Support to Retrofit Strategies: an European Perspective. In *Proceedings of the New Zealand Society for Earthquake Engineering Conference (NZSEE)*, number 14, pp. 1–10, Napier, New Zeland, 2006.

[GNDT-SSN 1994] GNDT-SSN. Scheda di Esposizione e Vulnerabilità e di Rilevamento Danni di Primo Livello e Secondo Livello (Muratura e Cemento Armato). Technical report, Rome, Italy, 1994.

[Grünthal 1998] G. Grünthal. European Macroseismic Scale. Working Group Macroseismic Scales. Centre Européen de Géodynamique et de Séismologie, Luxembourg, second edition, 1998.

[Gruppo Sismica srl 2009] Gruppo Sismica srl. 3D Macro - Il Software per le Murature: Computer Program for the Estimation of Masonry Buildings Seismic Vulnerability. Catania, Italy, 1.11103101 edition, 2009. User Manual.

[Guarenti and Petrini 1989] E. Guarenti and V. Petrini. Il caso delle Vecchie Costruzioni: verso una nuova legge danni-intensità. In *Proceedings of the* 12^{th} *National Conference on Earthquake Engineering*, Pisa, Italy, 1989. ANIDIS - Italian National Association of Earthquake Engineering.

[Hall 2011] S. S. Hall. At fault? *Nature*, 477:264–269, 2011.

[Indelicato 2010] D. Indelicato. *Valutazione e Riduzione della Vulnerabilità Sismica degli Aggregati Edilizi nei Centri Storici*. Phd thesis in architectural, urban and environmental renovation design, University of Catania, Catania, Italy, 2010.

[INE and LNEC 2013] INE and LNEC. O Parque Habitacional e a sua Reabilitação - Análise e Evolução 2001-2011. INE - National Institute of Statistics, Lisbon, Portugal, first edition, 2013.

[Ishiyama 2011] Y. Ishiyama. Introduction to Earthquake Engineering and Seismic Codes in the World. Hokkaido University, Hokkaido, Japan, 2011.

[Júlio *et al.* 2008] E. Júlio, C. Rebelo and D. Dias-da Costa. Structural Assessment of the Tower of the University of Coimbra by Modal Identification. *Elsevier Science Ltd - Engineering Structures*, 30(12):3468–3477, 2008.

[Karmazínová and Melcher 2012] M. Karmazínová and J. Melcher. Influence of Steel Yield Strength Value on Structural Reliability of Steel Yield Strength. *Recent Researches in Environmental and Geological Sciences*, pp. 1–6, 2012.

[Lagomarsino and Giovinazzi 2006] S. Lagomarsino and S. Giovinazzi. Mechanical Models for the Vulnerability Assessment of Current Buildings. In *Proceedings of the* 4^{th} *National Conference on Earthquake Engineering*, Vol. 1, Milan, Italy, 2006. ANIDIS - Italian National Association of Earthquake Engineering.

[Lagomarsino and Magenes 2009] S. Lagomarsino and G. Magenes. Evaluation and Reduction of the Vulnerability of Masonry Buildings. *The state of Earthquake Research in Italy: the ReLUIS-DPC 2005-2008 Project*, pp. 1–50, 2009.

[Lang 2002] K. Lang. *Seismic Vulnerability of Existing Buildings*. Phd thesis in technical sciences, Swiss Federal Institute of Technology, Zurich, Switzerland, 2002.

[Lourenço *et al.* 2010] P.B. Lourenço, N. Mendes, R. Marques and D.V. Oliveira. Análise de Estruturas Antigas e Novas em Alvenaria: possibilidade e aplicações. In *Proceedings of the* 8^{th} *National Congress of Sismology and Seismic Engineering*, pp. 1–14, Aveiro, Portugal, 2010. University of Aveiro.

[Magenes and Calvi 1997] G. Magenes and G.M. Calvi. In-plane seismic response of brick masonry walls. *Earthquake Engineering and Structural Dynamics*, 26(11):1091–1112, 1997.

[Mannari *et al.* 2011] A. Mannari, L. Scaramuzzino, S. Stefanelli and A. de Falco. Techniche di Consolidamento Ante e Post Sisma. In *Studi e Indagini sul Rischio Sismico del Centro Storico di San Pio delle Camere (AQ)*, chapter 9, pp. 251–285. University of Pisa, Pisa, Italy, ets edition, 2011.

[Marchetti 2002] L. Marchetti. Vulnerability of Historic Centres and Cultural Heritage. Technical report, Italy, 2002. 2^{nd} year of activity - Annual Report.

[Margottini *et al.* 1992] C. Margottini, D. Molin, B. Narcisi and L. Serva. Intensity versus Ground Motion: a new approach using Italian data. *Engineering Geology*, 33:45–48, 1992.

[Marques 2012] R. Marques. *Metodologias Inovadoras no Cálculo Sísmico de Estruturas em Alvenaria Simples e Confinada*. Phd thesis in structural engineering, University of Minho, Braga, Portugal, 2012.

[Marques and Lourenço 2011] R. Marques and P.B. Lourenço. Possibilities and Comparison of Structural Component Models for the Seismic Assessment of modern unreinforced masonry buildings. *Elsevier Science Ldt*, 89:2079–2091, 2011.

[Marques *et al.* 2012] R. Marques, G. Vasconcelos and P. B. Lourenço. Pushover Analysis of a Modern Aggregate of Masonry Buildings through Macro-element Modelling. In *Proceedings of the* 15^{th} *International Brick and Block Masonry Conference*, pp. 1–12, Florianopolis, Brazil, 2012. Federal University of Santa Catarina.

[Mendes 2012] N. Mendes. *Seismic Assessment of Ancient Masonry Buildings: Shaking Table Tests and Numerical Analysis*. Phd thesis in structural engineering, University of Minho, Braga, Portugal, 2012.

[Mendes and Lourenço 2004] N. Mendes and P. Lourenço. Redução da Vulnerabilidade Sísmica de Edifícios Antigos de Alvenaria. Technical report, Fundação para a Ciência e a Tecnologia, Lisbon, Portugal, 2004.

[Michel *et al.* 2009] C. Michel, E. Lattion, M. Oropeza and P. Lestuzzi. Vulnerability Assessment of Existing Masonry Buildings in Moderate Seismicity Areas using Experimental Techniques. *Proceedings of the 2009 Asian-Pacific Network of Centers for Earthquake Engineering Research (ANCER) Workshop*, 2009.

[Millennium 2004] Robot Millennium. Three Dimensional Static and Dynamic Finite Element Analysis and Design of Structures. Robot Office v17.5, 2004. User Manual.

[Modena *et al.* 2009] C. Modena, M. R. Valluzzi and M. Zenere. c-Sisma 3.0 PRO: Procedura Automatica per il Calcolo e la Verifica di Meccanismi di Pareti in Muratura. University of Padua, Padua, Italy, 2009. User Manual.

[Monaco *et al.* 2009] P. Monaco, G. Totani, G. Barla, A. Cavallaro, A. Costanzo, A. D'Onofrio, L. Evangelista, S. Foti, S. Grasso, G. Lanzo, C. Madiai, M. Maraschini, S. Marchetti, M. Maugeri, A. Pagliaroli, O. Pallara, A. Penna, A. Saccenti, F. Magistris, G. Scasserra, F. Silvestri, A. Simonelli, G. Simoni, P. Tommasi, G. Vannucchi and L. Verrucci. Geotechnical Aspects of the L'Aquila Earthquake. In *Proceedings of the* 15^{th} *International Conference on Soil Mechanics and Geotechnical Engineering*, pp. 1–50, Alexandria, Egypt, 2009.

[Monti and Vailati 2009] G. Monti and M. Vailati. Procedura di Analisi Non Lineare Statica per la Valutazione Sismica degli Edifici in Aggregato. In *Proceedings of the* 13^{th} *National Congress in Seismic Engineering*, Vol. 1, Bologna, Italy, 2009. ANIDIS - Italian National Association of Earthquake Engineering.

[Mouroux and Le Brun 2006] P. Mouroux and B. Le Brun. Presentation of RISK-UE Project. *Bulletin of Earthquake Engineering*, 4(4):323–339, 2006.

[Munari 2010] M. Munari. *Sviluppo di Procedure per Valutazioni Sistematiche di Vulnerabilità Sisimica di Edifici Esistenti in Muratura*. Phd thesis in preservation of the architectural and archaeological heritage, University of Padua, Italy, Padua, Italy, 2010.

[Munari and Valluzzi 2009] M. Munari and M. R. Valluzzi. Classificazioni di Vulnerabilità dal Calcolo Limite per Macroelementi: applicazione ad Aggregati Edilizi in Muratura in Centri Storici Umbri. In *Proceedings of the* 11^{th} *National Congress in Seismic Engineering*, pp. 1–10, Bologna, Italy, 2009. ANIDIS - Italian National Association of Earthquake Engineering.

[Munari *et al.* 2010] M. Munari, G. Busolo and M. R. Valluzzi. Mechanical Analysis for the Assessment of the Seismic Capacity of Masonry Building's Classes in the City Centre of Sulmona (Italy). *Advanced Materials Research*, 133-134:623–628, 2010.

[Murphy and O'Brien 1977] J.R. Murphy and L.J. O'Brien. The Correlation of Peak Ground Acceleration Amplitude with Seismic Intensity and other Physical Parameters. *Bulletin of the Seismological Society of America*, 67:877–915, 1977.

[Neves 2004] N. Neves. *Identificação Dinâmica e Análise do Comportamento Sísmico de um Quarteirão localizado na Cidade da Horta - Ilha do Faial*. Master's Thesis in Structural Engineering, University of Oporto, Oporto, Portugal, 2004.

[Nucera *et al.* 2012] F. Nucera, A. Santini, E. Tripodi and I. Caliò. Seismic Vulnerability Assessment of Confined Masonry Buildings by Macro-Element Modeling: a case study. In *Proceedings of the* 15^{th} *WCEE - World Conference of Earthquake Engineering*, pp. 1–9, Lisbon, Portugal, 2012.

[Oliveira 2008] C.S. Oliveira. Efeitos Naturais, Impacte e Mitigação. Sísmos e Edifícios. Orion, Alfgragide/Amadora, Portugal, 2008.

[Oliveira *et al.* 2004] C. Oliveira, M. Ferreira and M. Oliveira. Planning in Seismic Risk Areas: The Case of Faro - Algarve. A First Approach. In *Proceedings of the* 11^{th} *National Congress in Seismic Engineering*, pp. 1–12, Genoa, Italy, 2004. ANIDIS - Italian National Association of Earthquake Engineering.

[OPCM 2003] OPCM. Ordinaza 3274: Primi Elementi in Materia di Criteri Generali per la Classificazione Sismica del Territorio Nazionale e di Normative Tecniche per le Costruzioni in Zona Sismica. Ordinanza 3274, 2003.

[OPCM 2005] OPCM. Ulteriori Modifiche ed Integrazioni all'OPCM N.3274, Recante: Primi Elementi in Materia di Criteri Generali per la Classificazione Sismica del Territorio Nazionale e di Normative Tecniche per le Costruzioni in Zona Sismica. Ordinanza 3431, 2005.

[Ortolani *et al.* 2012] B. Ortolani, A. Borghini, S. Boschi, E. del Monte and A. Vignoli. Study of Vulnerability and Damage: the Case Study of Castelnuovo after L'Aquila Earthquake (Italy). In *Proceedings of the* 15^{th} *WCEE - World Conference of Earthquake Engineering*, pp. 1–10, Lisbon, Portugal, 2012.

[Pacor *et al.* 2010] F. Pacor, D. Bindi, L. Luzi, M. Massa, R. Paolucci and C. Smerzini. Characteristics of Strong Ground Motions from the L'Aquila mw 6.3 Earthquake and its Strongest Aftershocks. *International Journal of Earth Sciences - Bollettino di Geofisica Teorica e Applicata*, 52(3):471–490, 2010.

[Pagnini *et al.* 2011] L. C. Pagnini, R. Vicente, S. Lagomarsino and H. Varum. A Mechanical Model for the Seismic Vulnerability Assessment of Old Masonry Buildings. *Earthquakes and Structures*, 2(1):25–42, 2011.

[Palazzo and De Iuliis 2011] B. Palazzo and M. De Iuliis. L'Aquila Earthquake near-fault Accelerometer Registrations Seismic Demand in Terms of Damage Indexes. Technical report, University of Salerno, Salerno, Italy, 2011.

[Parisi 2010] F. Parisi. *Non-Linear Seismic Analysis of Masonry Buildings*. Phd thesis in structural engineering, University of Naples Federico II, Naples, Italy, 2010.

[Pellegrini 2007] R. Pellegrini. European Manual for in-situ Assessment of Important Existing Structures, chapter 2, pp. 1–182. Lessloss: Risk Mitigation for Earthquakes and Landslides. IUSS Press, Pavia, Italy, 2007.

[Pinto 2007] P. E. Pinto. Guidelines for Displacement-based Design of Buildings, chapter 5, pp. 1–218. Lessloss: Risk Mitigation for Earthquakes and Landslides. IUSS Press, Pavia, Italy, 2007.

[Pujades *et al.* 2012] L. G. Pujades, A. H. Barbat, R. González-Drigo, J. Avila and S. Lagomarsino. Seismic Performance of a Block of Buildings Representative of the Typical Construction in the Eixample District in Barcelona (Spain). *Bulletin of Earthquake Engineering*, 10(1):331–349, 2012.

[Ramos and Lourenço 2004] L. F Ramos and P. B. Lourenço. Modeling and Vulnerability of Historical City Centers in Seismic Areas: a Case Study in Lisbon. *Elsevier Science Ltd - Engineering Structures*, 26(9):1295–1310, 2004.

[Ravara *et al.* 2001] A. Ravara, C. S. Oliveira, E. C. Carvalho, M.S. Lopes, P. T. Costa, R. Delgado, R. Bairrão and V. C. Silva. Reducing the Seismic Vulnerability of the Building Stock. Technical report, Lisbon, Portugal, 2001.

[Reitherman 1999] R. Reitherman. Mitigation Division. HAZUS-MH MR3: Multi-Hazard Loss Estimation Methodology: Technical Manual. Technical report, Federal Emergency Management Agency, Washington DC, USA, 1999.

[Reitherman 2009] R. Reitherman. Unreinforced Masonry Buildings and Earthquakes - Developing Successful Risk Reduction Programs. Technical report, Federal Emergency Management Agency, Washington DC, USA, 2009.

[Restrepo-Velez and Magenes 2004] L. F. Restrepo-Velez and G. Magenes. Simplified Procedure for the Seismic Risk Assessment of Unreinforced Masonry Buildings. In *Proceedings of the* 13^{th} *WCEE - World Conference of Earthquake Engineering*, number 2561, pp. 1–15, Vancouver, Canada, 2004.

[Riuscetti *et al.* 1997] M. Riuscetti, R. Carniel and C. Cecotti. Seismic Vulnerability Assessment of Masonry Buildings in a Region of Moderate Seismicity. *Annali di Geofisica*, 40(5):1405–1413, 1997.

[Rush 2007] A. Rush. *Seismic Evaluation of Masonry Building conglomerations of Adjacent Structures*. Master's thesis in earthquake engineering, University of Pavia, Pavia, Italy, 2007.

[Salamon *et al.* 2010] A. Salamon, R. Amit, G. Baer, Y. Hamiel and A. Mushkin. The Mw 6.3, 2009, L'Aquila Earthquake, Central Italy: report of the GSI team visit to the affected area. Technical Report GSI/13/2010, The Ministry of National Infrastructures, Jerusalem, Israel, 2010.

[Sassu 2011] M. Sassu. Il Monitoraggio Sismico del Centro Storico di San Pio delle Camere (AQ). In *Studi e Indagini sul Rischio Sismico del Centro Storico di San Pio delle Camere (AQ)*, chapter 1, pp. 11–14. University of Pisa, Pisa, Italy, ets edition, 2011.

[Scheda di Aggregato 2010] Scheda di Aggregato. San Pio delle Camere Building Aggregate N.8800378. Technical report, University of Pisa, San Pio delle Camere, Italy, 2010.

[Schnepf *et al.* 2007] S. Schnepf, L. Stempniewski and D. Lungu. Application of the Capacity Spectrum Method for Seismic Evaluation of Structures. In *International Symposium on Strong Vrancea Earthquakes and Risk Mitigation*, Bucharest, Romania, 2007.

[Senaldi 2009] I. E. Senaldi. *Numerical Investigations on the Seismic Response of Masonry Building Aggregates*. Master's thesis in earthquake engineering, University of Pavia, Pavia, Italy, 2009.

[Shibata and Sozen 1976] A. Shibata and M. A. Sozen. Substitute-Structure Method to Determine Design Forces in Earthquake-Resistant Reinforced Concrete Frames. *Journal of the Structural Division, ASCE*, 102(ST1):1–18, 1976.

[Spacone *et al.* 2012] E. Spacone, V. Sepe and E. Raka. Safety Assessment of Masonry Building Aggregates in Poggio Picenze, following the L'Aquila 2009 Earthquake. In *Proceedings of the* 15^{th} *WCEE - World Conference of Earthquake Engineering*, pp. 1–11, Lisbon, Portugal, 2012.

[Spence *et al.* 2003] R. Spence, J. Bommer, D. del Re, J. Bird, N. Aydinoglu and S. Tabuchi. Comparison Loss Estimation with Observed Damage: A study of the 1999 Kocaceli Earthquake in Turkey. *Bulletin of Earthquake Engineering*, 1:83–113, 2003.

[STADATA 2007] STADATA. 3muri: Seismic Analysis Program for 3D Masonry Buildings - User Manual. STA DATA, Turin, Italy, 2007.

[STADATA 2011] STADATA. 3muri User Manual: a computer program for analysis of structures in masonry and mixed materials through a non-linear (pushover) and static analysis. , Turin, Italy, 2011.

[Ulrich *et al.* 2012] T. Ulrich, P. Gehl, C. Negulescu and E Foerster. Seismic Vulnerability Assessment of Masonry Building Aggregates. In *Proceedings of the* 15^{th} *WCEE - World Conference of Earthquake Engineering*, pp. 1–9, Lisbon, Portugal, 2012.

[Vailati *et al.* 2012] M. Vailati, G. Monti, M. J. Khazna, A. Napoli and R. Realfonzo. Probabilistic Assessment of Masonry Building Clusters. In *Proceedings of the* 15^{th} *WCEE - World Conference of Earthquake Engineering*, pp. 1–9, Lisbon, Portugal, 2012.

[Valluzzi *et al.* 2004] M. R. Valluzzi, G. Cardani, L. Binda and C. Modena. Seismic Vulnerability Methods for Masonry Buildings in Historical Centres: Validation and Application for Prediction Analyses and Intervention Proposals. In *Proceedings of the* 13^{th} *WCEE - World Conference of Earthquake Engineering*, pp. 1–12, Vancouver, Canada, 2004.

[Valluzzi *et al.* 2006] M. R. Valluzzi, V. Cóias and M. Munari. Avaliação da Vulnerabilidade Sísmica dos Edifícios Pombalinos utilizando a Abordagem dos Macro-Elementos. In *Proceeding of the 4^{th} JPEE, National Journeys of Structural Engineering*, pp. 1–15, Lisbon, Portugal, 2006. LNEC - National Laboratory of Civil Engineering.

[Varum 2003] H. Varum. *Avaliação, Reparação e Reforço sísmico de Edifícios Existentes*. Phd thesis in civil engineering, University of Aveiro, Aveiro, Portugal, 2003.

[Vasconcelos 2005] G. Vasconcelos. *Experimental Investigations on the Mechanics of Stone Masonry: characterization of granites and behaviour of ancient masonry shear walls*. Phd thesis, University of Minho, Braga, Portugal, 2005.

[Vicente 2008] R. Vicente. *Estratégias e Metodologias para Intervenções de Reabilitação Urbana - Avaliação da Vulnerabilidade e do Risco Sísmico do Edificado da Baixa de Coimbra*. Phd thesis in seismic and structural engineering, University of Aveiro, Portugal, 2008.

[Vicente *et al.* 2010] R. Vicente, H. Varum and S. Lagomarsino. Avaliação da Vulnerabilidade de Edifícios Antigos e do Risco Sísmico à Escala do Centro Histórico: o Caso da Baixa de Coimbra. *Riscos - Associação Portuguesa de Riscos, Prevenção e Segurança*, 17:189–200, 2010.

[Vicente *et al.* 2011] R. Vicente, H. Rodrigues, H. Varum and J. A. R. Mendes da Silva. Evaluation of Strengthening Techniques of Traditional Masonry Buildings: Case Study of a four-building Aggregate. *Journal of Performance of Constructed Facilities, ASCE*, 25(3):1–16, 2011.

[Vidic *et al.* 1994] T. Vidic, P. Fajfar and M. Fischinger. Consistent Inelastic Design Spectra: Strength and Displacement. *Earthquake Engineering and Structural Dynamics*, 23(5):507–521, 1994.